THE MODELLING OF THE BINARY ADSORPTION OF GOLD AND ZINC CYANIDES ONTO A STRONG BASE ANION EXCHANGE RESIN

Michael Richard Lister Glover

A dissertation submitted to the Faculty of Engineering, University of the Witwatersrand, Johannesburg, in fulfilment of the requirements for the degree of Master of Science in Engineering.

Johannesburg, 1989.

ABSTRACT

The homogeneous surface diffusion model with external film transfer is solved for the two–component adsorption of gold and zinc cyanides onto the strong–base anion exchange resin, Duolite A161. The binary equilibriums between the solid and liquid phases are non–linear and may be described using the empirical relationship given by Fritz and Schlunder (1974).

Isothermal mini–column adsorption experiments for single and binary adsorption are performed, and the external film and intraparticle surface diffusion parameters are fitted to the experimentally measured breakthrough curves.

The binary mass transfer parameters obtained are similar to those obtained from the single component studies. Furthermore the fitted surface diffusion parameters are found to be independent of the Reynolds number. This is noteworthy and suggests that the intraparticle diffusion coefficient is indeed a measure of an internal transport mechanism.

The characteristics of the model are investigated by "semi–quantitatively" comparing existing experimentally measured gold and zinc intraparticle loading profiles to model predictions using realistic values of the mass transfer parameters. Broad agreement between the binary homogeneous surface diffusion model and the independently measured experimental results is obtained.

ACKNOWLEDGEMENTS

I wish to thank

— my supervisors, Professor A. W. Bryson and Mr B. D. Young.

— MINTEK for providing the necessary funding.

— Nicky Keddy.

DECLARATION

I declare that this dissertation is my own, unaided work, except where spe... acknowledgement is made. It is being submitted for the Degree of Master of Scienc... (Engineering) to the Faculty of Engineering, University of the Witwatersrand, Johannesburg. It has not been submitted before for any degree or examination to any other university.

M.R.L.G

Michael Richard Lister Glover

23 day of JANUARY 1989

CONTENTS

LIST OF FIGURES

LIST OF TABLES

1. INTRODUCTION

The separation of components from a fluid stream by adsorption is a well–established industrial practice. The adsorption of a single component from an aqueous solution onto various adsorbents has been successfully modelled by a number of researchers including van Deventer (1985), van Lier (1983), and Weber and Lui (1980). Relatively little model development has been done for the binary or multi–component case however, which has to be handled in practice. As a first step towards modelling a multi–component adsorption system, a binary system is attempted. In this study, the binary adsorption of gold and zinc cyanides onto a strong–base anion exchange resin is investigated. Zinc cyanide is chosen to be the second component, as not only is it found in most real solutions, but it is often used to elute gold and silver from strong–base anion exchange resins.

For the experimental determination of the kinetic parameters, the mini–column technique as described by Weber and Lui (1980) is used. This technique provides accurate estimates of the mass transfer parameters on the basis of the characteristic breakthrough which are experimentally measured. The essence of the technique is to use columns of sufficiently short adsorbent length so that immediate or incipient effluent concentration breakthrough occurs. As shown by Weber and Lui (1980), the mini–column technique gives accurate estimates of both the external film and internal intraparticle mass transfer coefficients.

The resin chosen for the study is Duolite A161, a strong–base anion exchange resin manufactured by A.C.I.X., a division of National Chemical Products Ltd., South Africa.

1.1 THE USE OF RESIN IN THE EXTRACTION OF GOLD

1.1.1 HISTORICAL BACKGROUND

Fleming and Cromberge (1984) describe the historical development of the use of resins to extract gold from cyanide solutions and pulps. This is summarised below.

An investigation into resins was first performed in South Africa in 1961, although the U.S. Bureau of Mines conducted an earlier study in 1949. In the latter case, the process failed owing to the inability of weak–base resins to extract anions efficiently at the high pH values of cyanide leach liquors. Burstal et. al. (1953), and Burstal and Wells (1955) observed that gold in a cyanide solution could readibly be adsorbed onto strong–base anion exchange resins together with other metal cyanide complexes. By using a series of selective eluting agents, they found it possible to remove the various metals from the resin successively and to obtain a number of discrete eluates containing relatively high concentrations of the various metals.

Davidson *et. al.* (1961), using strong–base anion exchange resins also demonstrated the potential of the Resin–In–Pulp (RIP) process and expressed the view that it could compete with the conventional zinc–precipitation process providing that the pregnant solution was high in gold and relatively free of competing metal cyanide complexes. Using real solutions they observed that gold loading on the resin was related to the contact time between the resin and the solutions. Their design philosophy was to extract gold as selectively as possible, followed by non–selective elution.

More recent progress in the development of the RIP process made in the Soviet Union and Roumania has been detailed by Demidov *et al* (1967), Fridman *et al* (1971), and Tataru (1973), with one of the largest Soviet gold mines using an anion exchange resin to extract gold in an RIP application. In their process, non–selective adsorption is followed by selective elution.

In Canada, Stamboliades *et al* (1978) recently investigated using strong–base resins to extract gold from cyanide solutions. They concluded that the non–selectivity of gold adsorption, coupled with the high cost of elution, rendered the process unfavourable as compared with zinc precipitation. In their study however, only clarified solutions were investigated and the economic benefits to be gained from the elimination of solid–liquid separation by using an RIP process were ignored.

More recently, Riveros and Cooper (1988) investigated the intraparticle diffusion of adsorbing anions into a strong–base anion exchange resin using a shrinking core model. They found that the intraparticle diffusional resistances for gold and silver cyanides are lower than those for copper, zinc, and iron cyanide complexes. This explains why gold and silver cyanides load onto the resin relatively quickly. However, they also found that gold and silver cyanides were then slowly eluted from the resin if it was left in the solution. The driving force for this displacement was attributed to the resin's equilibrium preference for the base metal cyano complexes.

At present in South Africa, an increasing amount of work is being focussed on RIP technology by MINTEK, which also includes this project. Other MINTEK projects include the development of a gold and silver selective strong–base anion exchange resin, and applying the RIP process on a commercial scale (Golden Jubilee Gold Mine).

1.1.2 RESIN–IN–PULP AS AN ALTERNATIVE TO CARBON–IN–PULP

The advantages and dissadvantages of the RIP process over the CIP process as stated by Fleming and Cromberge (1984) are listed below.

Advantages of the RIP Process

(a) Anion exchange resins are superior to currently available activated carbons with respect to both rate and equilibrium loading of the aurocyanide ion. This means that either the resin inventory, or the plant, will be smaller in the RIP process.

(b) Resins may be eluted at room temperature whereas carbon must be eluted at high temperature, preferably around 120^{0}C in a pressurised vessel.

(c) Activated carbon requires periodic thermal reactivation for the removal of adsorbed organic materials.

(d) Resins do not load calcium carbonate to the same extent as activated carbon, and the acid–washing step in the CIP process will therefore probably be unnecessary in an RIP application.

(e) Resins do not appear to be 'poisoned' by organic species which severly inhibit the loading of gold on activated carbon. Indeed Golden Jubilee Gold Mine is using resins due to the high organic content of their pulp.

(f) South Africa has developed a resin manufacturing facility, whereas all gold application activated carbon is presently imported and hence its supply is less assured.

Dissadvantages of the RIP process

(i) Anion exchange resins are less selective than activated carbon for the aurocyanide ion over the base metal cyanide complexes prevalent in cyanide leach liquors.

(ii) The particles of resin are smaller than those of carbon, and hence more sophisticated screening techniques are necessary. Work in this field is presently being done by MINTEK.

(iii) The physical strength of resins and their resistance to abrasion and attrition in pulps is largely unknown.

(iv) Resins are less dense than activated carbon and tend to accumulate at the surface of the pulp unless agitated properly.

(v) Resins are generally more expensive than activated carbon.

1.2 THE CHEMISTRY OF ADSORPTION

Fleming and Cromberge (1984) have examined the chemistry of the interactions between the aurocyanide ion, the zinc tetracyanide ion and the anion-exchange resin. A brief summary is presented below.

The functional group of a strong-base anion exchange resin is a quaternary amide possesing a permanent positive charge. The adsorbing anions are extracted by an ion-exchange reaction, which is shown here for the aurocyanide anion adsorbing onto resin in the sulphate form:

$$|-\overset{+}{N}R_3HSO_4^- + Au(CN)_2^- \rightleftharpoons |-\overset{+}{N}R_3Au(CN)_2^- + HSO_4^- \qquad (1)$$

where the symbol |— denotes the inert backbone or matrix of the resin, which for Duolite A161 is polystyrene, and $\overset{+}{N}R_3$ denotes the quaternary amide. The elution of the aurocyanide ion from the resin by zinc cyanide is depicted by equation (2),

$$2\ |\!-\overset{+}{N}R_3Au(CN)_2^- + Zn(CN)_4^{2-} \rightleftharpoons (|\!-\overset{+}{N}R_3)_2Zn(CN)_4^{2-} + 2\ Au(CN)_2^- \qquad (2)$$

This is due to the zinc tetracyanide anion being adsorbed more strongly onto the strong-base resin Duolite A161. Once eluted, the resin is regenerated before being recycled to adsorption. This may be done with a dilute mineral acid as the zinc tetracyanide anion decomposes in acid solution. The regeneration action is depicted by equation (3),

$$(|\!-\overset{+}{N}R_3)_2Zn(CN)_4^{2-} + 3\ H_2SO_4 \longrightarrow 2\ |\!-\overset{+}{N}R_3HSO_4^- + ZnSO_4 + 4\ HCN \qquad (3)$$

1.3 LITERATURE REVIEW ON THE APPROACH TO MODELLING

1.3.1 ADSORPTION ISOTHERMS

Adsorption isotherms, or equilibrium data are the basic requirements of any adsorption system. Whereas the single component isotherms are easily obtainable, the multicomponent isotherms require a tedious procedure in order to be obtained experimentally.

As reported by McKay and al Duri (1989), Butler and Ockrent (1930) were the first to develop the Langmuir model. This model assumes a homogeneous surface with respect to the energy of adsorption, no interaction between adso ing species and that all adsorption sites are equally available to all adsorbing species. This was later modified by Jain and Snoeyink (1973) who assumed that a portion of adsorption takes place without competition as not all adsorption sites are available to all species. However, for more than two components these models were found to be inapplicable. This led Myers and Prausnitz (1965), and later Radke and Prausnitz (1972) to develop the Ideal Adsorbed Solution (IAS) theory. This theory assumes that, when multisolutes adsorb simultaneously at the same temperature and spreading pressure as each species would, the adsorbed phase forms an ideal solution. The mathematics and computational effort required however is substantial which has restricted this theory to limited applications. This then led to the development of empirical formulae by some researchers including Fritz and Schluender (1974).

The purpose of this study is not to obtain a fundamental understanding of the intricacies of isotherm theory, all that is required is to obtain an accurate mathematical description of the equilibrium relationship so that it is possible to proceed with the modelling of the kinetics. For this reason the empirical relationship proposed by Fritz and Schluender (1974) is fitted to the experimentally determined isotherm data.

1.3.2 ADSORPTION DYNAMICS

According to Liapis and Rippin (1976), the transport of adsorbate from solution to it's ultimate adsorbed state is considered to proceed via two sequential mass transfer processes. The first comprises the transport of the adsorbate from the bulk solution through a boundary layer immediately adjacent to the adsorbent particles to the exterior surface of the particles. The rate of transfer across the film being described by a linear liquid concentration driving force expression. The second involves a combination of intraparticle surface and pore diffusion. Intraparticle surface diffusion takes place along the inner walls of the pores, whilst intraparticle pore diffusion takes place in the liquid phase down the pores. Unsteady–state radial surface and pore concentration gradients being the driving forces, respectively.

The surface diffusion model has been compared with pore diffusion for the adsorption of phenol onto activated carbon by Neretnieks (1977) and for a number of organics by van Lier (1974). These researchers conclude that both diffusion mechanisms occur in parallel and it is difficult to separate them. This means that for adequate modelling they may be lumped into a single effective diffusion coefficient. The homogeneous intraparticle surface diffusion model with external film transfer is chosen to describe this system.

2. THEORY

2.1 BINARY ADSORPTION ISOTHERMS

As discussed in Section 1, Fritz and Schlunder (1974) have suggested a general empirical equation for calculating the adsorption equilibria of organic solutes in aqueous solutions. The expression is of the following form:

$$C_{si} = \frac{a_{io} C_{ci}^{b_{io}}}{c_i + \sum_{j=1}^{n} a_{ij} C_{cj}^{b_{ij}}} = f_i(C_{c1}, C_{c2} \cdots C_{cn}) \qquad (2.1.1)$$

where, $a_{io} \cdots a_{ij}, b_{io} \cdots b_{ij}, c_i$ are constants

C_{ci} is the liquid phase concentration of component i, mg l^{-1}

C_{si} is the solid phase concentration of component i, mg g^{-1}

n is the number of components

Liapis and Rippin (1976) have discussed some wellknown relationships which are special cases of Equation (2.1.1).

For $b_{io} = b_{ij} = c_i = 1$, it becomes the well known Langmuir equation:

$$C_{si} = \frac{a_{io} C_{ci}}{1 + \sum_{j=1}^{n} a_{ij} C_{cj}} \qquad (2.1.2)$$

For a single solute Equation (2.1.1) becomes:

$$C_s = \frac{a_0 \, C_c^{b_0}}{c + a_1 \, C_c^{b_1}} \qquad (2.1.3)$$

In the special case where c is identically zero, the well known Freundlich equation is obtained:

$$C_s = \frac{a_0}{a_1} C_p^{b_0 - b_1} \qquad (2.1.4)$$

Fritz and Schlunder (1974) have used Equation (2.1.1) to satisfactorily fit experimental data for the two–component equilibrium adsorption of *p*–nitophenol and phenol onto activated carbon.

In order to fit Equation (2.1.1) to a binary adsorption system, the 14 parameters (a_{10}, a_{20}, a_{11}, a_{12}, a_{21}, a_{22}, b_{10}, b_{20}, b_{11}, b_{12}, b_{22}, b_{21}, c_{10}, c_{20}) are chosen to minimise the sum of squared errors between the experimental data and the isotherm predicted data. As discussed in Section 1.3, the nature of the isotherm relationship is empirical and the object of the isotherm relationship in this work is to obtain an accurate mathematical relationship so that it is possible to proceed with the modelling of the kinetics.

The constants obtained are merely fitting parameters and have no physical significance. Furthermore owing to the large number of parameters there will probably be a number of regions of the parameters which will give a good fit to the experimental data.

2.2 ADSORPTION DYNAMICS

The predictive modelling of the adsorption process requires determination of equilibrium and rate parameters. The equilibrium parameters must rigorously describe the experimental isotherms. The rate parameters must fully characterise the external and internal mass transport dynamics. As discussed in Section 1, for each component, the external mass transfer is characterised by an interfacial film transfer coefficient and intraparticle transport by an effective surface diffusion coefficient. Ideally, as is the case in this study, the equilibrium and rate parameters should be obtained from independent experiments and applied along with appropriate operational variables, in the framework of a mathematical model for the simulation and prediction of the expected performance characteristics of an adsorption system.

The following assumptions are made in obtaining the rate expression:

i. The system is isothermal, ie. heats of adsorption are low in relation to the heat capacities of the resin and solution.

ii. Equilibrium exists between the solid and the liquid at at all times at the particle / liquid interface.

iii. The external film transfer coefficients for each component are independent.

iv. The intraparticle surface diffusion coefficients for each component are independent.

Under the above assumptions, the concentration profile inside the resin bead of species i is obtained by solving Equation (2.2.1)

$$\frac{\partial C_{si}}{\partial t} = \frac{D_{si}}{r^2}\frac{\partial}{\partial r}\left[r^2\frac{\partial C_{si}}{\partial r}\right] \qquad (2.2.1)$$

where, C_{si} is the solid adsorbate concentration of component i, mg g^{-1}

D_{si} is the effective surface diffusion coefficient of component i, m^2s^{-1}

r is the radius, m

t is time, s

The boundary conditions for this equation are:

$$C_{si}(r,0) = 0 \qquad (2.2.2)$$

$$\frac{\partial C_{si}}{\partial r}(0,t) = 0 \qquad (2.2.3)$$

$$\rho_p\frac{\partial C_{si}}{\partial r}(r_0,t) = \frac{k_{fi}}{D_{si}}(C_{cio} - C_{pi}) \qquad (2.2.4)$$

where, C_{cio} is the bulk liquid adsorbate concentration of component i, mg l^{-1}

k_{fi} is the film transfer coefficient of component i, m s^{-1}

ρ_p is the particle density, kg (dry adsorbent) m^{-3} (particle)

2.3. INFINITE BATH

For the simple system of an infinite bath the bulk liquid concentrations remain constant with time. The complete solution to the model may then be obtained by solving Equation (2.2.1) coupled to the isotherm Equation (2.1.4). This is done numerically using the NAG FORTRAN software library routine D03PGF. The program written to solve the model is presented in Appendix 8.

2.4 MINI-COLUMN

In addition to the assumptions presented in Section 2.2, the following is assumed in deriving the non steady-state material balance for the packed adsorber:

i. The liquid is in plug flow

ii. The effect of longitudinal dispersion is negligible. This is verified by Weber and Lui (1980).

iii. The volumetric flowrate is constant as the adsorbate concentrations are low.

The non steady-state column material balance as derived in Appendix 3 is:

$$\frac{V}{\varepsilon}\frac{\partial C_{ci}}{\partial Z} + 3\left[\frac{1-\varepsilon}{\varepsilon}\right]\frac{k_{fi}}{r_0}(C_{ci} - C_{pi}) + \frac{\partial C_{ci}}{\partial t} = 0 \quad (2.4.1)$$

where, C_{ci} is the liquid adsorbate concentration of component i, mg l^{-1}

C_{pi} is the liquid adsorbate concentration of component i at the particle / liquid interface, mg l^{-1}

k_{fi} is the film transfer coefficient of component i, m s^{-1}

t is time, s

V is the superficial velocity, m s^{-2}

Z is the longitudinal coordinate, m

ε is the column voidage

The boundary conditions for this equation are:

$$C_{ci}(0,t) = C_{cio} \quad (2.4.2)$$

$$C_{ci}(Z,0) = 0 \quad (2.4.3)$$

where C_{cio} is the column inlet concentration of component i, mg l^{-1}

As shown by Young and van Vliet (1987), at small times the loading of adsorbates on the adsorbent particles are small and may be neglected. This means that the concentrations of the adsorbates at the particle / liquid interface are effectively zero and film transfer dominates the

rate expression. Under these conditions the initial effluent breakthrough concentration may easily be shown to be given by Equation (2.4.4).

$$C_{cie} = C_{cio} \exp\left[-\frac{3\ (1-\varepsilon)\ L\ k_{fi}}{V\ r_0}\right] \qquad (2.4.4)$$

where C_{cie} is the liquid concentration of adsorbent i in the effluent, mg l^{-1}

L is the adsorbent packing length, m

Hence using Equation (2.4.4), the external film transfer coefficients may be estimated independently from the effective surface diffusion coefficients from the incipient effluent concentration breakthrough

The complete solution to the model is obtained numerically by solving the partial differential Equations (2.4.1) and (2.2.1) simultaneously coupled with the isotherm Equation (2.1.4). Equation (2.4.1) which is the non steady-state column mass balance is a first order hyperbolic partial differential equation. An adaption of the method of characteristics is used to solve it. Briefly it involves reducing the hyperbolic partial differential equation to an ordinary differential equation along certain conditions or characteristics by transformation of the independent vaiables. The characteristics in this case are the shock waves of solution passing down the column in plug flow, which are merely the trajectories of the interface between the resin adsorbate and the solution. The characteristics as derived in Appendix 4 are:

$$t = t_o + \frac{\varepsilon\ L\ s}{V}$$

where, ε is the adsorbent packing voidage

t is the time of the shock wave of solution passing down the column, entering the column at time t_0, s

L is the adsorbent packing length, m

s is the parameterising variable for both time and adsorbent length

V is the superficial solution velocity, m s^{-1}

Under these conditions or characteristics, the column mass balance as shown in Appendix 4 becomes:

$$\left.\frac{dC_{ci}}{ds}\right|_{I} = -3\left[\frac{1-\varepsilon}{\varepsilon}\right]\frac{k_{fi}}{V r_o}(C_{ci}-C_{pi})\tau$$

where, I denotes the characteristics

τ is the residence time of the shock wave of solution within the column.

In essence the characteristics are conditions under which the partial differential equation becomes an ordinary differential equation. The ordinary differential equation may then be solved numerically simultaneously with the rate expression along the discretised solution shock waves down the discretised column. As stated by Acrivos (1956), the method of characteristics technique is strictly speaking an approximate one, yet it is straightforward, systematic and capable of producing numerical results of great accuracy. Equation (2.2.1) is a parabolic partial differential equation and is solved numerically using the NAG FORTRAN software library routine D03PGF simultaneously with the parameterised column equation. The solution to these equations is discussed fully in Appendix 4.

2.3 FILM TRANSFER COEFFICIENT CORRELATION

The liquid side mass or film transfer coefficients may be linked to the system parameters via dimensionless numbers, namely the Reynolds, Schmidt and Sherwood Numbers. Williamson *et al* (1963), obtained a correlation for similar low Reynolds numbers by experimenting with a column system packed with dissolving benzoic acid spheres (this is similar to the experimental conditions used in this study. The correlation has the following form:

$$Sh = 2.4\,\varepsilon^{0.66}\,Re^{0.34}\,Sc^{0.42} \qquad (2.5)$$

where, Sh is the Sherwood Number, $k_f d_p/D$

Re is the Reynolds Number, $d_p V\rho/\mu$

Sc is the Schmidt Number, $\mu/\rho D$

D is the free liquid diffusivity of the adsorbate, $m^2\,s^{-1}$

d_p is the particle diameter, m

k_f is the film transfer coefficient, $m\,s^{-1}$

ε is the column voidage

μ is the liquid viscoscity, $kg\,m\,s^{-1}$

ρ is the liquid density, $kg\,m^{-3}$

Young and van Vliet (1987) have noted that this correlation has an intrinsic weakness in that the surface roughness, and hence the film transfer coefficients, of the benzoic acid spheres changes as the dissolution progresses. They found the correlation to fit adsorption data for a

BACM spherical activated carbon / phenol system reasonably well. Unfortunately as there are no literature values for the free liquid diffusivities of the gold and zinc cyanides and it is beyond the scope of this study to measure them, the Sherwood and Schmidt Numbers could not be evaluated.

The equation proposed by Williamson *et al* (1963) is assumed to be correct. This equation is then fitted to the experimental results by minimising the sum of the squared differences between the experimental data and the correlation prediction using the free liquid diffusivity as the fitting parameter.

The accuracy of the fitted values of the free liquid diffusivities are dependent on the applicability of the correlation. These values should however allow for good estimates of the film transfer coefficients for gold and zinc cyanide systems when used in conjunction with the Williamson *et al* (1963) correlation.

3. CHARACTERISTICS OF THE MODEL

3.1 INTRODUCTION

The purpose of this Section is to illustrate the characteristics of the homogeneous surface diffusion model and to show that it is in broad agreement with existing experimental results, and not to make detailed quantitative comparisons.

Existing time related gold and zinc intraparticle concentration profiles experimentally measured by Pillay (1989) are "semi quantitatively" compared with model predictions using realistic values for the mass transfer parameters. The homogeneous binary surface diffusion model with external film transfer is used as described in Section 2.

The Fritz and Schluender (1974) relationship discussed in Section 2.1, and presented in Section 5.1 is used to mathematically describe the equilibrium or isotherm behaviour. The experimental conditions under which the isotherms were measured are presented in Section 4.1.

3.2 THEORY

Binary Kinetics

As discussed previously in Section 2, the kinetics are modelled using a binary version of the homogeneous surface diffusion model which includes both external film transfer and intraparticle surface diffusion. Ideally, as in this case, the equilibrium and rate parameters should be obtained from independent experiments and applied along with appropriate operational variables, in the framework of a mathematical model for simulation and prediction of the expected performance characteristics of an adsorption system. In this case, the simple system of an infinite bath is used. The model is presented, and it's solution discussed in Section 2.3.

3.3 EXPERIMENTAL

Loading Profiles

The intraparticle loading profiles of gold and zinc cyanides were measured experimentally by Pillay (1989) usind a Scanning Electron Microscope (SEM) technique. The experimental conditions under which the loading profiles were measured were different to those used to evaluate the isotherm. An excess of 1000 mg per litre of potassium cyanide and a pH of 10,0 was used for the isotherm studies, whilst an excess concentration of 200 mg per litre of potassium cyanide and a pH of 11,0 was used for measuring the loading profiles.

Loading of the resin was done by contacting 8 to 10 Duolite A161L resin beads in 50 ml of solution. The metal concentrations were 100 mg per litre each. The solutions containing the beads were mixed using a rotary agitator for different times. At the end of each loading test, the beads were removed and prepared for SEM examination. This was done by rapidly freezing the beads using liquid nitrogen in order to quench the adsorption and diffusion processes. Following this the beads were freeze–dried and mounted for SEM examination.

3.4 RESULTS AND DISCUSSION

Loading Profiles

The experimentally measured loading profiles for times of 2, 3, 4 and 6 hours are given on Figures 3.1 to 3.4. It is clear from these figures that the zinc boundary moves progressively towards the center of the bead with more zinc loading with time. The zinc is almost fully loaded in 6 hours.

For the loading profiles of gold however, it is seen that gold initially loads more quickly within the resin particles. At two hours the gold has a maximum loading somewhere between the centre and the outside of the bead. This maximum moves to the centre of the bead within 3 hours, after which the gold loadings inside the resin bead progressively decrease. At 6 hours the gold is clearly near it's final eluted state.

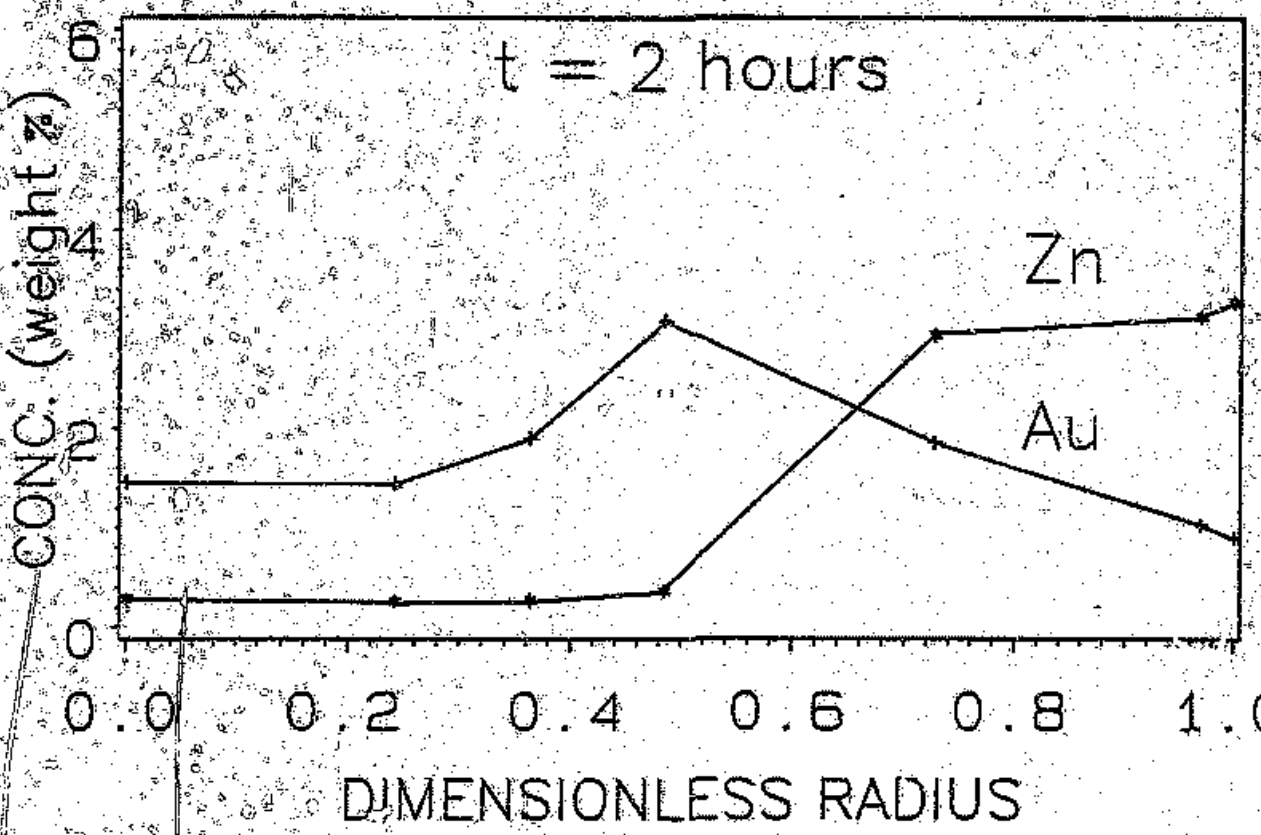

Fig. 3.1: Experimental Intraparticle Loading Profile

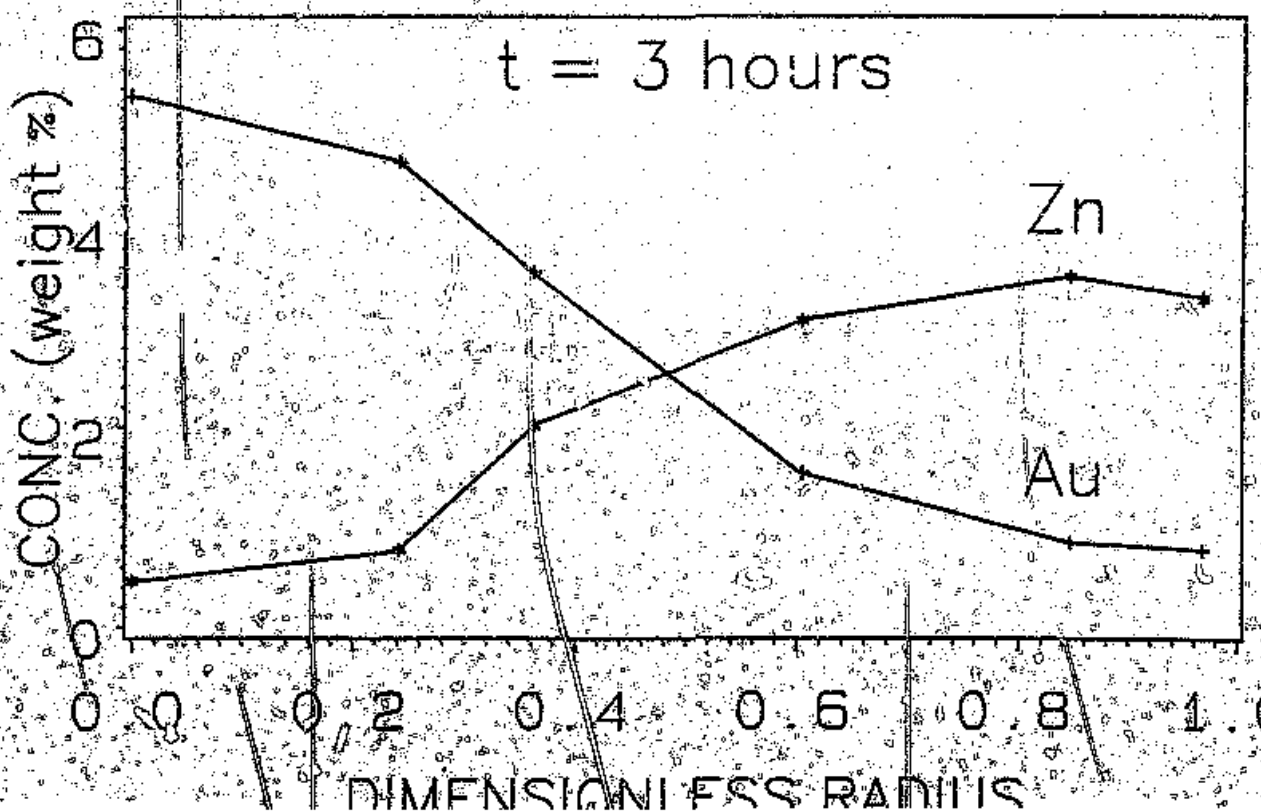

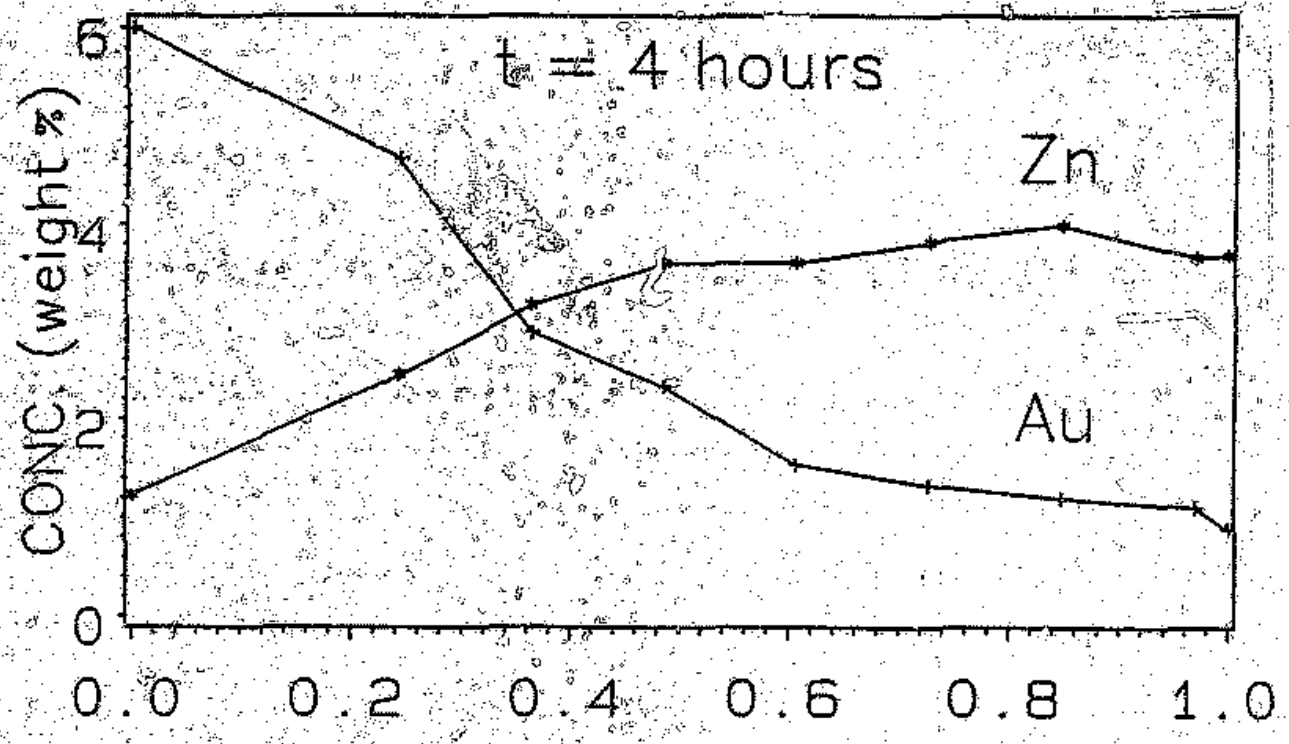

Fig. 3.3: Experimental Intraparticle Loading Profile

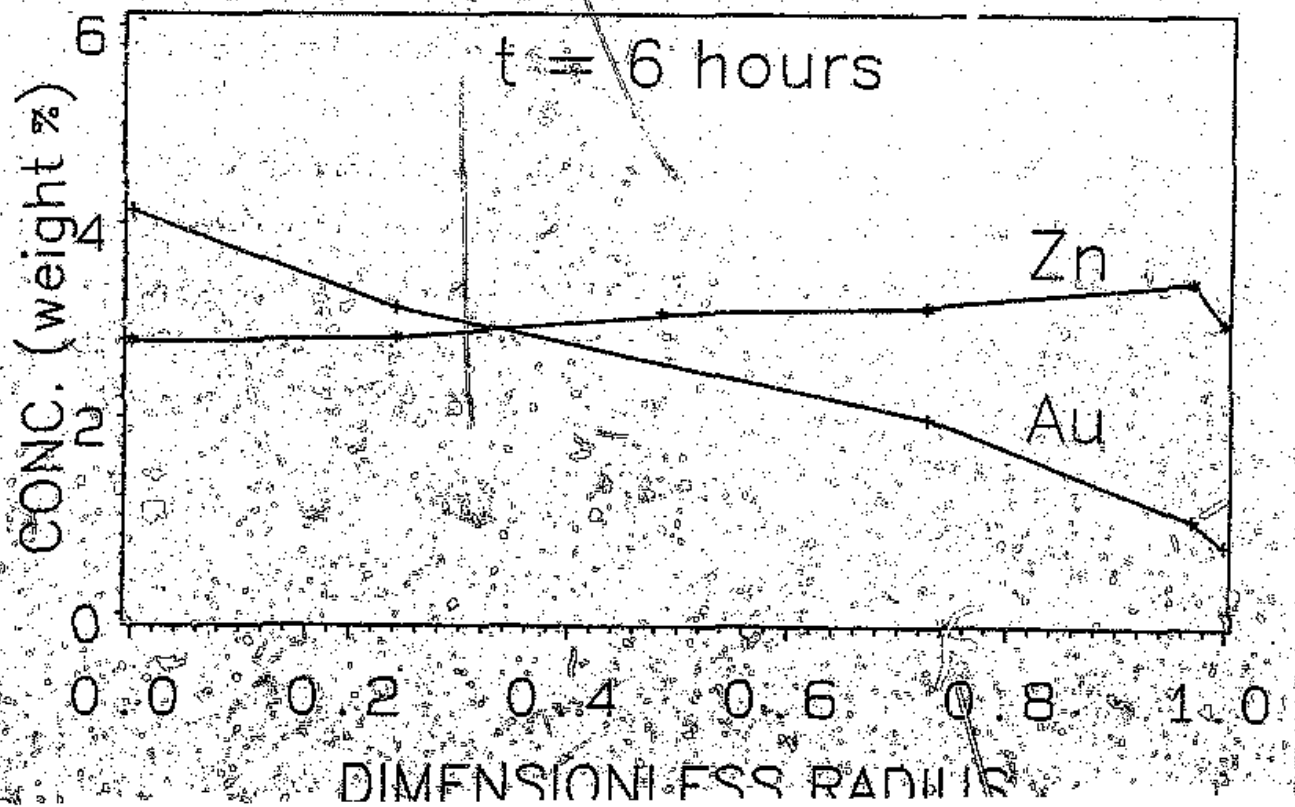

Model Predictions

The mass transfer parameters chosen to represent the system are given in Table 3.1.

Table 3.1:: Kinetic Parameters Used for Model Solution

Adsorbate	$k_{fi} * 10^5$ [$m \cdot s^{-1}$]	$D_{si} * 10^{12}$ [$m^2 s^{-1}$]
$Au(CN)_2^-$	5,00	5,00
$Zn(CN)_4^{2-}$	0,35	1,50

These surface diffusion parameters are of the same order as those fitted to the binary mini–column adsorption experimental studies presented in Section 5.2. They were adjusted slightly in order to obtain broad agreement with the experimental loading profiles. The solutions to the model at 2, 3, 4 and 6 hours are presented on Figures 3.5 to 3.9.

It is clear from these figures that very similar loading profiles are obtained bearing in mind that different conditions existed when the two sets of profiles were obtained. It is clear therfore that the binary homogeneous surface diffusion model is in broad agreement with the experimentally measured loading profiles.

The model explanation is as follows: Firstly, when the beads come into contact with solution, the relative gold cyanide concentration at the particle interface is higher than that for zinc cyanide, since the film transfer coefficient for gold cyanide is higher than that for zinc cyanide. Therefore gold loads highly on the resin at the particle interface, and since gold has a high surface diffusion coefficient, it migrates into the resin rapidly. However as adsorption progresses and the liquid concentrations of both species at the particle interface increase, the isotherm conditions change and by the nature of the isotherm the zinc loading rises whilst the gold loading drops at the interface. This means that the concentration gradient for gold is reversed and gold actually starts to diffuse out of the bead. As significant quantities of gold have diffused towards the center of the bead, the gold loading passes through a maximum inside the resin bead. As the loading of zinc at the interface always increases, the zinc loadings throughout the bead continually rise and do not have a maximum.

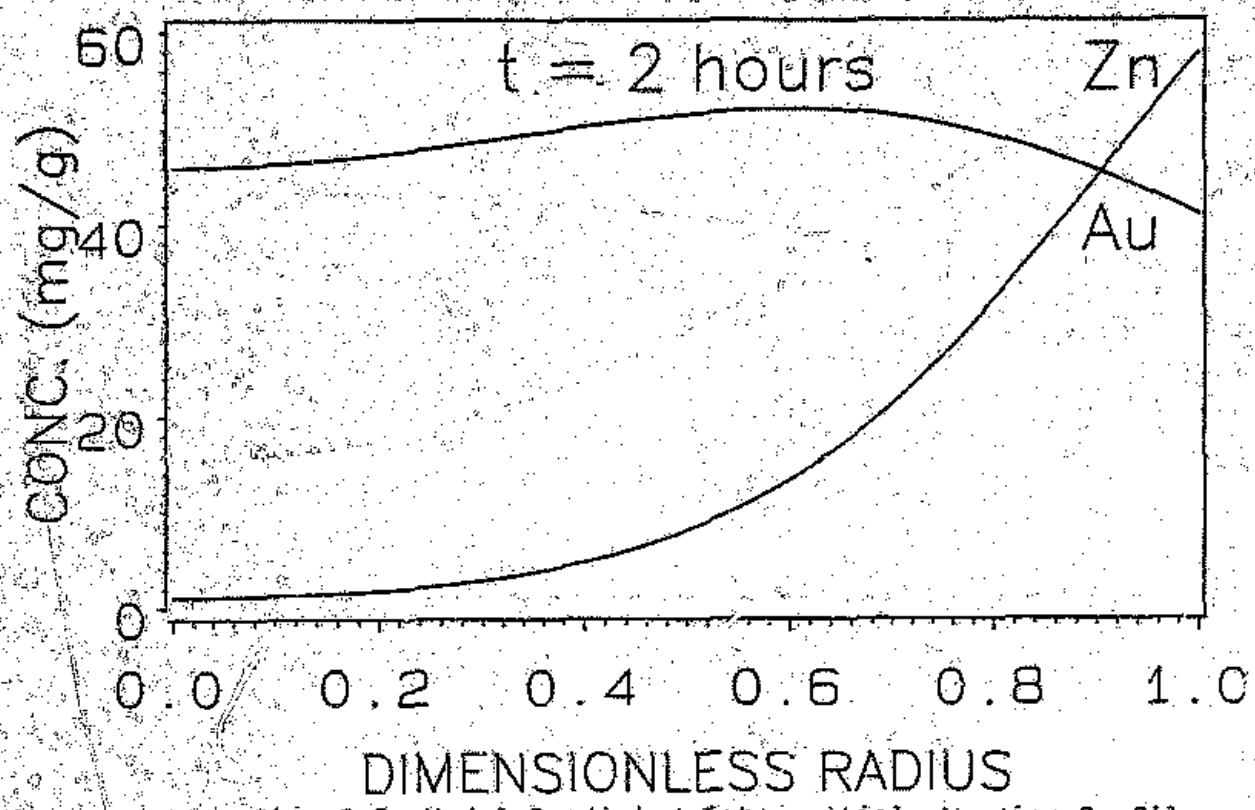

Fig. 3.5: Model Predicted Intraparticle Loading Profile

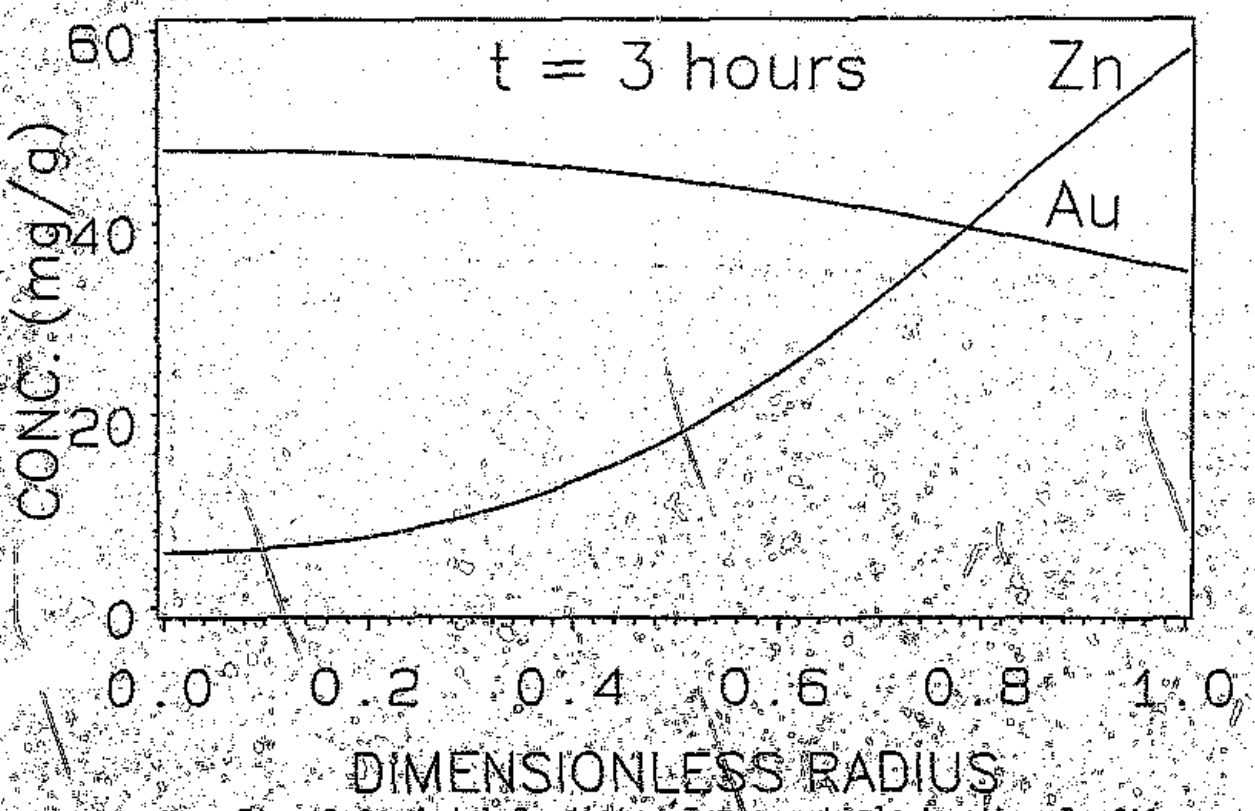

Fig. 3.6: Model Predicted Intraparticle Loading Profile

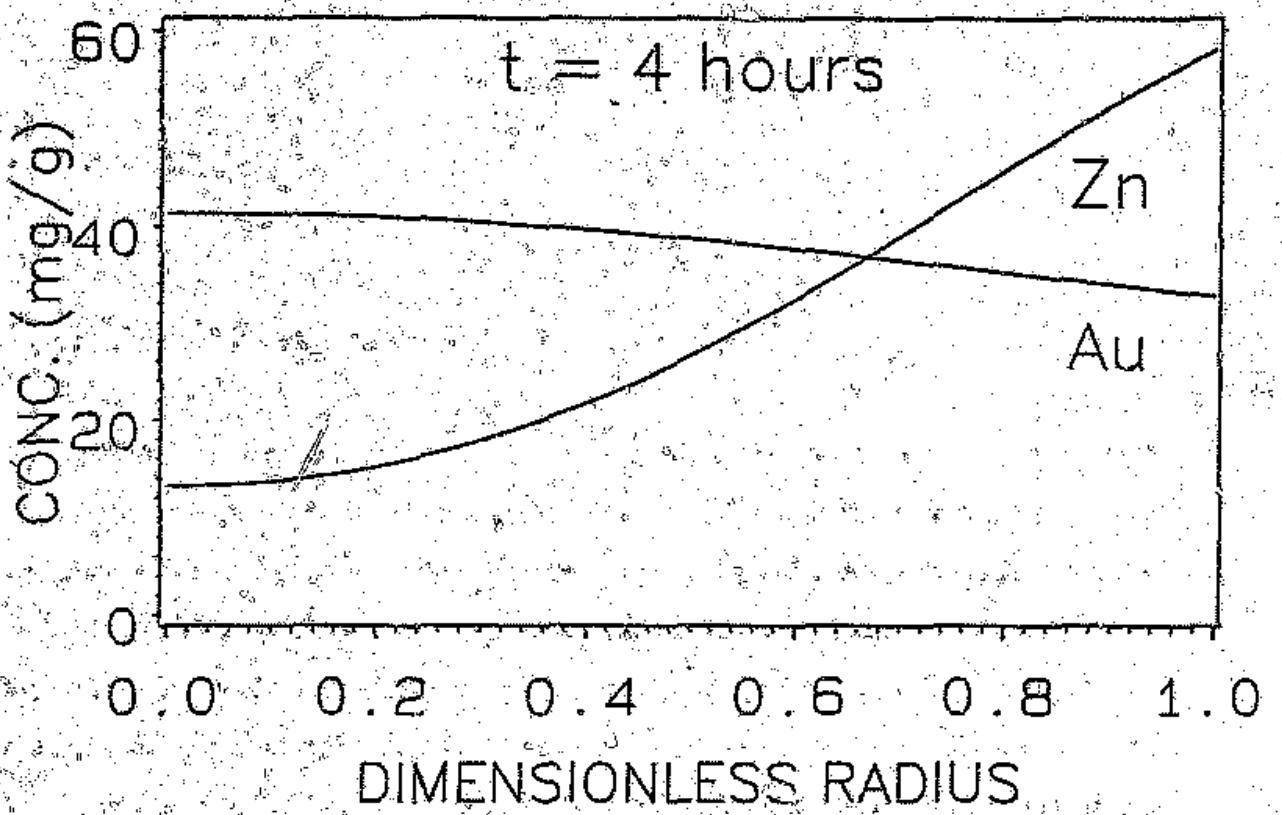

Fig. 3.7: Model Predicted Intraparticle Loading Profile

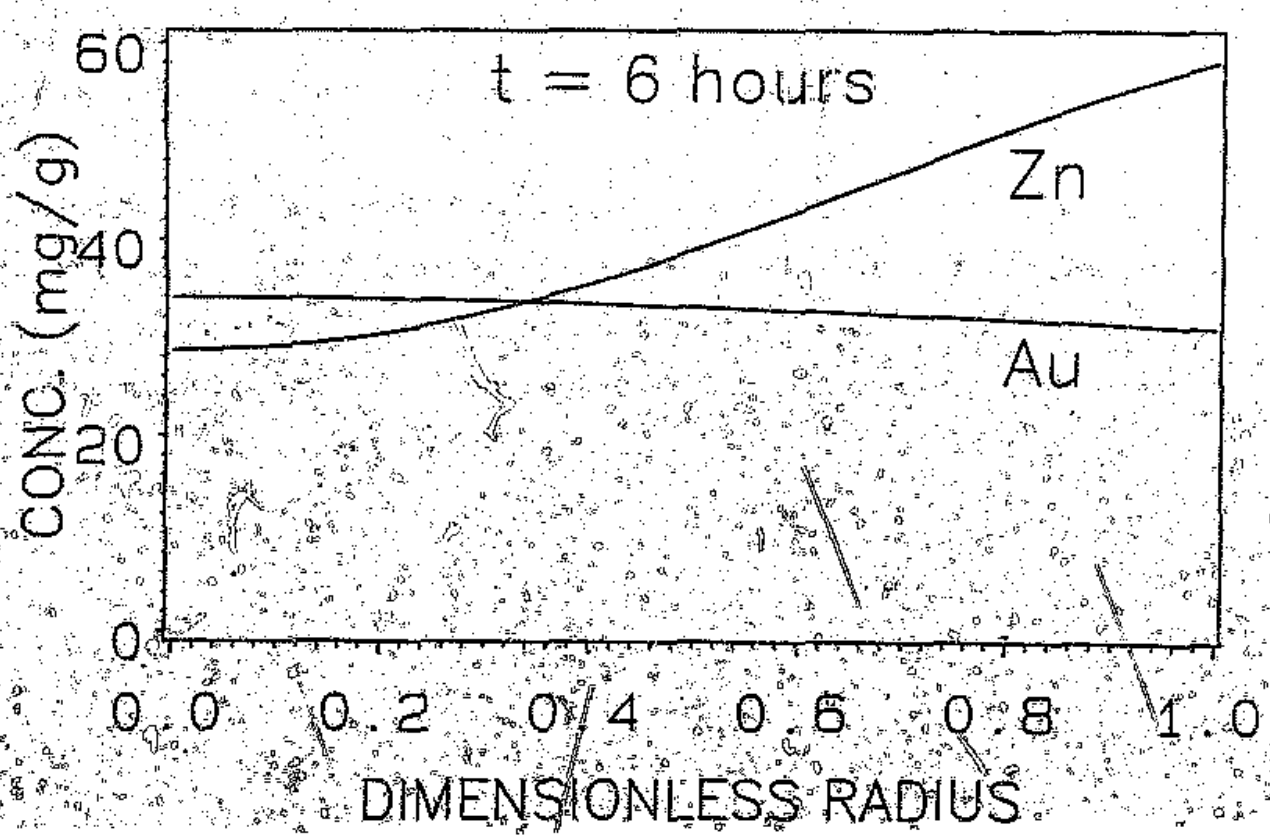

4 EXPERIMENTAL

4.1 PREPARATION OF THE RESIN

The resin is manufactured with chloride ions attached to the quaternary amide functional groups. Since in practice the resin is regenerated after elution with sulphuric acid, it must be converted to the sulphate form. This was done simply by washing the resin beads alternately with dilute sulphuric acid and sodium hydroxide solutions until no chloride ions were found in the sodium hydroxide wash solutions. The beads were then left in dilute sulphuric acid solution overnight after which they were stored under distilled water. The sulphuric acid and sodium hydroxide solution concentrations were each 5% by mass. Silver nitrate solution was used to check for chloride ions in the sodium hydroxide wash solutions.

The resin was then sieved into a series of particle size fractions, as, the smaller the particle size, the higher the rate of adsorption, although particle size has no effect on the equilibrium loading. The resin beads used were in the 0.85 mm to 1.00 mm size range.

The weighing of the resin required a special technique as the characteristics of the resin are damaged if allowed to dry. This method is described by van Vliet, Weber and Hozumi (1980) and involves dewatering the resin beads to a state of being "touch dry" by centrifuging it at 4000 r.p.m. for two minutes in a sintered glass funnel. The moisture contents of the "touch dry" resin was investigated and the results are presented in Appendix 1.

4.2 PREPARATION OF THE SOLUTIONS

There are many factors affecting adsorption that must be eliminated if meaningful estimates of the various mass transfer parameters are to be obtained, these factors are.

(i) Pulp density: An increase in the pulp density reduces the initial rate of loading. This may be due to a decrease in the mixing efficiency as a result of increased apparent viscosity, or due to physical blinding of the pores on the resin by slimes in the pulp. For the experiments only clear solutions are used.

(ii) pH: Fleming and Cromberge (1984) have shown that the pH value of a solution ranging between 2 and 12 has little effect on either the rate of loading or the equilibrium loading on the strong base anion exchange resin IRA 400. Even so the pH of the solutions was mantained at 10,0. For the equilibrium studies this was done simply by adjusting the pH at regular time intervals. For the column studies the head solution was made up to a pH of 10,0 and the pH of the effluent was monitored. It was found that the effluent pH did not drop below 9,5. The pH values of the solutions were attained by the addition of small quantities of sulphuric acid and potassium hydroxide as required.

(iii) Ionic strength and free cyanide level: Fleming and Cromberge (1984) have shown that, for the resin IRA 400, the ionic strength of the solution has little effect on the initial rate of loading. However, a fairly significant effect on the equilibrium loading is noticed. They attribute this to competition between the aurocyanide ion and the other anions present, which in their case was the chloride ion. A free cyanide level of 0,1% Potassium cyanide by mass was chosen as it maintains a high solution ionic strength as well as being a typical level used in industry. By maintaining a high solution ionic strength, small changes in it will have small effects on the adsorption characteristics.

(iv) Temperature: Fleming and Cromberge (1984) have shown that for the resin IRA 400, an increase in temperature supresses the equilibrium capacity of the resin, whilst changes in the initial rates of loading are negligible. The mini-column and isotherm experiments were therefore done in a constant temperature room maintained to within 1^0 C of 25^0 C.

(v) Organics present: It is known that anion exchange resins adsorb organic compounds from aqueous solutions. To what extent and how this affects the adsorption of gold and zinc cyanides onto the resin is unknown. To prevent organics from the leaching of plastics etc, into the system only glass equipment and silicone rubber tubing was used.

(vi) Oxygen content: An increase in the dissolved oxygen content of the solution has little effect on the initial rate of adsorption, however the equilibrium loading is suppressed. In the isotherm studies, the oxygen content of the solutions was maintained by repeatedly opening the stoppered solutions to the atmosphere.

For the single component and binary mini-column adsorption experiments, the gold and zinc head concentrations were chosen to be approximately 10 ppm and 20 ppm respectively. The source of the gold and zinc are $KAu(CN)_2$ and $Zn(CN)_2$ respectively.

4.3 BINARY ADSORPTION ISOTHERM

The isotherm or equilibrium tests were undertaken by contacting different masses of resin with gold and zinc cyanide solutions. The solutions were made as described in Section 3.3, the only difference being that the standard solution concentrations of gold and zinc were higher for the isotherm studies than for the mini-column studies.

The equipment used for the isotherm experiments includes:

(i) 10 x 500 ml stopped glass flasks

(ii) Standard gold and zinc cyanide solutions of approximately 200 ppm each of the metal ion in solution

(iii) Shaker table

The procedure used is as follows:

(i) The desired concentration of gold and zinc cyanide solution is made from the standard gold and zinc solutions.

(ii) 400,00 grams of the solution is weighed and placed into the glass flasks.

(iii) Resin is weighed accurately in the 'touch-dry' state, as described in Appendix 1, and placed into the flasks containing the solution.

(iv) The bottles are sealed and placed into the shaker table which is then set in motion.

(v) Every 24 hours the pH of the solutions are checked and adjusted accordingly with small quantities of potassium hydroxide or sulphuric acid. The flasks are also left open for 1 hour in order to allow the free transport of oxygen to or from the solution.

(vi) The samples are agitated in this manner for one week, after which the metal concentrations in solution are determined using Atomic Absorption Spectroscopy.

(vii) The metal loadings on the resin are determined by mass balance on the solution phase.

The raw data from these tests is tabulated in Appendix 2. The results are presented in Section 5.1.

4.4 MINI-COLUMN EXPERIMENTS

4.4.1 APPARATUS

The experimental apparatus is shown in Figure 4. It consists of a 40 litre glass constant head reservoir in which the gold and zinc cyanide feed solution is stored, a glass control valve used to regulate the flow which is monitored using a rotameter, and the glass adsorption column which contains a packed bed of virgin resin beads. The virgin resin beads are packed between two layers of glass beads of 1 mm diameter, which is approximately the same size as the resin, in order to minimise entrance and exit effects. The inside diameter of the column is 3.60 cm. Bird, Stewart and Lightfoot (1960) suggest an internal column diameter of at least 30 times the particle diameter to prevent excessive wall effects. The height of the resin packing was approximately 2.0 cm.

4.4.2 PROCEDURE

The required solutions of gold and zinc cyanides are made up as described in Section 4.2, the metal concentrations are then accurately measured using Atomic Absorption Spectroscopy. The 40 litres of solution is then pumped up into the constant head reservoir, which is situated approximately 1,5 meters above the column outlet.

The resin is packed into the column between the glass beads (of 1,00 mm diameter) as shown on Figure 4. This is done under distilled water so as to avoid air bubble entrainment in the column. The water level is then reduced to just above the glass bead packing in order to minimise dilution.

The experiment is commenced by opening the control valve, and the flowrate is monitored using the rotameter placed before the column. Samples of the effluent are taken at predetermined time intervals and the gold and zinc metal concentrations are measured using Atomic Absorption Spectroscopy.

Figure 4: Experimental Apparatus

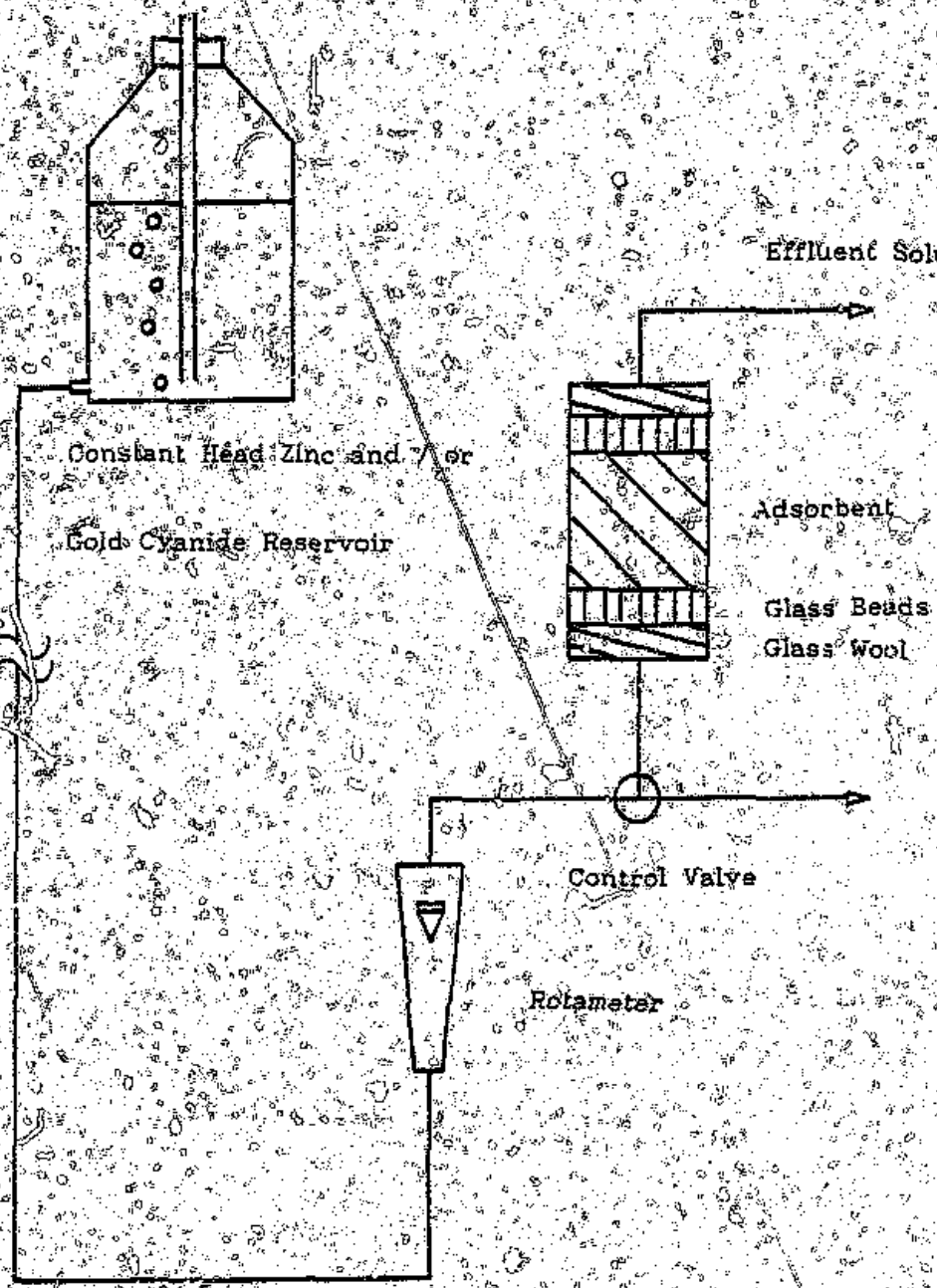

5. RESULTS AND DISCUSSION

5.1 BINARY ISOTHERMS

The fitted Fritz and Schluender binary isotherms relating the equilibria between gold and zinc loadings on the resin to gold and zinc cyanides in solution are given by Equations (5.1.1) and (5.1.2) respectively. These equations were fitted to the experimental data presented in Appendix 2 by minimising the sum of the squared differences between the equation predictions and the experimental data. This is described in detail in Appendix 5.

$$C_{s1} = \frac{87,7876\ C_{c1}^{0,677}}{1 + 0,1624\ C_{c1}^{0,677} + 6,3458\ C_{c2}^{0,385}} \qquad (5.1.1)$$

$$C_{s2} = \frac{213,2535\ C_{c2}^{0,439}}{1 + 0,2526\ C_{c1}^{0,653} + 2,9712\ C_{c2}^{0,439}} \qquad (5.1.2)$$

where: C_s is the solid metal concentration; mg g^{-1}

C_c is the liquid adsorbate concentration; mg l^{-1}

Subscripts 1 and 2 refer to gold and zinc respectively.

The mathematical expressions describe the loading of one species on the resin in the presence of both species in solution. Figures 5.1.1 and 5.1.2 are the 3-dimensional graphical representations of Equations (5.1.1) and (5.1.2) respectively.

The goodness of fit for these equations are represented by Figures 5.1.3 and 5.1.4 where the experimentally measured loading data as presented in Appendix 2 is compared to the loadings predicted by Equations (5.1.1) and (5.1.2). The purpose of the goodness of fit plots is to show how well the experimental results fit the isotherm. If perfect agreement between the experimental results and the isotherm were obtained, all the experimental data would lie on the 45^0 line shown on the figures. It can be seen that the deviations are not large and furthermore are randomly scattered about the 45^0 lines indicating that there are no systematic deviations between the isotherm equations and the experimental results. Equations (5.1.1) and (5.1.2) describe the equilibrium data well.

From Figure 5.1.1, it is clear that the presence of small amounts of zinc cyanide in solution greatly reduce the propensity for gold to be adsorbed on the resin. However, as may be seen from Figure 5.1.2, the presence of gold cyanide in solution hardly influences the loading of zinc on the resin.

FIG. 5.1.1: Binary Isotherm - Gold Equilibrium

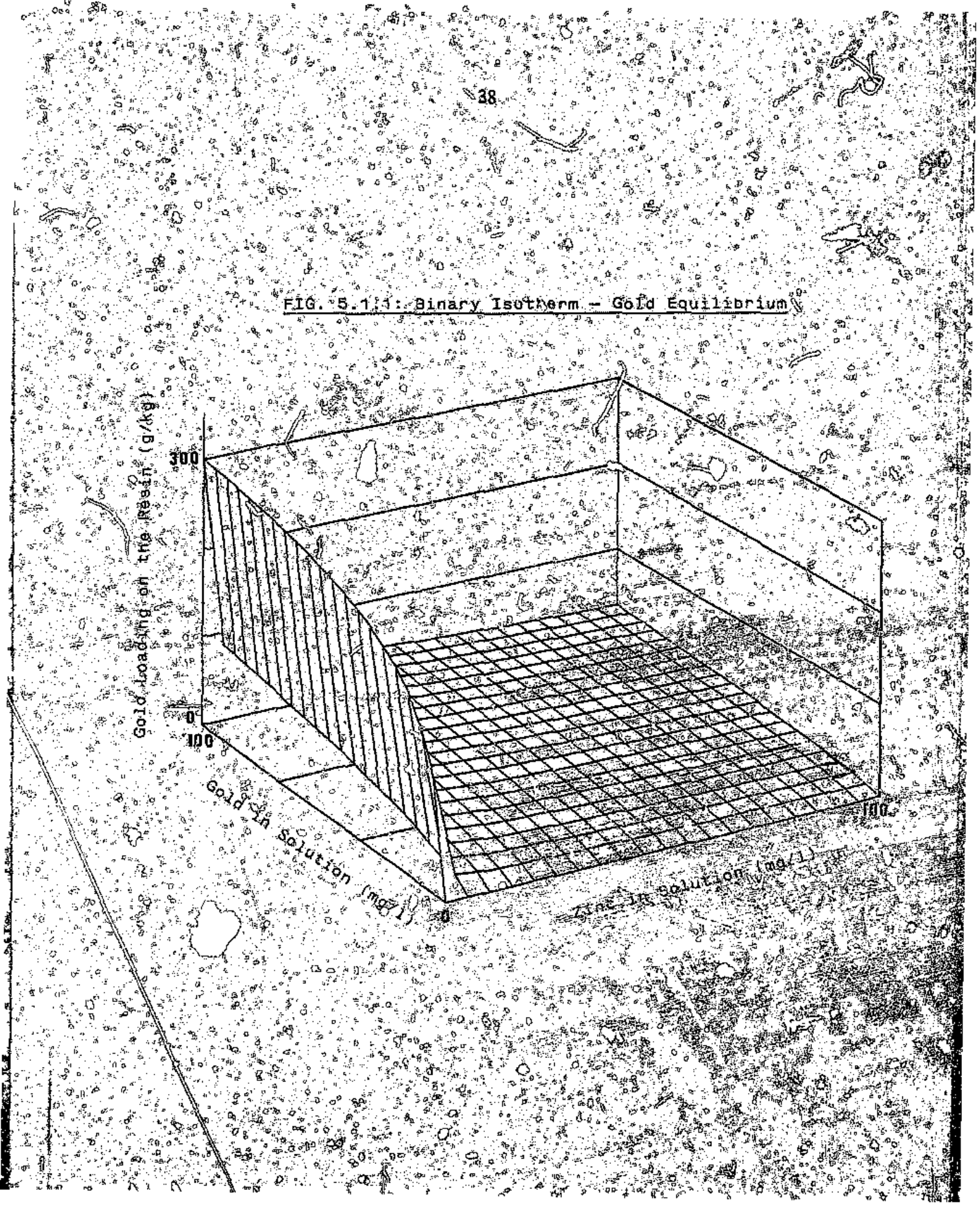

Fig. 5.4.2: Binary Isothem - Zinc Equilibrium

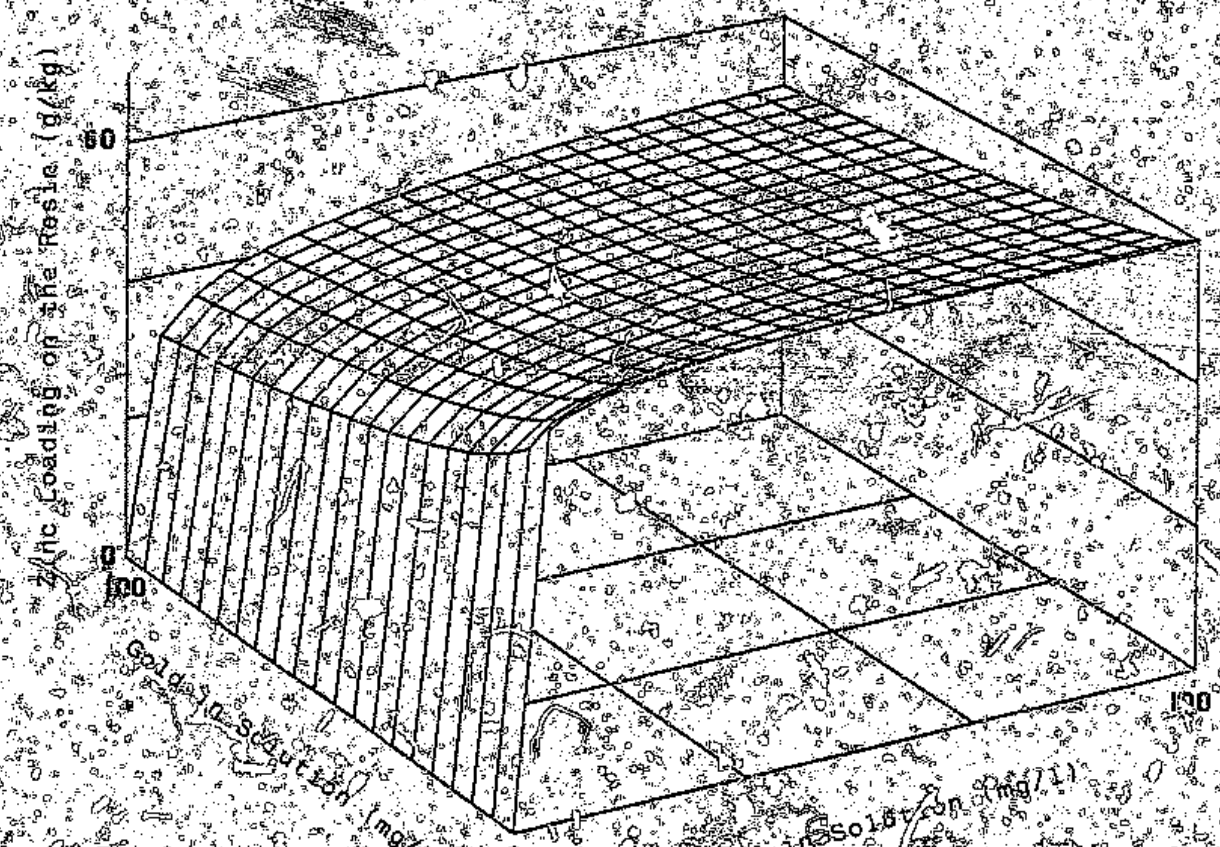

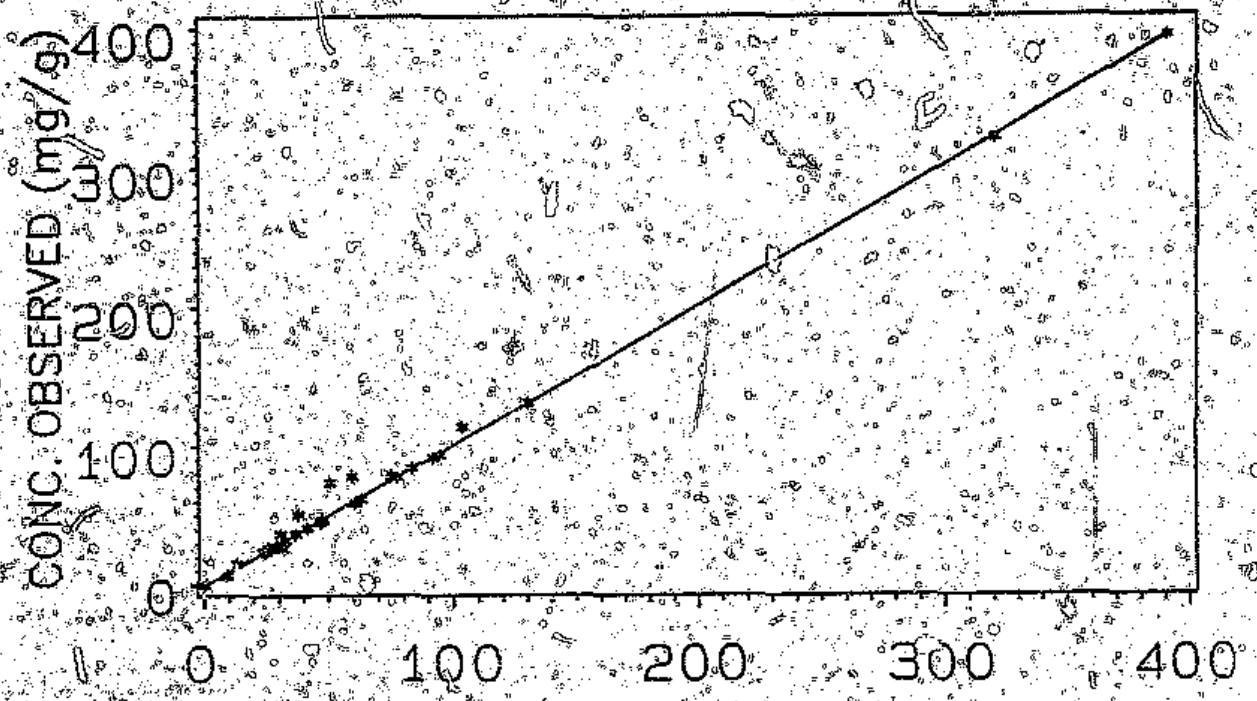

Fig. 5.1.3: Goodness of Fit - Gold Equilibrium

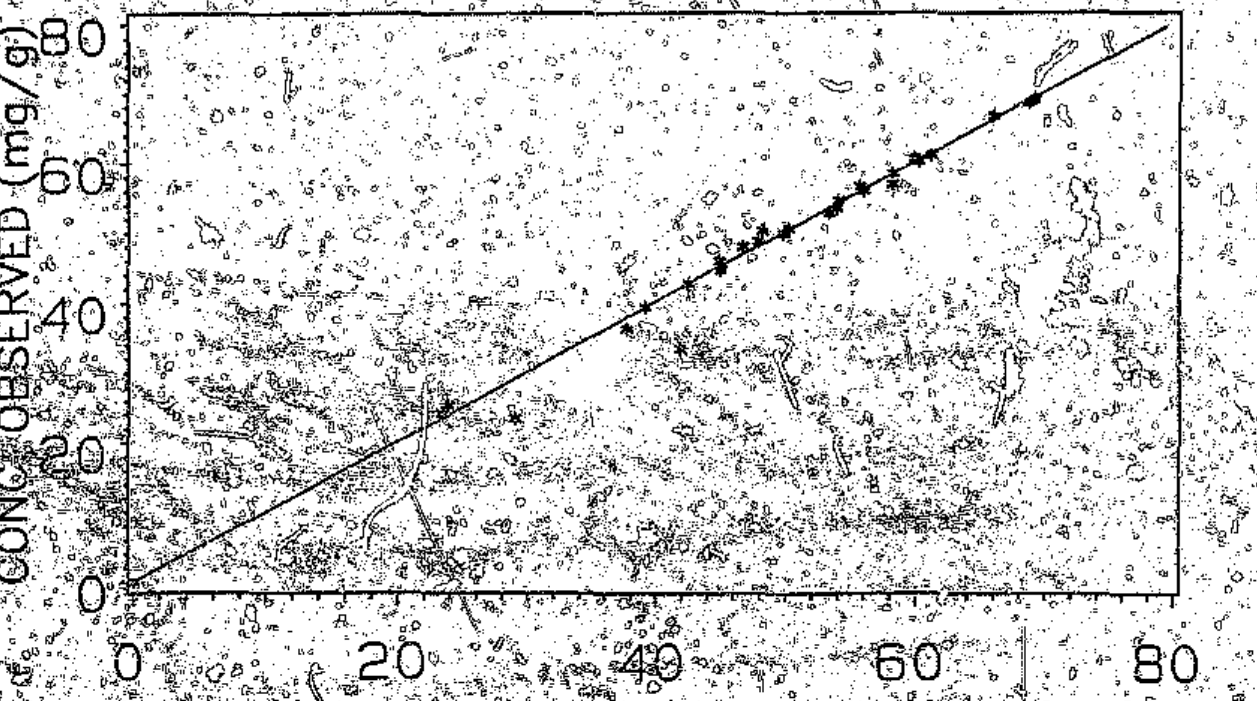

Fig. 5.1.4: Goodness of Fit - Zinc Equilibria

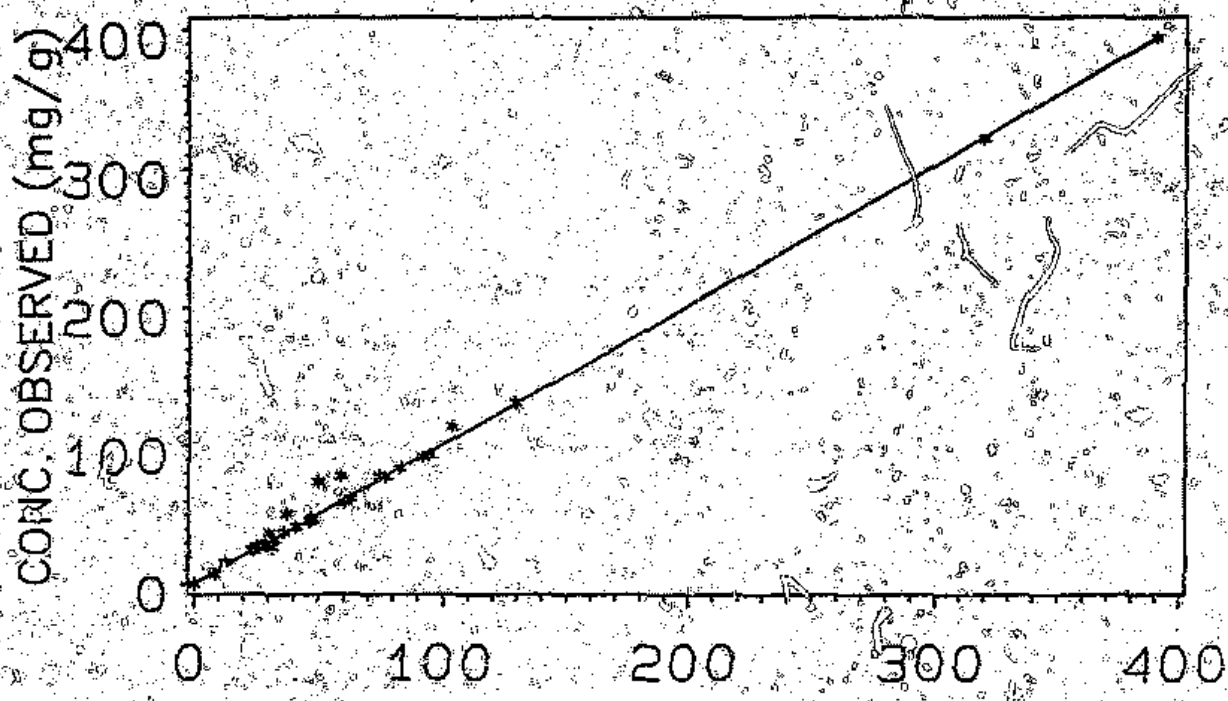

Fig. 5.1.3: Goodness of Fit - Gold Equilibrium

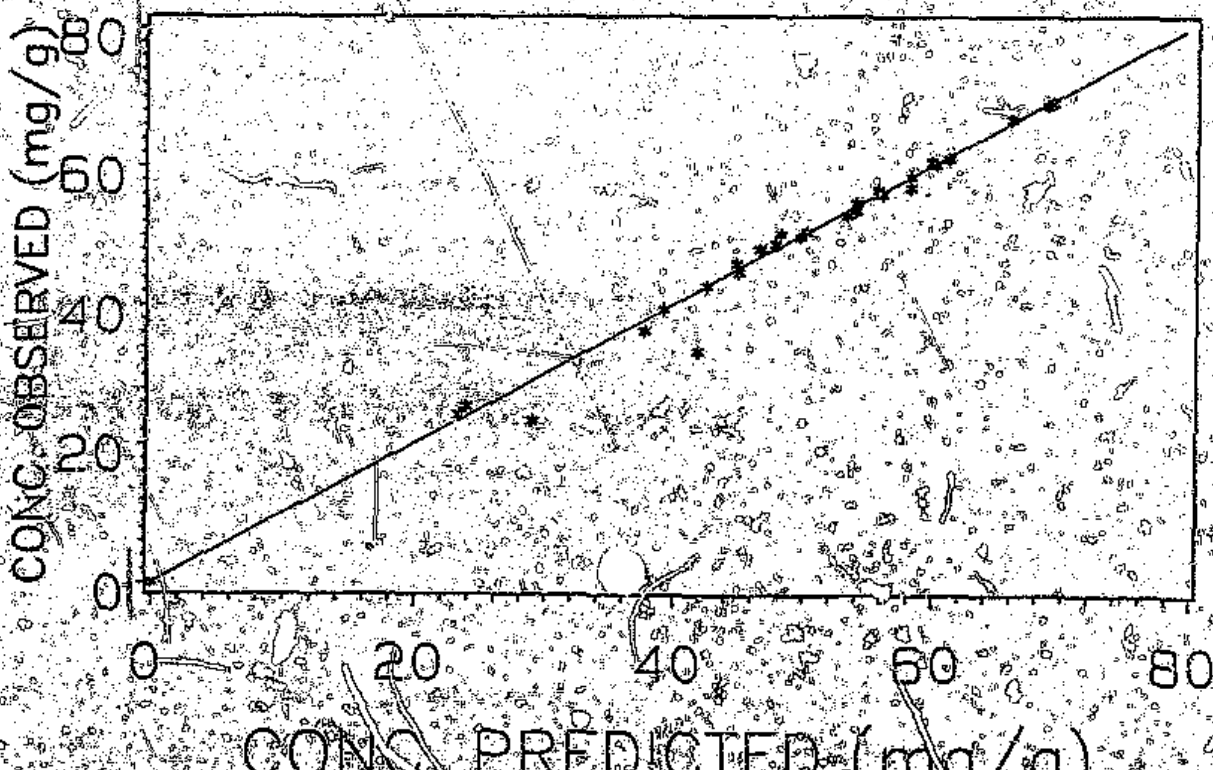

Fig. 5.1.4: Goodness of Fit - Zinc Equilibrium

5.2 MINI–COLUMN ADSORPTION

As described in Section 2.2, the homogeneous surface diffusion model is fitted to the experimental mini–column breakthrough curves by minimising the sum of the squared differences between the experimental results and the model predictions. This is done by minimising the sum of the squared differences between the experimentally measured concentrations and the model predicted concentrations by choice of the two kinetic parameters, namely the film coefficient and the surface diffusion coefficient for each component. The experimental conditions and data are presented in Appendix 7. The model is solved using an adaption of the method of characteristics. This is described in Appendix 4. The FORTRAN programs used to fit the external film and intraparticle surface diffusion coefficients for both the single component and binary adsorption cases are presented in Appendix 6. The program written to solve the single component adsorption model was tested against an existing solution by Weber and Lui (1980). Agreement between the model and the existing solution was obtained. The program written to solve the binary adsorption model was then tested against the single component model by setting each component's inlet concentration in turn, to zero. Agreement was obtained.

Sensitivity analyses of breakthrough curves with respect to the two mass transfer processes are useful indicators of how these parameters influence fixed bed adsorber dynamics. The use of such analyses has been well described by Weber and Lui (1980) who performed sensitivity analyses on an identical model for the adsorption of *para*–bromophenol and dodecylbenzenesulphonate in fixed beds of granular activated carbon. The values of the external film and effective intraparticle surface diffusion mass transfer parameters used for

their analyses are of the same order as those fitted to the experimental breakthrough curves in this study. The conclusions which they drew are hence applicable in this study. These conclusion are:

(1) The initial stage of the breakthrough curve is always dominated by film transfer.

(2) For the same degree of change in the external film and / or surface diffusion coefficients, the response of a mini–column is more sensitive than that of a long column.

Hence if the column is of sufficiently short length so that the incipient breakthrough occurs then the initial stage of the breakthrough curve is dominated by film transfer. Hence the film transfer coefficients may be estimated independently using the initial portion of the mini–column breakthrough curve. This was verified by Young and van Vliet (1987) who performed experiments on the adsorption of phenol onto a number of adsorbates using a mini–column technique. Young and van Vliet (1987) also noted that owing to the practical limitations in the experimental equipment it is not possible to measure the concentrations at very small times and so the determination of the film transfer becomes less accurate at higher Reynolds numbers. They illustrated this point by testing the sensitivity of the model to the film transfer coefficient. The film transfer coefficients are therefore estimated using Equation (2.4.4) given in Section 2.4. The initial effluent concentration was estimated by extrapolating from the experimental data. This approach is valid provided a good estimate of the initial effluent concentration may be obtained. This may not be possible in cases where the initial effluent concentration changes rapidly. Any experimental points taken before about 100 ml of solution had passed through the column were ignored as they were artificially low due to dilution with interstitial water.

The only unknown parameters remaining are the effective surface diffusion coefficients. These, as discussed in Section 2.4, are estimated by minimising the sum of the squared differences between the measured concentrations and the model–predicted concentrations by choice of the diffusion coefficients. As shown by Weber and Liu (1980) the later portion of the breakthrough curve is usually sensitive to the surface diffusion coefficients for reasonable values of the kinetic parameters. This means that good estimates of both kinetic parameters may be obtained from the mini–column experiment. Although the mini–column technique is more difficult to deal with from a mathematical modelling perspective than a batch system, it is attractive because it allows good estimates of the kinetic parameters to be made.

The single component and binary mini–column breakthrough results are presented in Section 5.2.1 and 5.2.2 respectively. The corresponding experimental data and conditions are given in Appendix 7.

5.2.1 SINGLE COMPONENT GOLD ADSORPTION

The fitted mass tranfer parameters for the adsorption of gold cyanide are presented in Table 5.2.1 together with their corresponding Reynolds numbers.

Table 5.2.1: Fitted Film Transfer Parameters for Gold Adsorption

Reynolds Number	$k_f * 10^5$ [m s^{-1}]	$D_s * 10^{12}$ [$m^2 s^{-1}$]
1,49	2,72	2,37
2,60	3,44	2,40
3,94	3,91	2,42
5,16	4,19	2,39
6,48	4,63	2,41

It is clear that the effective surface diffusion coefficient D_s is independent of the Reynolds number. This is consistent with the fact that D_s is a measure of intraparticle diffusion and should be independent. The film transfer coefficient on the other hand is expected to increase with the Reynolds number as predicted by the Williamson *et al* (1963) correlation. This is found to be the case. The experimental breakthrough data points and the corresponding model fits are presented on Figures 5.2.1 to 5.2.5. On the whole the agreement can be seen to be very good. At low Reynolds Numbers, the breakthrough curve is dominated by film transfer,

and as the Reynolds Number increases, the period of film transfer domination decreases. This is illustrated on Figure 5.2.6 where the sensitivity of the model to the film coefficient is shown. It is noted that the model is least sensitive to the film coefficient when the Reynolds number is high. The present results are well within the region of accuracy of the method since the model curves are still sensitive to the film coefficient.

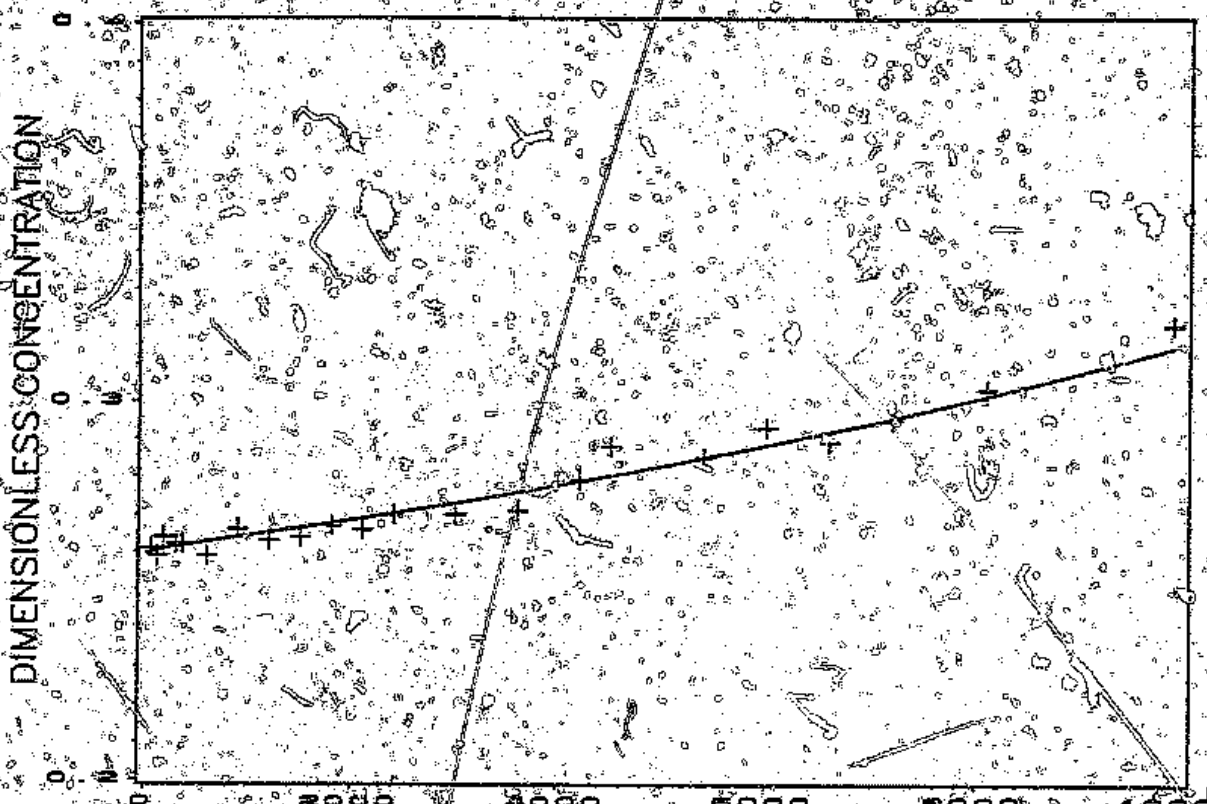

Fig. 5.2.1: Gold Cyanide Breakthrough Curve, Re = 1.49

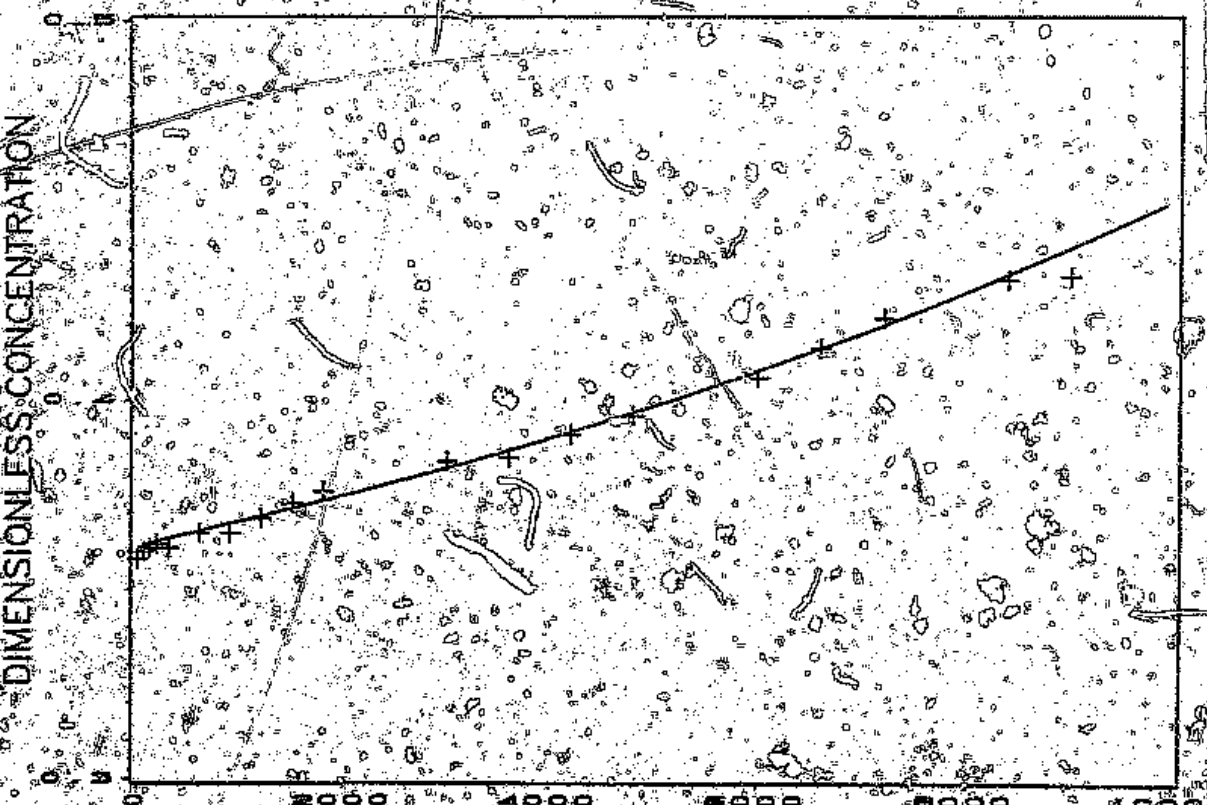

Fig. 5.2.2: Gold Cyanide Breakthrough Curve, Re = 2.60

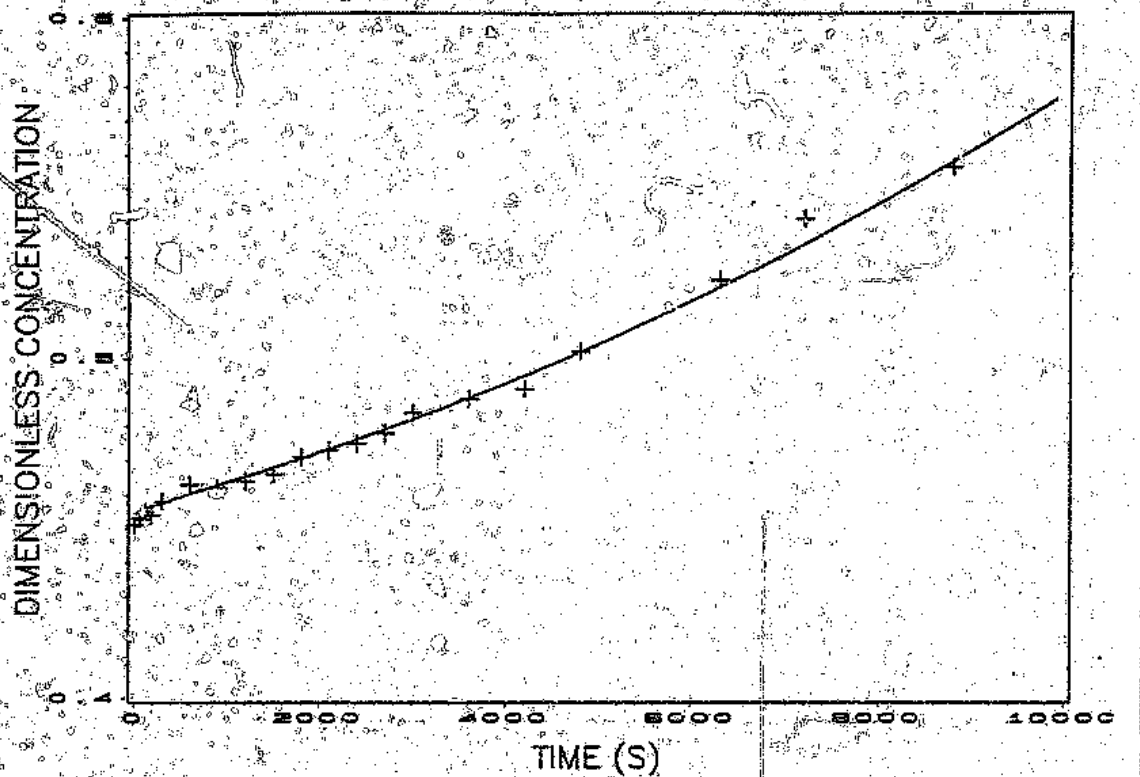

Fig. 5.2.3: Gold Cyanide Breakthrough Curve, Re = 3,94

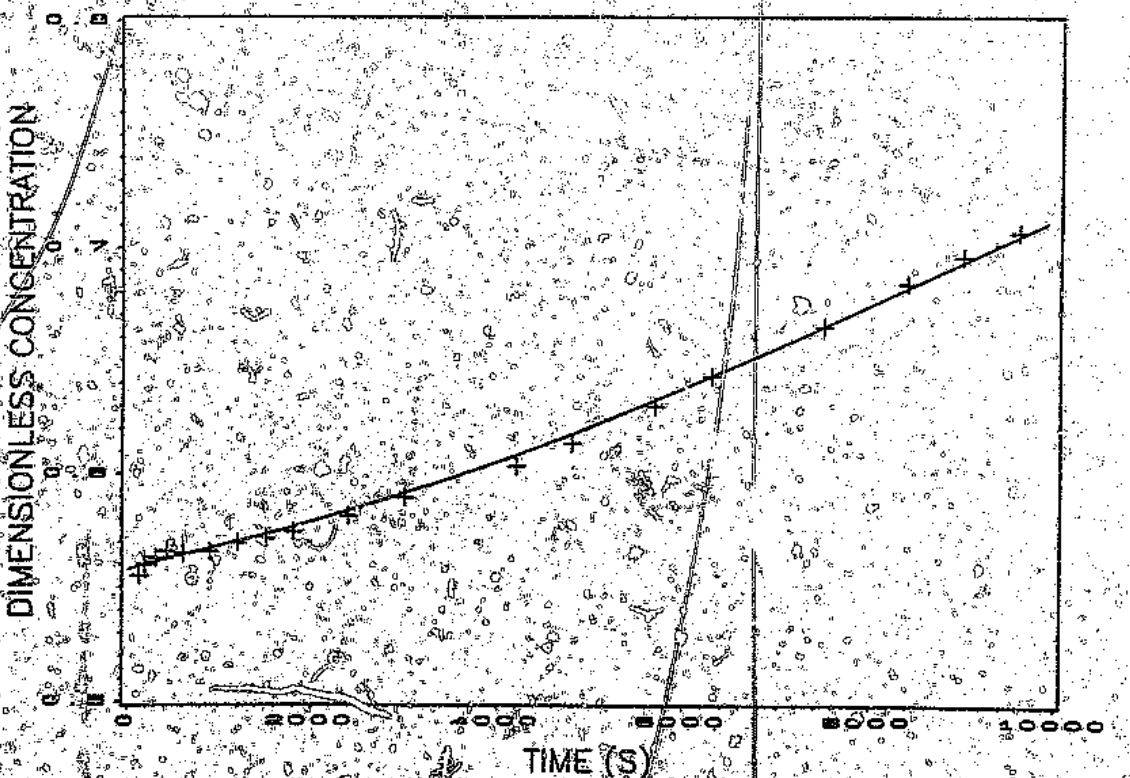

Fig. 5.2.4: Gold Cyanide Breakthrough Curve, Re = 5,16

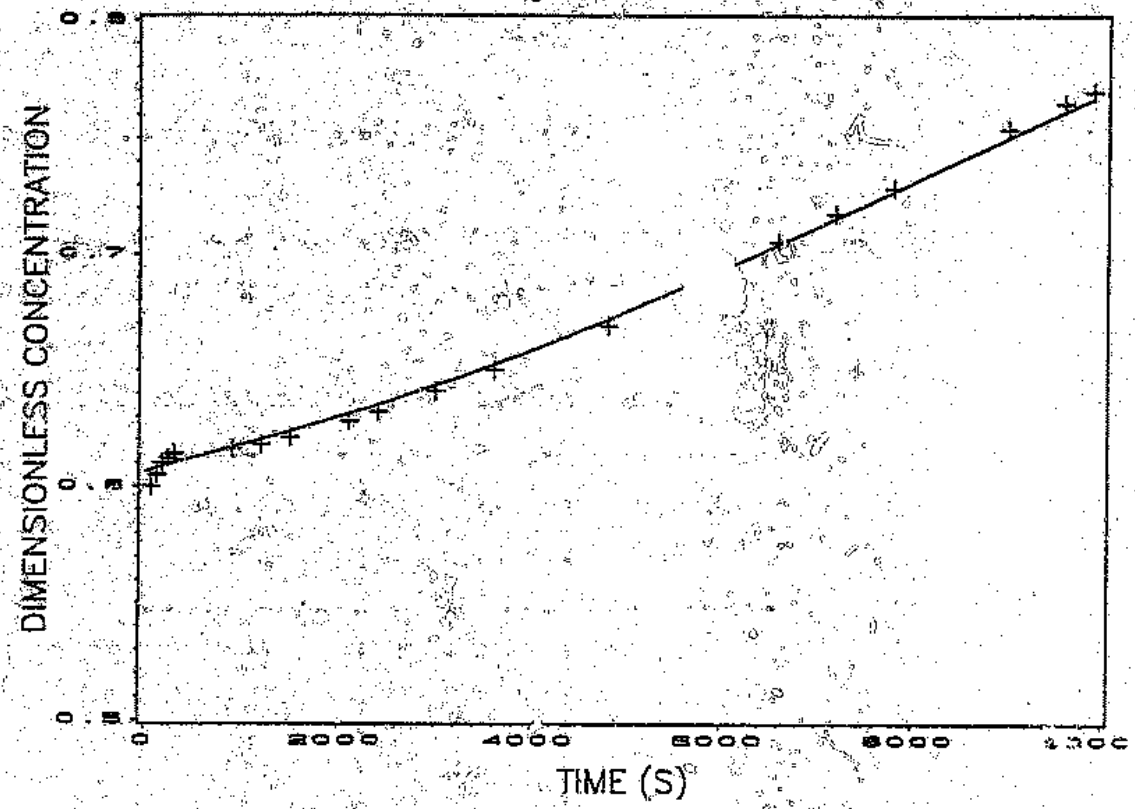

Fig. 5.2.5: Gold Cyanide Breakthrough Curve, Re = 6,48

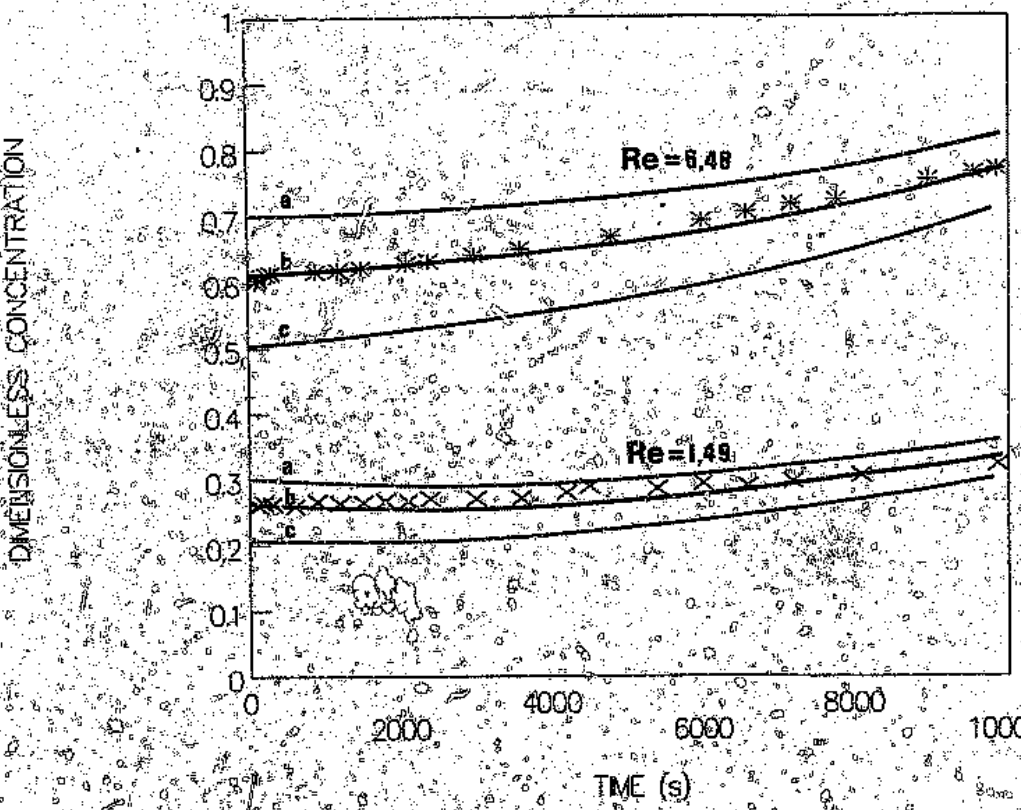

Figure 5.2.6: Film Thanswer Sensitivity Analysis
a = K_f + 50%, b = k_f, c = k_f - 50%

5.2.2 SINGLE COMPONENT ZINC ADSORPTION

The fitted mass tranfer parameters for the adsorption of zinc cyanide are presented in Table 5.2.2 together with their corresponding Reynolds numbers.

Table 5.2.2: Fitted Film Transfer Parameters for Zinc Adsorption

Reynolds Number	$k_f * 10^5$ [m s^{-1}]	$D_s * 10^{12}$ [$m^2 s^{-1}$]
1,49	2,45	1,64
2,60	3,05	1,57
3,94	3,51	1,60
5,16	3,99	1,59
6,48	4,06	1,62

It is clear that the effective surface diffusion coefficient D_s is independent of the Reynolds number. This is consistent with the fact that D_s is a measure of intraparticle diffusion and should be independent. The film transfer coefficient on the other hand is expected to increase with the Reynolds number as predicted by the Williamson *et al* (1963) correlation. This is found to be the case. The experimental breakthrough data points and the corresponding model fits are presented on Figures 5.2.7 to 5.2.11. On the whole the agreement can be seen to be very good. At low Reynolds Numbers, the breakthrough curve is dominated by film transfer,

and as the Reynolds Number increases, the period of film transfer domination decreases. This is illustrated on Figure 5.2.12 where the sensitivity of the model to the film coeffic... shown. It is noted that the model is least sensitive to the film coefficient when the Reyn... number is high. The present results are well within the region of accuracy of the method since the model curves are still sensitive to the film coefficient.

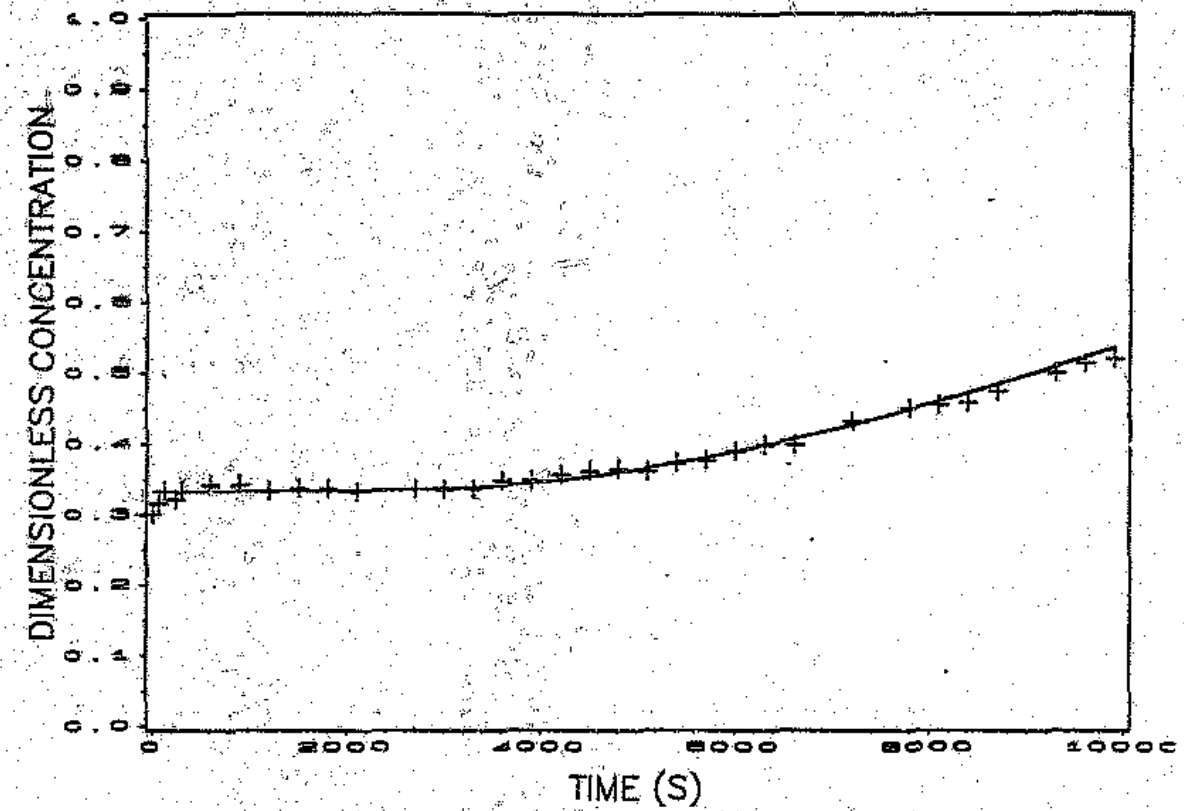

Fig. 5.2.7: Zinc Cyanide Breakthrough Curve, Re = 1,49

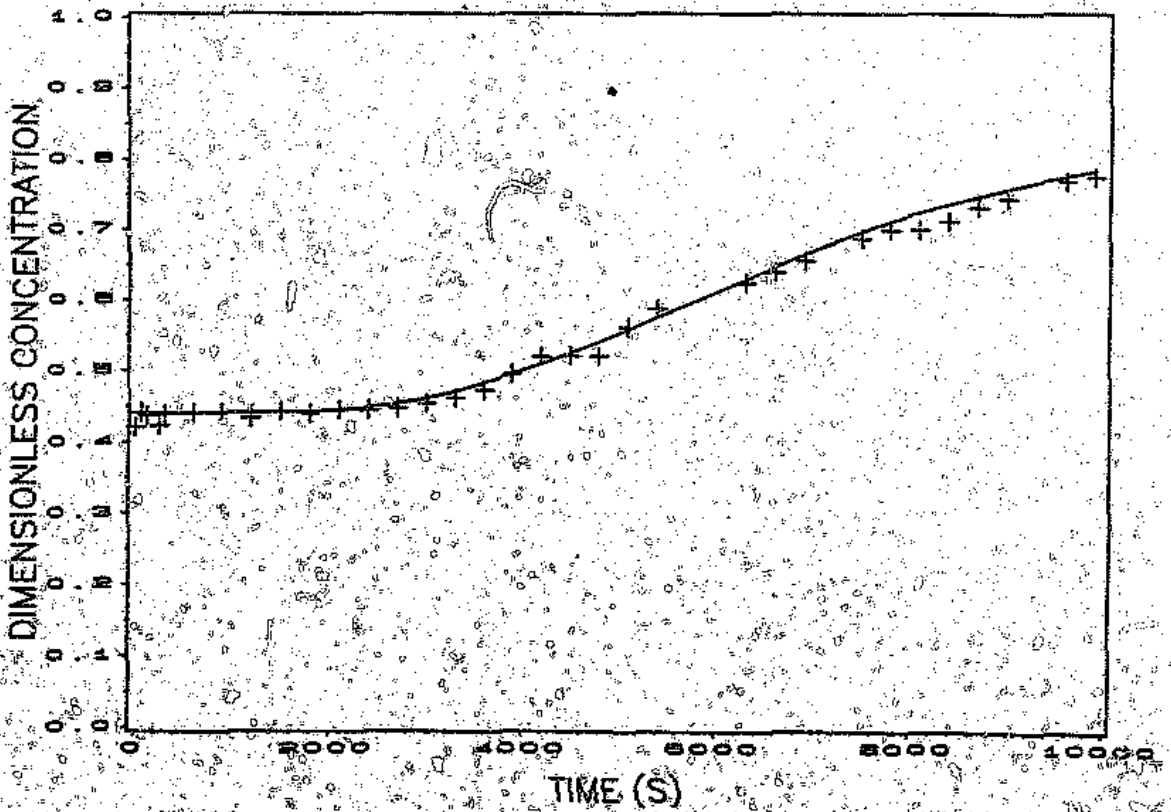

Fig. 5.2.8: Zinc Cyanide Breakthrough Curve, Re = 2,60

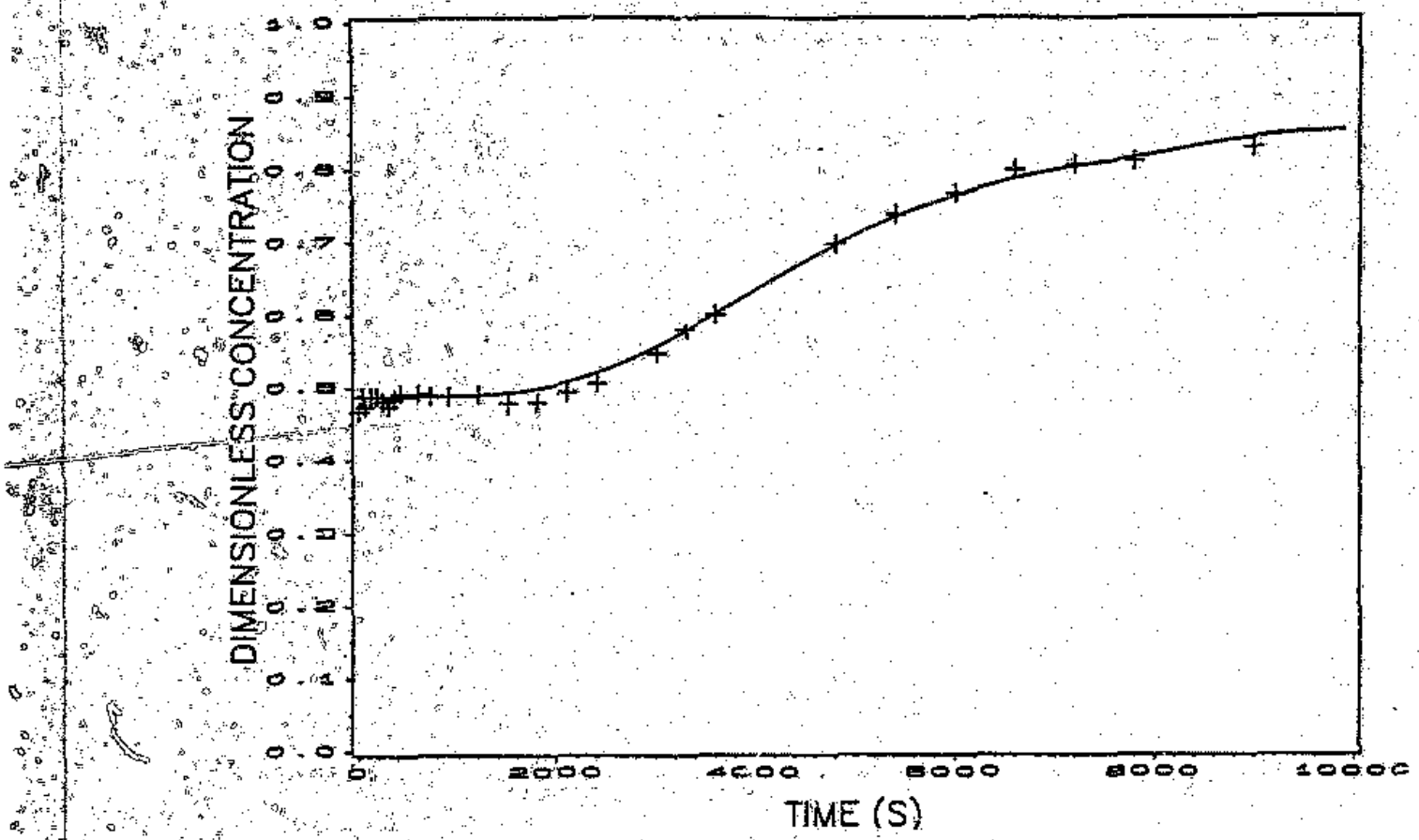

Fig. 5.2.9: Zinc Cyanide Breakthrough Curve, Re = 3,94

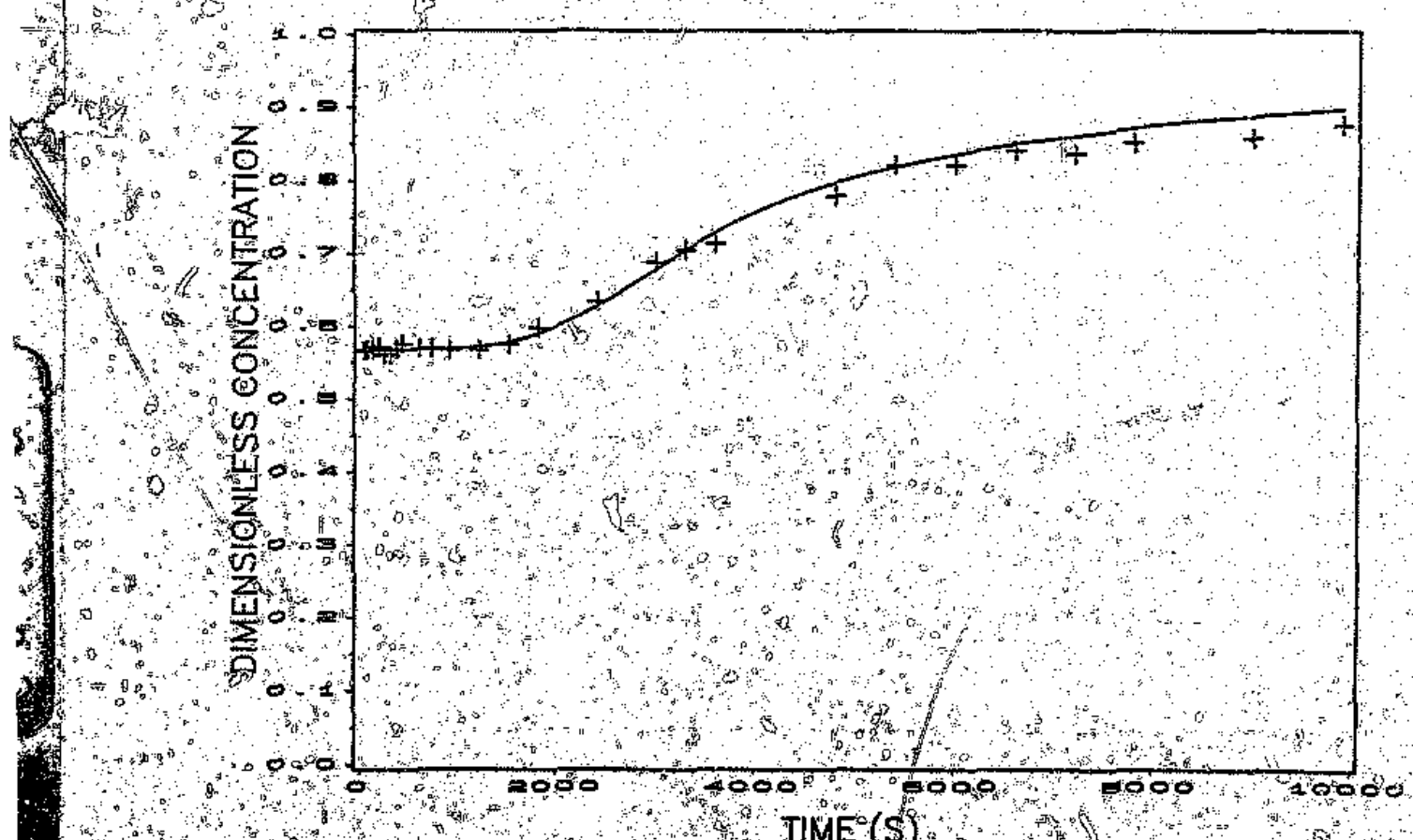

Fig. 5.2.10: Zinc Cyanide Breakthrough Curve Re = 5,16

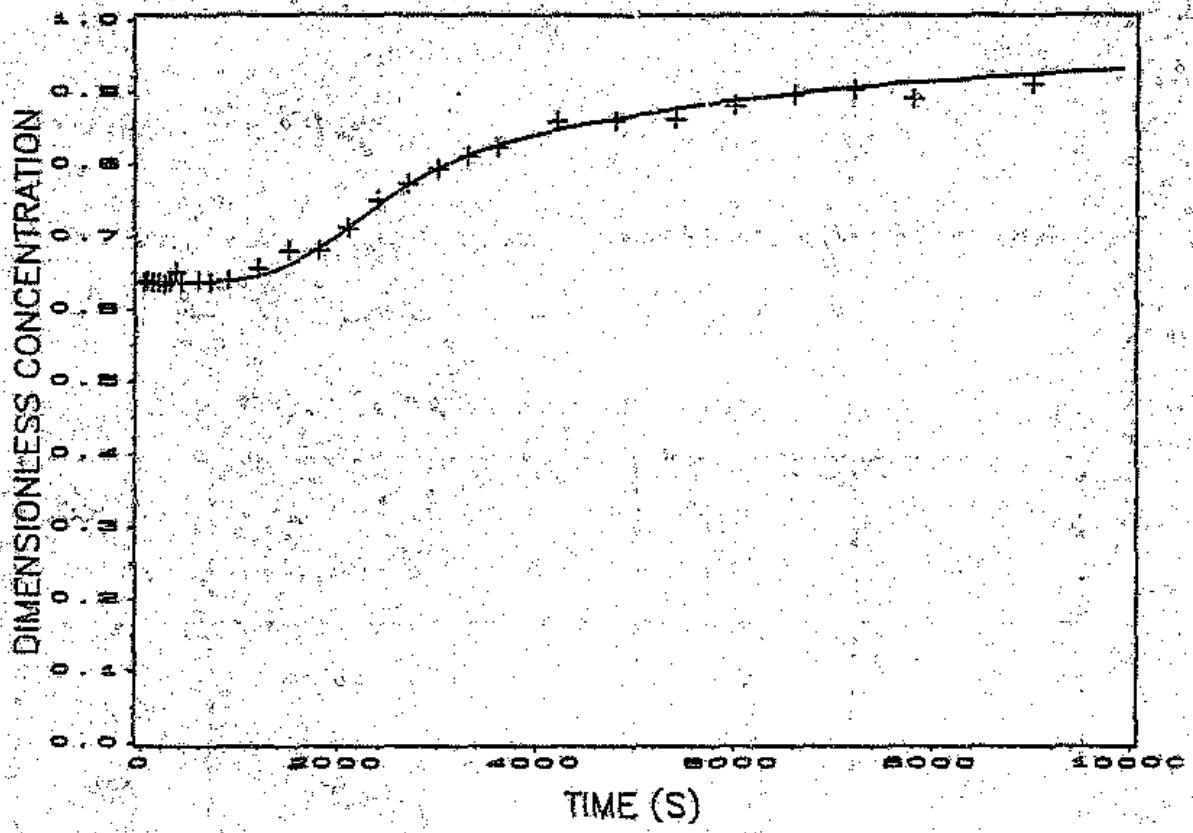

Fig. 5.2.11: Zinc Cyanide Breakthrough Curve, Re = 6,48

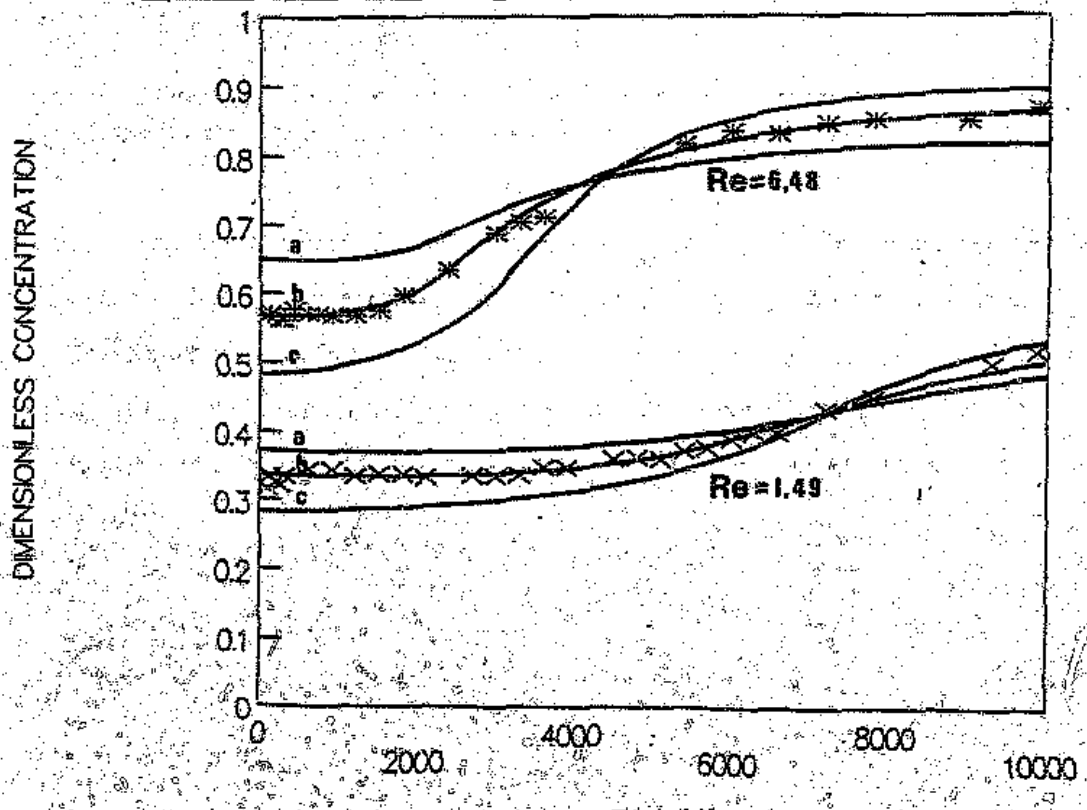

Figure 5.2.12: Film Transfer Sensitivity Analysis
a = k_f + 50%, b = k_f, c = k_f - 50%

5.2.3 BINARY ADSORPTION

The fitted mass tranfer parameters for the simultaneous adsorption of gold and zinc cyanides are presented in Table 5.2.3.

Table 5.2.3: Fitted Film Transfer Parameters for Binary Adsorption

Reynolds Number	$k_{f1} * 10^5$ [m s^{-1}]	$k_{f2} * 10^5$ [m s^{-1}]	$D_{s1} * 10^{12}$ [$m^2 s^{-1}$]	$D_{s2} * 10^{12}$ [$m^2 s^{-1}$]
1,49	2,70	2,44	2,29	1,51
2,60	2,98	2,77	2,28	1,44
3.94	3,58	3,20	2,24	1,50
5,16	3,82	3,69	2,25	1,49
6,48	4,56	3,47	2,31	1,53

Subscripts 1, and 2 refer to gold and zinc respectively.

It is clear that the effective surface diffusion coefficients D_{s1} and D_{s2} are independent of the Reynolds number. This is consistent with the fact that D_{s1} and D_{s2} are measures of the intraparticle diffusion and should be independent of the Reynolds number. The experimental breakthrough data points and the corresponding model fits are presented on Figures 5.2.13 to 5.2.17. As in the single component adsorption studies the agreement can be seen to be very good.

When comparing the binary and single component surface diffusion coefficients obtained it is noted that those obtained for the binary studies are slightly lower for both gold and zinc cyanide than those for the single component studies. This suggests that there is only a small degree of interaction between the intraparticle diffusion coefficients for gold and zinc. This means that the assumption that the gold and zinc intraparticle diffusion coefficients are independent is reasonable. It is also worth noting that the film coefficients are similar, this is to be expected since the only difference in the transfer coefficients will be due to the free liquid diffusivities of gold and zinc cyanides being supressed in the binary system. All these factors are extremely encouraging since it suggests that the mass transfer parameters are not only independent from each other, but they are also good measures of both the external film transfer and intraparticle diffusion mechanisms. In fact the interactions between zinc and gold cyanides are explained by the nature of the isotherm. The fact that small amounts of zinc have a negative effect on gold adsorption is sufficient to satisfactorily explain the results.

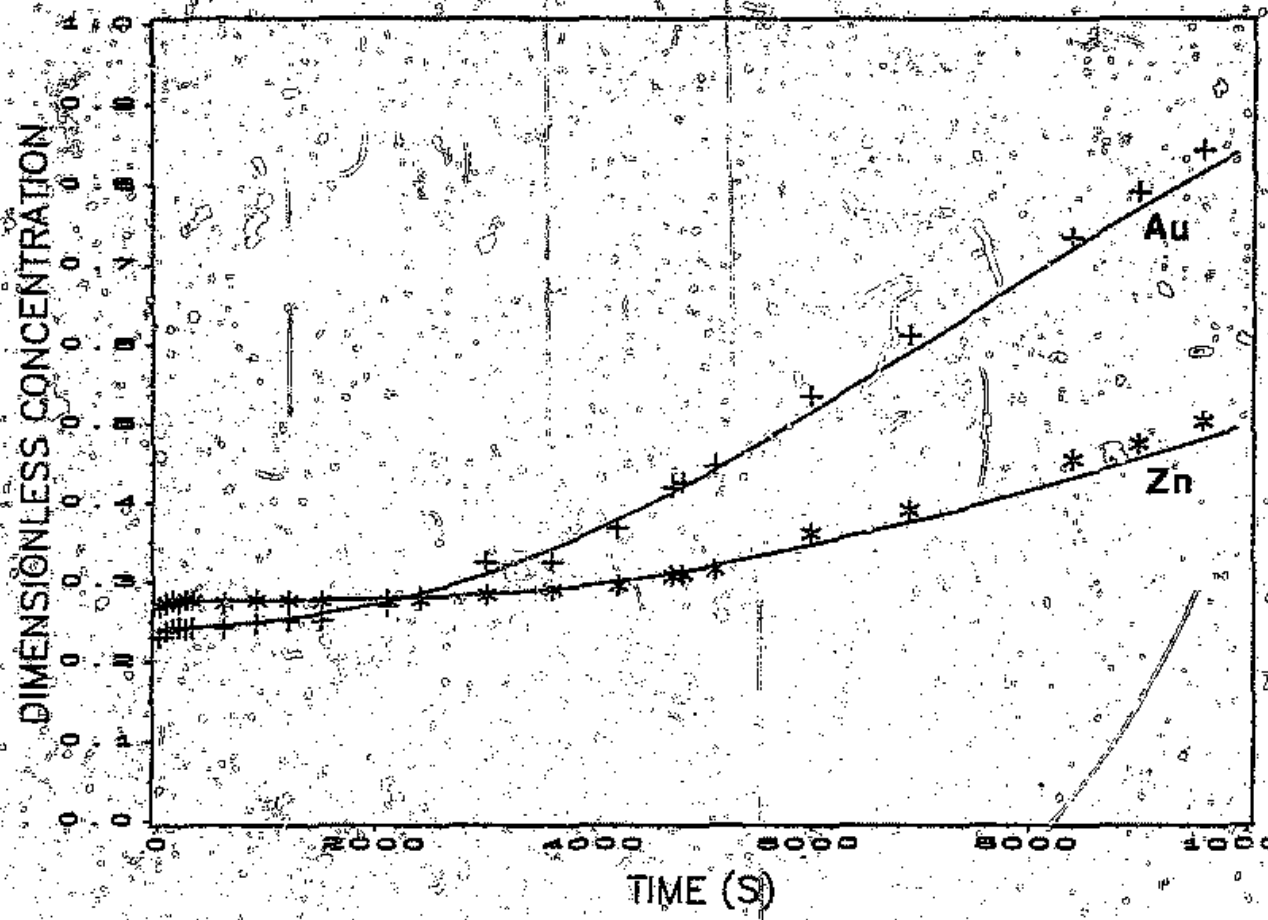

Fig. 5.2.13: Binary Adsorption Breakthrough Curve, Re = 1.49

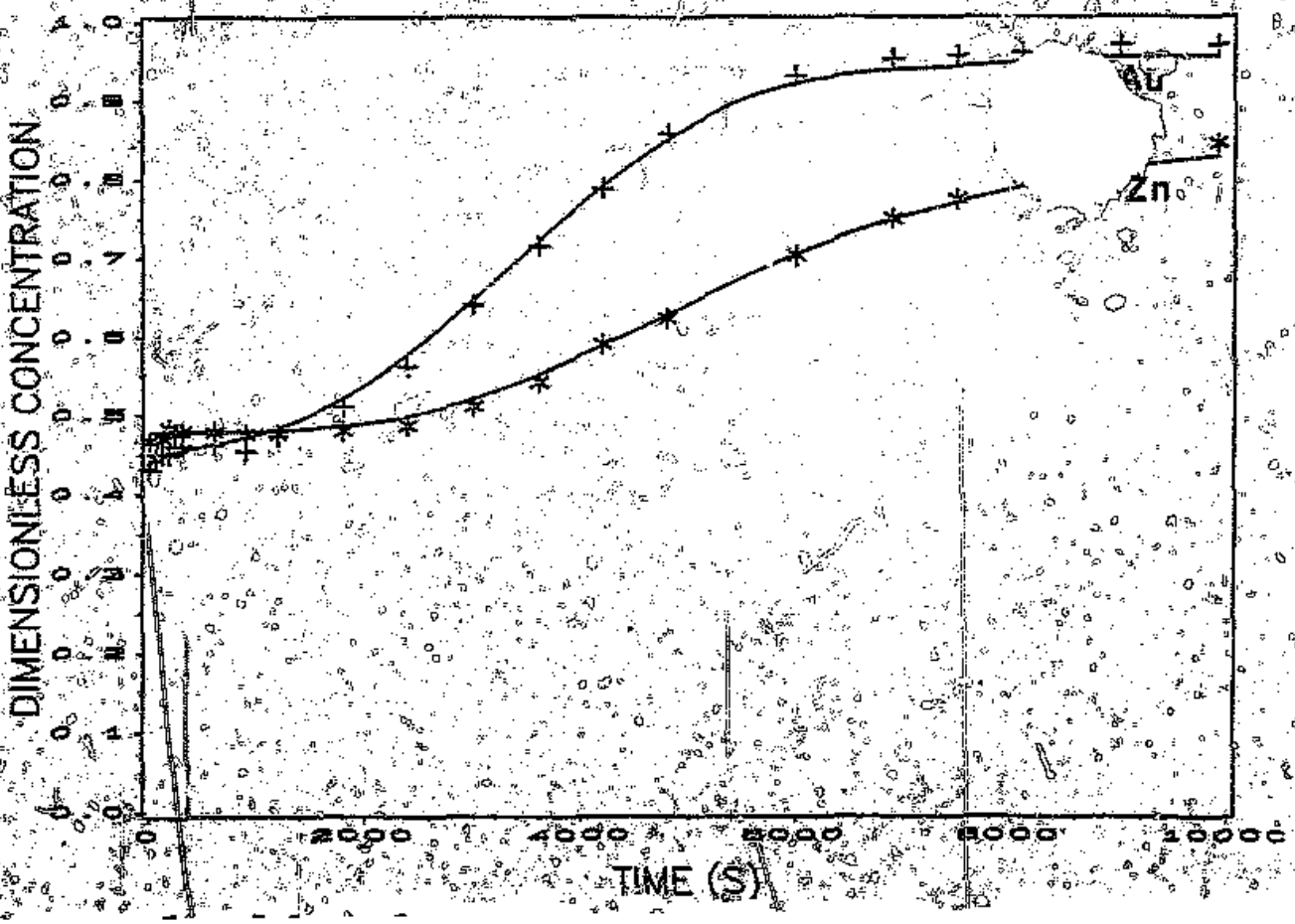

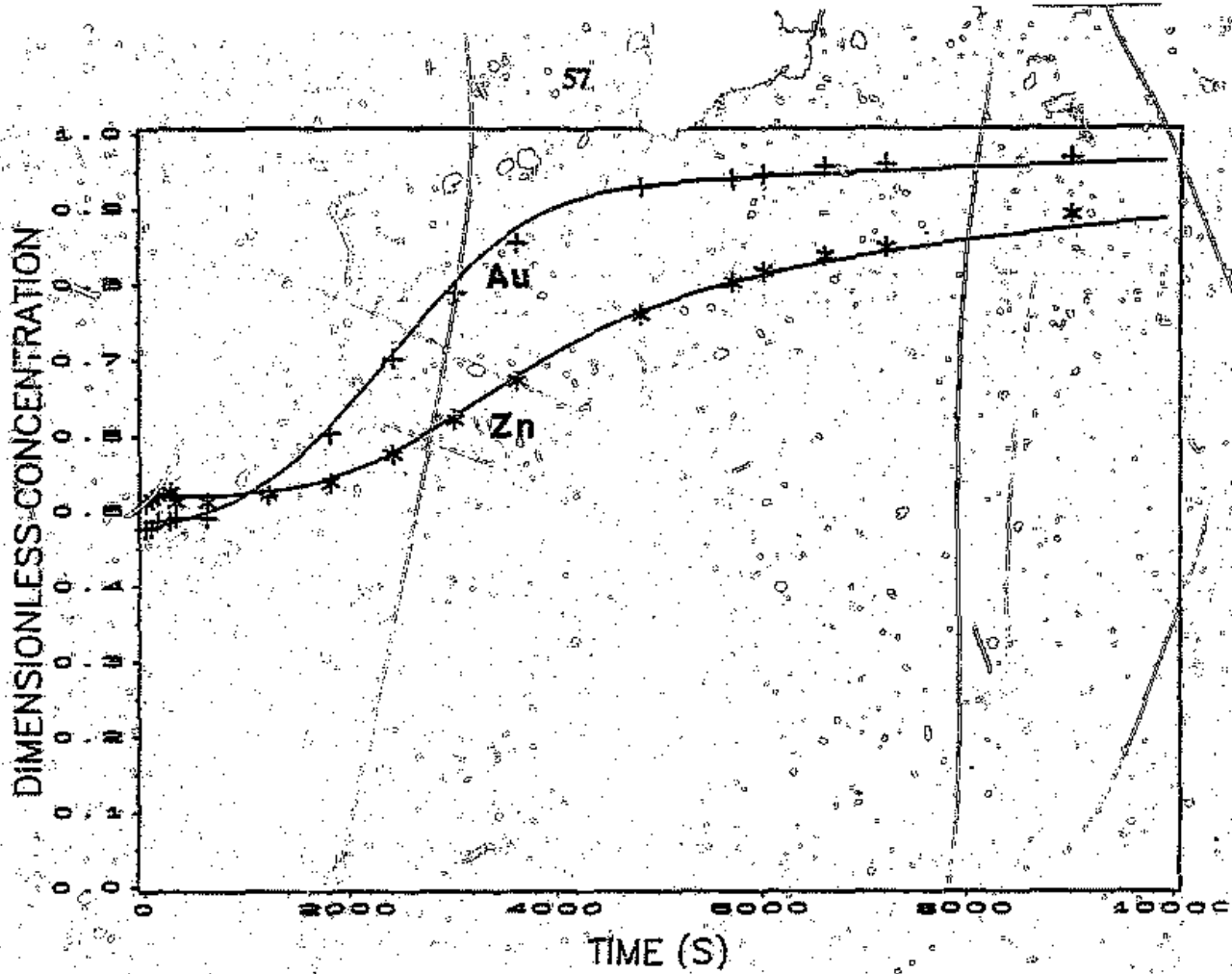

Fig. 5.2.15: Binary Adsorption Breakthrough Curve, Re = 3,94

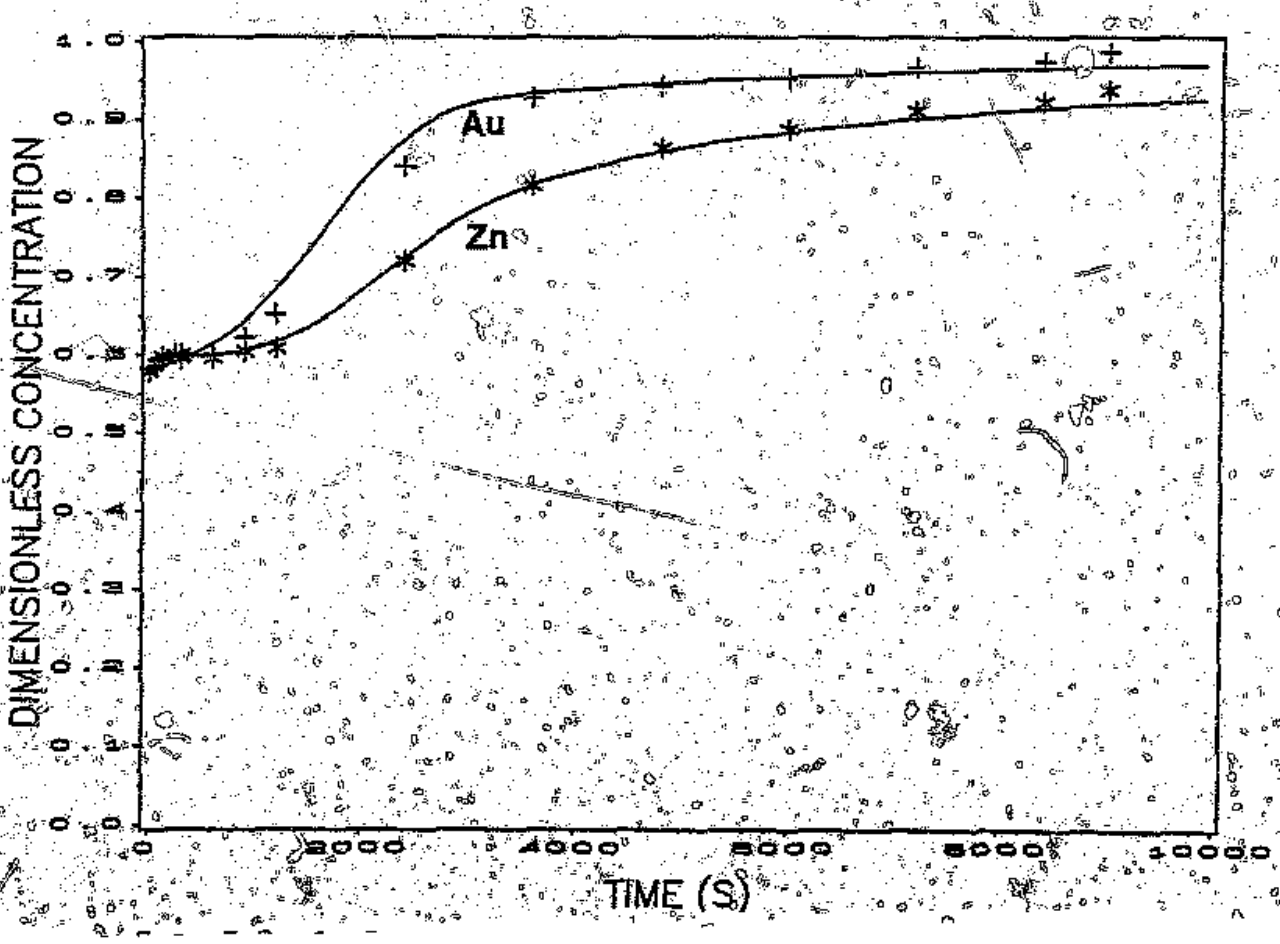

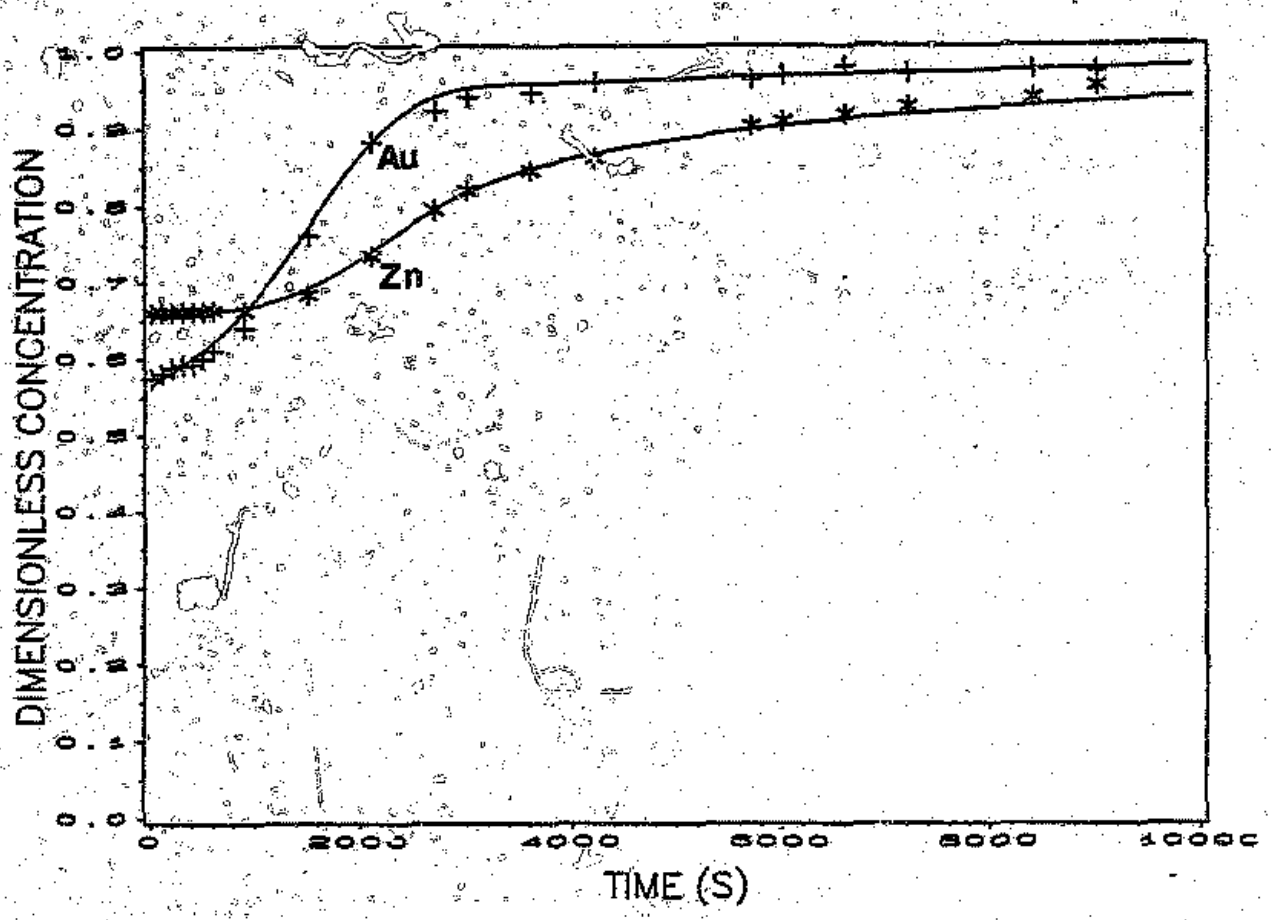

Fig. 5.2.17: Binary Adsorption Breakthrough Curve, Re = 5,48

5.3. FILM TRANSFER CORRELATION

As presented in Section 5.2, the film transfer coefficients as fitted to the mini-column experimental breakthrough curves are consolidated on Table 5.3 together with their corresponding Reynolds numbers, where subscripts 1 and 2 refer to gold and zinc cyanides respectively.

Table 6.3: Experimental Film Transfer Coefficients

System	Reynolds Number	$k_{f1} * 10^5$ [m s^{-1}]	$k_{f2} * 10^5$ [m s^{-1}]
Au	1,49	2,72	—
Au	2,60	3,44	—
Au	3,94	3,91	—
Au	5,16	4,19	—
Au	6,48	4,63	—
Zn	1,49	—	2,45
Zn	2,60	—	3,05
Zn	3,94	—	3,51
Zn	5,16	—	3,99
Zn	6,48	—	4,06
Au/Zn	1,49	2,70	2,44
Au/Zn	2,60	2,98	2,77
Au/Zn	3,94	3,58	3,20
Au/Zn	5,16	3,82	3,69
Au/Zn	6,48	4,56	3,47

As discussed in Section 2.5, there are no literature values for the free liquid diffusivities of gold and zinc cyanides, and hence the Sherwood and Schmidt numbers are unable to be evaluated. The purpose of this section is to provide a suitable expression from which the film transfer coefficients may be estimated. As described in Section 2.5, the correlation described by Williamson *et al* (1963) is assumed to describe the system adequately. The correlation is fitted to the experimental results presented in Table 5.3.1 by minimising the sum of the differences squared between the experimental results and the correlation predictions using the free liquid diffusivities as the fitting parameters. The fitted free liquid diffusivities are presented in Table 5.3.2.

Table 5.3.2 : Fitted Free Liquid Diffusivities

System	$D_1 * 10^{10}$ [m^2s^{-1}]	$D_2 * 10^{10}$ [m^2s^{-1}]
Au	8,38	–
Zn	–	6,96
Au/Zn	7,19	5,93

Subscripts 1, and 2 refer to gold and zinc cyanides respectively

It is interesting to note for gold and zinc cyanide, that the fitted free liquid diffusivities for the binary adsorption studies are approximately 85 % of those for the single component adsorption studies. Indeed it is expected that the presence of a second species will supress the free liquid diffusivity of the first species.

Using these fitted free liquid diffusivities, the correlations are compared with the experimental results on Figure 5.3. It is clear from this figure that the fitted correlations describe the experimental data well. It can be seen that the deviations are not large and furthermore are randomly scattered about the correlation predictions. This indicates no systematic deviation between the correlation and the experimental results.

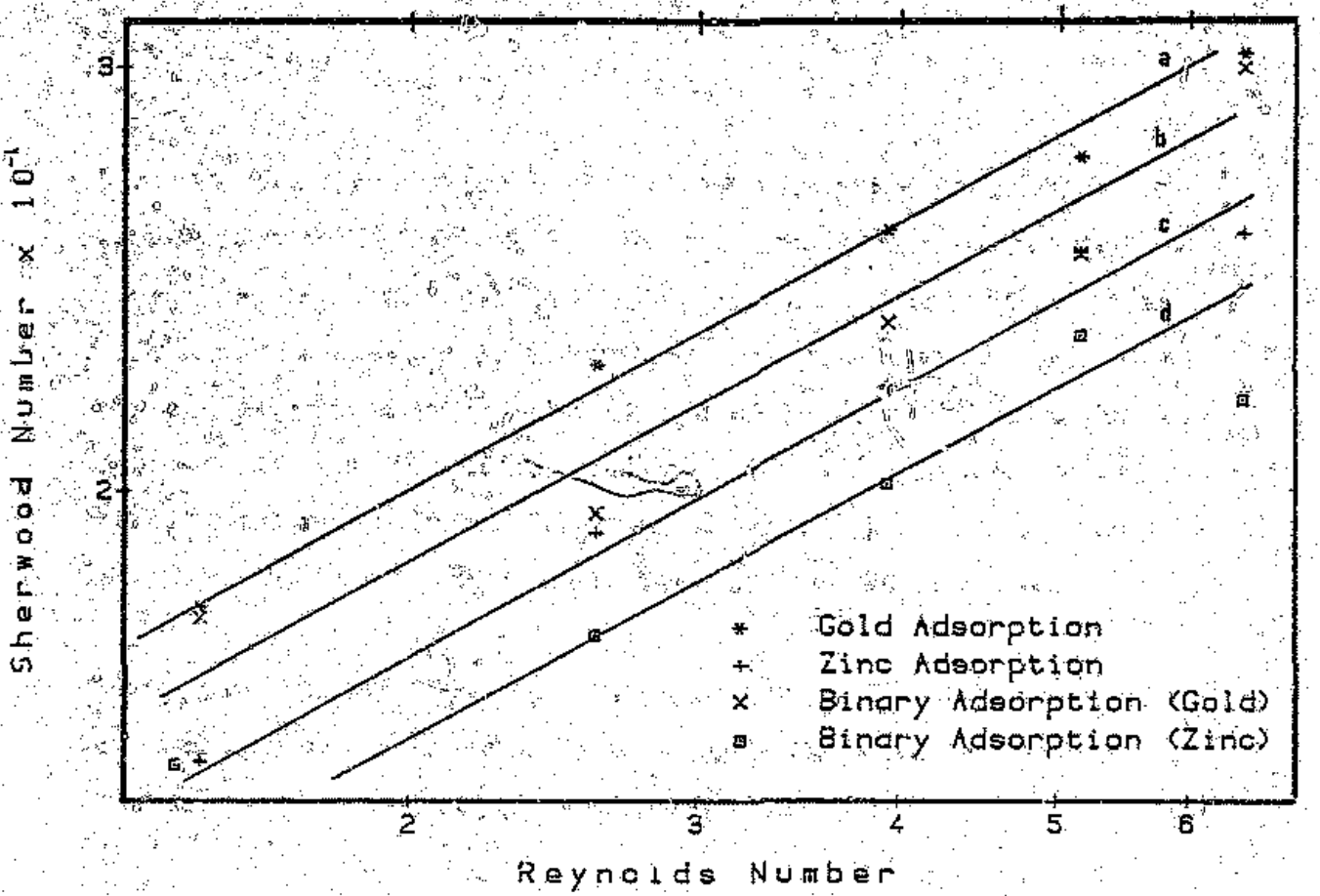

Fig. 5.3: Film Transfer Coefficient Correlation

a - Single Component Gold Adsorption Correlation

b - Binary Adsorption Correlation (Gold)

c - Single Component Zinc Correlation

d - Binary Adsorption Correlation (Zinc)

6. CONCLUSIONS

In this work the homogeneous surface diffusion model with external film transfer has been sucessfully solved for the binary adsorption of gold and zinc cyanides onto the strong-base anion exchange resin Duolite A161 in a mini-column system. The values for the mass transfer parameters obtained for the single component adsorption studies are similar to those obtained for the binary adsorption studies. Also the effective intraparticle surface diffusion coefficients are found to be independent of the Reynolds number. This is consistent with a measure of intraparticle diffusion. Furthermore the measured film coefficients display a dependence on the Reynolds number that is consistent with an existing correlation.

The empirical Fritz and Schluender (1974) binary isotherm relationship was found to mathematically fit the experimental equilibrium data well. The 3-dimensional isotherm plots illustrated the elution properties of zinc cyanide over gold cyanide.

The external film transfer was able to be adequately correlated to the Williamson *et al* (1963) relationship by choice of suitable values of the free liquid diffusivities.

The characteristics of the homogeneous surface diffusion model with external film tarnsfer were illustated by "semi-quantitatively" modelling it to existing time related gold and zinc intraparticle concentration profiles experimentally measured by Pillay (1979). This was done for the case of an infinite bath using realistic values for the mass transfer parameters. Broad agreement between the model predictions and the experimental results was obtained.

REFERENCES

1. A Acrivos, Method of Characteristics Technique Application to Heat and Mass Transfer Problems, *Ind. Eng. Chem.* 48, 703–710 (1956)

2. R.B. Bird, W.E. Stewart and E.N. Lightfoot, Transport Phenomena, John Wiley & Sons, Inc (1960)

3. F.H. Burstall, N.F. Kember, P.J. Forrest and R.A. Wells, Ion Exchange Processes for the Recovery of Gold from Cyanide Solutions, *Ind. Eng. Chem.*, 45, 1648 (1953)

4. F.H. Burstall and R.A. Wells, Recovery of gold from cyanide solution by ion exchange, *Ion Exchange and Its Applications*. London, Society of Chemical Industry, 83 (1955)

5. J.A.V. Butler and C. Ockrent, *J. Phys. Chem.* 34, 2841 (1930)

6. J. Davidson, F.O. Reid, F.D.L. Noakes and T.V. Arden, Ion exchange for gold recovery, *Trans. Instn Min. Metall.* 70, 247 (1961)

7. V. I. Demidov, R. Z. Kreienes, M. I. Ivanova and A. S. Kartasheva, Pilot plant tests on adsorptive extraction of gold from waste cyanide solutions. *Soviet J. Non–ferrous Me.*, 8 (8), 53 1967

8. C. A. Fleming, and G Cromberge, Small scale pilot plant tests on the resin–in–pulp extraction of gold from cyanide media, *J of S.A.I.M.M* (1984)

9. C. A. Fleming, and G Cromberge, The extraction of gold from cyanide solutions by strong and weak base anion exchange resins, *J of S.A.I.M.M* (1984)

10. C. A. Fleming, and G Cromberge, The elution of aurocyanide from strong– and weakbase resins *J of S.A.I.M.M* (1984)

11. I. D. Fridman, E. P. Zdorova, L. E. Eochkina, R. Yu. Bek, A. I. Maslii and S. N. Il'ichev, Pilot plant tests on extracting gold and silver from cyanide pulp employiong the coninious electroelution method. *Soviet J. Non–ferrous Met*, 12, 1971

12. W. Fritz, and E. U. Schluender, Simultaneous adsorption equilibria of organic solutes in dilute aqueous solutions on activated carbon, *Chem. Eng. Sci.* 29, 1279–1282 (1974)

13. I.S. Jain and V.L. Snoeyink, *J. WPCF*, 45, 2463 (1973)

14. G. Mc Kay and B. al Duri, Prediction of multicomponent adsorption data using empirical correlations, *The Chem. Eng. Jnl*, 41, 9–23 (1989)

15. A. I. Liapis, and D. W. T. Rippin, A general model for the simulation of multi–component adsorption from a finite bath, *Chem. Eng. Sci.* 32, 619–627 (1976)

16. A.L. Myers and J.H. Prausnitz, *AIChE J.*, 11 121 (1965)

17. I. Neretnieks, Analysis of some adsorption experiments with activated carbons, *Chem. Engng Sci.* 31, 1029–1035 (1976).

18. R.G. Peel, A. Benedek and C.M. Crowe, A branched pore kinetic model for activated carbon adsorption, *AIChE Journal*, 27(1), 26–32 (1981)

19. V. Pillay , Loading profiles of competing base metal complexes on the adsorption of gold cyanide onto anion exchange resin, Internal MINTEK Report, (1989)

20. C.J. Radke and J. H. Prausnitz, *AIChE J.*, 11 (4) 761 (1972)

21. P.A. Riveros and W.C. Cooper, Kinetic aspects of the ion exchange extraction of gold, silver and base metal cyano complexes, *Solvent Extraction and Ion Exchange*, 6(3), 479–503 (1988)

22. E. Stamboliades, J. McHardy, and T. Salman, Ion exchange techniques for the recovery of gold from cyanide solutions, *Can. Min. Metall. Bull.*, 71 124 (1978)

23. S. A. Tataru, Recovery of gold from cyanide solution by ion exchange, *Tenth Int. Min. Proc. Congress 1973. M. J. Jones (ed)*. London, The Inst. of Mining and Metallurgy, 26, 1135–1145, 1974.

24. J.S.J. van Deventer, Kinetic models for the adsorption of gold onto activated carbon, *Mintek 50: Proceedings of the International Conference on Mineral Science and Technology*, 2, 487–494 (1985)

25. W.C. van Lier, On the kinetics of adsorption on activated carbon from the aqueous phase, Activated carbon... a fascinating material, Norit, 129 (1983)

26. B.M. van Vliet, Comparitive adsorption performance of synthetic adsorbents and activated carbons, Ph.D. thesis, University of Michigan, Ann Arbor, Michigan (1980)

27. B. M. van Vliet, W. J. Weber, Jr. and H. Hozumi, Modelling and prediction of specific compound adsorption by activated carbon and synthetic adsorbents, *Water Res.* 14, 1719–1728 (1980)

28. W.J. Weber and K.T. Lui, Determination of mass transport parameters for fixed–bed adsorbers, *Chem. Engng Commun.* 6, 49–60 (1980)

29. J.E. Williamson, K.E. Bazaire and C.J. Geankoplis, Liquid–phase mass transfer at low reynolds numbers, *I & EC Fundam*, 3, 126–129 (1963)

30. B.D. Young and B.M. van Vliet, The effect of surface roughness on fluid–to–particle mass transfer in a packed bed adsorber, *Int. J. Heat Mass Transfer*, 31, 27–34 (1987)

APPENDIX 1: Mass Determination of Moist Resin Beads

The weighing of the resin requires a special procedure as the characteristics of the resin are damaged if allowed to dry. The resin is weighed in a moist but "touch dry" state. The method used to dewater the resin is well described by van Vliet, Weber and Hozumi (1980), and involves centrifuging the resin beads at 400 r.p.m. for two minutes in a covered sintered glass funnel. The method was tested for a few samples of resin and the moisture contents of the "touch dry" resin samples is given in table A1.

Table A.1: Moisture Contents of "Touch Dry" Resin Samples

Mass of "dry" Resin /g	Mass of dry Resin /g	% Water (w/w)
5,220	2,715	47,98
2,939	1,531	47,90
4,002	2,099	47,55
4,904	2,557	47.86
3,133	1,6423	47,58

The resin was dried in an oven at 120° C for 24 hours. The average moisture content of the "touch dry" resin is 47,77% (w/w), and the standard deviation is 0,196%. It can be seen that this is an accurate and reliable way of determining the mass of resin without damaging it's properties.

APPENDIX 2: Isotherm Data

1. Solution : 190,80 ppm Au
   0.00 ppm Zn
   pH : 10,00
   Temperature : 25°C

Mass of Resin /g	Gold Concentration (ppm)	Gold Loading (g/ton)
1,0210	0,18	31 340
0,8086	0,42	46 089
0,6078	0,70	62 503
0,5029	1,04	76 866
0,4000	1,44	93 891
0,3050	2,72	129 331
0,2085	-	-
0,1062	25,80	619 784
0,0524	83,60	809 160

2. Solution : 150,91 ppm Au
   43,97 ppm Zn
   pH : 10,0
   Temperature : 25°C

Mass Resin (g)	Gold Conc. (ppm)	Zinc Conc. (ppm)	Gold (g/t)	Zinc (g/t)
1,0017	0,306	0,00	30 071	-
0,8089	0,510	0,00	37 186	-
0,5998	1,184	0,00	49 927	-
0,5065	1,877	0,00	58 850	-
0,9019	3,551	0,06	60 034	33 851
0,3093	8,49	0,08	91 306	29 002
0,2000	51,02	1,68	103 258	41 861
0,0986	114,25	22,35	82 549	44 834
0,0561	127,76	34,42	74 290	46 623

3. Solution: 50,31 ppm Au
131,91 ppm Zn

pH : 10,0

Temperature : 24°C

Weight Resin (g)	Gold Conc. (ppm)	Zinc Conc. (ppm)	Gold (g/t)	Zinc (g/t)
1,4958	0,08	0,02	8 336	23 311
0,9925	0,55	0,126	12 603	37 714
0,7878	4,00	1,382	25 713	47 816
0,6238	10,2	10,4	23 046	58 177
0,3991	13,47	17,8	24 217	58 206
0,1993	26,8	50,9	25 311	60 217
0,1052	42,9	93,5	29 148	59 896
0,0622	61,1	126,9	28 500	61 192

4. Solution : 100,62 ppm Au

87,94 ppm Zn

pH : 10,0

Temperature : 25°C

Mass Resin (g)	Gold Conc. (ppm)	Zinc Conc. (ppm)	Gold (g/t)	Zinc (g/t)
1,0066	5,02	1,99	24 912	48 127
0,8000	7,31	2,43	32 089	49 773
0,6023	11,7	3,88	36 121	50 167
0,4000	23,7	10,7	40 867	53 264
0,3022	39,1	20,1	46 389	53 896
0,2000	55,0	35,9	47 118	53 992
0,1500	91,4	84,4	46 912	56 002

5. Solution : 171,43 ppm Au
0,00 ppm Zn

pH : 10,00

Temperature : 24°C

Mass of Resin /g	Gold Concentration (ppm)	Gold Loading (g/ton)
2,0000	0,13	39 106
1,0118	0,20	42 515
1,3030	0,26	45 012
1,0118	1,71	55 679
0,5065	31,59	65 992
0,4000	107,01	68 636
0,2056	134,55	69 007
0,1027	153,25	69 198

APPENDIX 3:- Multi-Component Column Mass Balance

Using the assumptions detailed in Section 2.4, the mass balance for the column of component i is presented below.

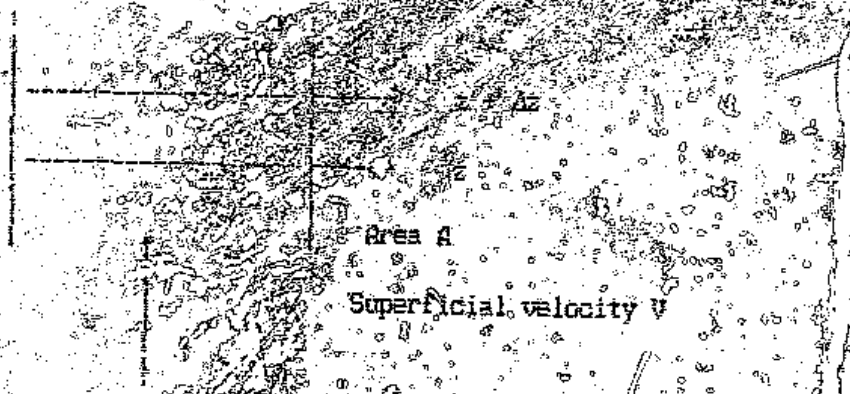

$$\begin{vmatrix}\text{Component i}\\ \text{in at z}\end{vmatrix} = \begin{vmatrix}\text{Component i}\\ \text{in at z+}\Delta z\end{vmatrix} + \begin{vmatrix}\text{Component i}\\ \text{accumulated}\end{vmatrix} + \begin{vmatrix}\text{Component}\\ \text{adsorbed}\end{vmatrix}$$

Component i out at $z + \Delta z = A\ V\ C_{ci}\Big|_{z+\Delta z}$

Component i adsorbed $= A\ \Delta z\ (1-\varepsilon)\ \rho_p \dfrac{\partial \bar{C}_i}{\partial t}$

Component i accumulated

in solution $= \varepsilon\ A\ \Delta z \dfrac{\partial C_{ci}}{\partial t}$

where:

ρ_p is the particle density, kg (dry particle) per m^3 (fully swelled resin bead)

C_{si} is the average solid phase concentration of component i, g/ton

Hence the mass balance yields (for component i)

$$A V C_{ci}|_z = A V C_{ci}|_{z+\Delta z} \Delta z (1-\varepsilon) \rho_p \frac{\partial C_{si}}{\partial t} + \varepsilon A \Delta z \frac{\partial C_{ci}}{\partial t}$$

Dividing through by Δz and taking limits as $\Delta z \to 0$, get:

$$V \frac{\partial C_{ci}}{\partial z} + \frac{(1-\varepsilon)}{\varepsilon} \rho_p \frac{\partial C_{si}}{\partial t} + \frac{\partial C_{ci}}{\partial t} = 0$$

where C_{si} is defined by:

$$C_{si} = \frac{3}{r_0^3} \int_0^{r_0} C_{si}(r,t)\, r^2\, dr$$

With boundary conditions:

$$C_{ci}(0,t) = C_{cio}$$

$$C_{ci}(0,z) = 0$$

However the average increase in the solid adsorbate concentration is simply the amount of adsorbate in by diffusion namely;

$$\rho_p \frac{\partial \bar{C}_{si}}{\partial t} = k_{fi}(C_{ci} - C_{pi})$$

Hence $$\rho_p \frac{\partial \bar{C}_{si}}{\partial t} = \frac{3\, k_{fi}}{r_0}(C_{ci} - C_{pi})$$

Substituting this into the column expression yields:

$$\frac{V}{\varepsilon}\frac{\partial C_{ci}}{\partial z} + 3\left[\frac{1-\varepsilon}{\varepsilon}\right]\frac{k_{fi}}{r_0}(C_{ci} - C_{pi}) + \frac{\partial C_{ci}}{\partial t} = 0$$

APPENDIX 4 Solution of the Model using the Method of Characteristics

As presented in Section 2, the unsteady–state column mass balance for adsorbing speies i, is:

$$\frac{V}{\varepsilon}\frac{\partial C_{ci}}{\partial z} + 3\left[\frac{1-\varepsilon}{\varepsilon}\right]\frac{k_{fi}}{r_0}(C_{ci} - C_{pi}) + \frac{\partial C_{ci}}{\partial t} = 0 \qquad \text{(A4.1)}$$

where, C_{ci} is the liquid adsorbate concentration of component i, mg l^{-2}

C_{pi} is the liquid adsorbate concentration of component i at the particle / liquid interface, mg l^{-1}

k_{fi} is the film transfer coefficient of component i, m s^{-1}

r_0 is the outside radius of the resin bead, m

t is time, s

V is the superficial velocity, m s^{-2}

Z is the longitudinal coordinate, m

ε is the column voidage

ρ_p is the resin density, g m^{-3}

The boundary conditions for this equation are:

$$C_{ci}(0,t) = C_{cio} \qquad \text{(A4.2)}$$

$$C_{ci}(Z,0) = 0 \qquad \text{(A4.3)}$$

A shell balance of radially diffusing species i, into the spherical resin bead as stated by Liapis and Rippin (1976) is:

$$\frac{\partial C_{si}}{\partial t} = \frac{D_{si}}{r^2}\frac{\partial}{\partial r}\left[r^2\frac{\partial C_{si}}{\partial r}\right] \qquad \text{(A4.4)}$$

where, C_{si} is the solid adsorbate concentration of component i, mg g^{-2}

t is time, s

D_{si} is the effective surface diffusion coefficient of component i, m^2s^{-1}

r is the radius of the resin bead, m

The boundary conditions for this equation are:

$$C_{si}(r,0) = 0 \qquad \text{(A4.5)}$$

$$\frac{\partial C_{si}}{\partial r}(0,t) = 0 \qquad \text{(A4.6)}$$

$$\frac{\partial C_{si}}{\partial r}(r_0,t) = -\frac{k_{fi}}{D_{si}}(C_{cio} - C_{pi}) \qquad \text{(A4.7)}$$

where, C_{ci} is the liquid adsorbate concentration of component i, mg l^{-2}

C_{pi} is the liquid adsorbate concentration of component i at the particle / liquid interface, mg l^{-1}

k_{fi} is the film transfer coefficient of component i, m s^{-1}

r_0 is the outside radius of the resin bead, m

The complete solution of the model is obtained by solving Equations (A4.1) and (A4.4) simultaneously. Equation (A4.1) is a hyperbolic partial differential equation and is solved using the method of characteristics as described by Acrivos (1956) and Murray (1988).

The solution to Equation (A4.1) is as follows:

The concentration of adsorbate in the solution of component i may be expressed as:

$$\Psi(s) = C_{ci}(Z(s),t(s))$$

on a curve parameterised as $z = z(s)$, and $t = t(s)$ with s being a parameter along the curve.

Differentiating $\Psi(s)$ with respect to s:

$$\frac{d\Psi(s)}{ds} = \frac{\partial C_{ci}}{\partial Z}\frac{dZ(s)}{ds} + \frac{\partial C_{ci}}{\partial t}\frac{dt(s)}{ds}$$

or, $$\Psi'(s) = \frac{\partial C_{ci}}{\partial Z}Z' + \frac{\partial C_{ci}}{\partial t}t'$$

where the prime denotes differentiation with respect to s.

Rearanging this expression:

$$\Psi'(s)\left[\frac{\partial C_{ci}}{\partial Z}Z'\right] = \frac{\partial C_{ci}}{\partial \tau_0}t'$$

Substituting this expression into the column material balance yields:

$$\frac{\partial C_{ci}}{\partial z}\left[\frac{\Psi}{\varepsilon}t' - Z'\right] = -\Psi'(s) - 3\left[\frac{1-\varepsilon}{\varepsilon}\right]\frac{k_{fi}}{r_0}(C_{ci} - C_{pi})\,t'$$

Hence when, $\frac{dZ}{dt} = \frac{V}{\varepsilon}$

$$\Psi'(s) = -3\left[\frac{1-\varepsilon}{\varepsilon}\right]\frac{k_{fi}}{r_0}(C_{ci} - C_{pi})\,t'$$

The slope of the characteristic is $\frac{dZ}{dt}$ ie.

$$t = t_0 + \frac{\varepsilon L s}{V}$$

where $Z = Ls$ (for convenience)

and, L is the height of the bed.

Also:

$$\tau = t' = \frac{\varepsilon L}{V}$$

Therefore:

$$\left.\frac{dC_{ci}}{ds}\right|_I = -3\left[\frac{1-\varepsilon}{\varepsilon}\right]\frac{k_{fi}}{r_0}(C_{ci} - C_{pi}) \qquad \text{(A4.8)}$$

where I denotes the characteristic $t = t_0 + \frac{\varepsilon L s}{V}$

Along this characteristic it is noted that the hyperbolic partial differential equation is reduced to an ordinary differential equation. The characteristic is merely a shock wave of solution passing down the column in plug flow. It is the trajectory of the interface between the resin adsorbate and the solution. This is shown on Figure A 4.1.

The simultaneous solution of the parameterised ordinary differential column equation (Equation (A4.8)) and the rate equation (Equation (A4.4)) is as follows:

(1) Break the surface into a fine grid as shown on Figure A 4.1.

(2) Solve Equation (A4.4) at Z = 0 ($C_{ci} = C_{cio}$) at the various grid times for C_{si}. This is done using the NAG FORTRAN software library routine D03PGF.

(3) Solve for the C_{pi}'s using the isotherm relationship (Equation (2.1.1), Section 2.1) at the various grid times.

(4) Using these C_{pi}'s, solve Equation (A4.8) along the characteristics from Z = 0 to Z = ΔZ to obtain the C_{ci}'s for the grid times at Z = ΔZ. This is done assuming the C_{pi}'s are constant over the integral step, which is a good assumption if the step length is small.

(5) Use these C_{ci}'s to solve Equation (A4.4) at Z = ΔZ to obtain C_{pi}'s at the various times.

(6) Repeat steps (4) and (5) until s = 1, ie. Z = L.

Fortran programs were written to solve the single and binary adsorption models. These programs are presented in Appendix 6.

Figure A4.1: Boundary Conditions for the Model with Representative Characteristics in the (Z,t) Plane

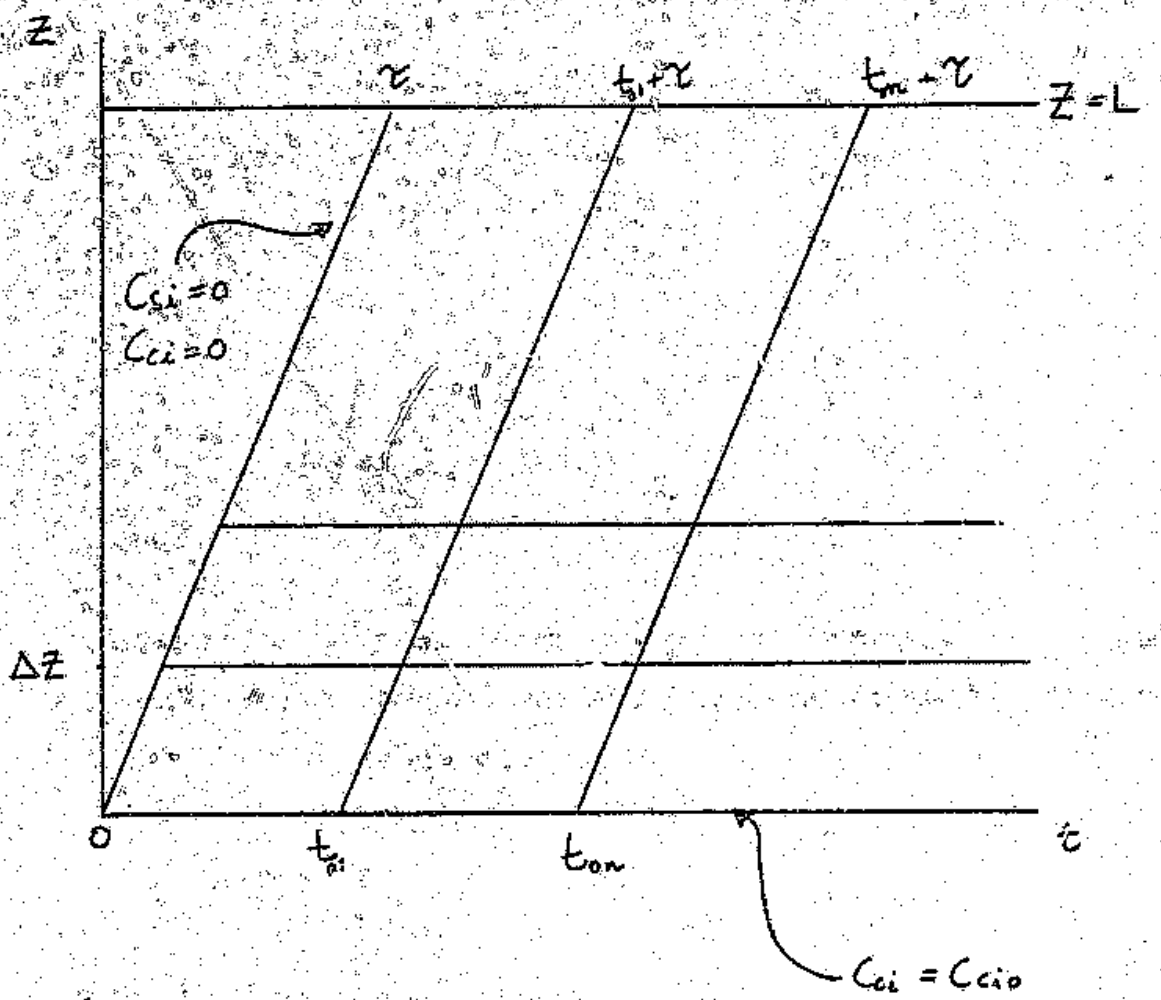

APPENDIX 5 : FITTING OF THE ISOTHERM DATA

For two components, the Fritz and Schluender(1974) relationship becomes:

$$C_{s1} = \frac{a_{10}\, C_{p1}^{b_{10}}}{c_1 + a_{11}\, C_{p1}^{b_{11}} + a_{12}\, C_{p2}^{b_{12}}}$$

and,

$$C_{S2} = \frac{a_{20}\, C_{p2}^{b_{20}}}{c_2 + a_{21}\, C_{p1}^{b_{21}} + a_{22}\, C_{p2}^{b_{22}}}$$

The above relationships have seven parameters each. Obviously there are many more parameters than are required to get a good fit to the experimental data. For convenience therefore the following parameters are set:

$$c_1 = c_2 = 1{,}0$$

$$b_{10} = b_{11}$$

$$b_{20} = b_{22}$$

To solve for the rest of the parameters two Fortran programs were written to minimise the sum of the squared differences between the model and the experimental data. There were two programs written as five optimum parameters were required and the computer was unable to

cope with the task. This was overcome by choosing the powers or b's and solving for only three optimum parameters (the a's). The a's were then substituted into a second program where the b's were optimised. The b's were then used in the first program to find new estimates of the optimum a's etc.

The optimisation routine used is the IMSL FORTRAN software library routine, ZXMIN.

```
C   *
C   *  PROGRAM TO FIND THE OPTIMUM
C   *  COEFFICIENTS FOR A1 AND A2 IN THE
C   *  FRITZ AND SCHLUENDER ISOTHERM
C   *
$JOB
      EXTERNAL FUNCT
      INTEGER N,NSIG,MAXFN,IOPT
      REAL A(8),H(99),G(9),W(99),F
      COMMON NP,X1(60),X2(60),Y1(60),Y2(60)
      NP=43
      DO 10 I=1,NP
   10 READ(5,*) X1(I),X2(I),Y1(I),Y2(I)
      N=3
      NSIG=4
      MAXFN=500
      IOPT=0
C
C   *  INITIAL GUESSES FOR THE
C   *  ISOTHERM PARAMETERS A1, A2, AND A3
C
      A(1)=504792.1
      A(2)=10.
      A(3)=1000.
C   *
C   *  OPTIMISATION ROUTINE USED IS ZXMIN
C   *
      CALL ZXMIN (FUNCT,N,NSIG,MAXFN,IOPT,A,H,G,F,W,IER)
      WRITE (1,*) F
      DO 40 I=1,N
   40 WRITE(1,*) A(I)
      STOP
      END
C
C
```

```
C
      SUBROUTINE FUNCT (N,A,F)
      COMMON NP,X1(60),X2(60),Y1(60),Y2(60)
      INTEGER N
      REAL A(N),F
      SUM=0.0
      DO 20 I=1,NP
      S1=A(1)*X1(I)**0.697/(A(2)*X1(I)**.697+A(3)*X2(I)**.394)
      SUM=SUM+(S1-Y1(I))**2
   20 CONTINUE
      F=SUM
      WRITE(1,4) F
      RETURN
      END
$ENTRY
```

```
C    *
C    *  PROGRAM TO FIND THE OPTIMUM
C    *  COEFFICIENTS FOR B1 AND B2 IN THE
C    *  FRITZ AND SCHLUENDER ISOTHERM
C    *
$JOB
      EXTERNAL FUNCT
      INTEGER N,NSIG,MAXFN,IOPT
      REAL B(8),H(99),G(9),W(99),F
      COMMON NP,X1(60),X2(60),Y1(60),Y2(60),B1,B2
      NP=42
      DO 10 I=1,NP
   10 READ(5,*) X1(I),X2(I),Y1(I),Y2(I)
      N=2
      NSIG=4
      MAXFN=500
      IOPT=0
C
C    *  INITIAL GUESSES FOR THE
C    *  ISOTHERM PARAMETERS B1, B2
C
      B(1)=0.9663
      B(2)=0.6094
C    *
C    *  OPTIMISATION ROUTINE USED IS ZXMIN
C    *
      CALL ZXMIN (FUNCT,N,NSIG,MAXFN,IOPT,B,H,G,F,W,IER)
      WRITE (1,*) F,B1,B2
C     DO 40 I=1,N
C 40  WRITE(1,*) B(I)
      STOP
      END
C
C
```

```
C
      SUBROUTINE FUNCT (N,B,F)
      COMMON NP,X1(60),X2(60),Y1(60),Y2(60),B1,B2
      INTEGER N
      REAL B(N),F
      SUM=0.
      B1=1.6*(SIN(B(1)))**2
      B2=1.0*(SIN(B(2)))**2
      DO 20 I=1,NP
C     WRITE(6,*)X1(I),X2(I),B(1),B(2)
      AAA=2.4820*X1(I)**B1
      BBB=32.378*X2(I)**B2
      SMY=(AAA+BBB)
      SUMY1=501493.*X1(I)**B1/SMY
      SUM=SUM+(SUMY1-Y1(I))**2
20    CONTINUE
      F=SUM
      WRITE(1,*) F,B1,B2
      RETURN
      END
$ENTRY
```

APPENDIX 6: FORTRAN PROGRAMS TO SOLVE THE MODEL

There are two programs presented. The first program solves the single component adsorption case. It was checked against a solutions presented by Young and van Vliet (1987) and Weber and Lui (1980). In every case agreement was obtained.

The second program solves the two component adsorption case. It was checked by setting in turn the two inlet concentrations to zero, and using the program to solve for single component model for both components individually. Agreement was then obtained with the single component programs.

```
C
C     ***********************************************
C     *                                             *
C     * PROGRAM TO SOLVE FOR THE INTERNAL SURFACE *
C     * DIFFUSION AND EXTERNAL FILM  TRANSFER     *
C     * COEFFICIENTS FOR GOLD GOLD AND ZINC       *
C     * CYANIDE ADSORPTION ONTO DUOLITE A161      *
C     *                                             *
C     ***********************************************
C
      IMPLICIT REAL*8 (A-H,O-Z)
      REAL*8 X(50),Y(2,50),CP1(10000)
      REAL*8 CP2(10000),CC1(10000),CC2(10000)
      COMMON DS1,DS2,RO,RH0,XFILM1,XFILM2,CC,C1,C2,NX
C
C     THE REQUIRED DATA IS SPECIFIED HERE
C     ***********************************
C
C     SUBSCRIPTS 1 AND 2 REFER TO GOLD AND
C     ZINC RESPECTIVELY
C
C     INLET CONCENTRATION (G/M**3)
      CC1O=45.8
      CC2O=19.5
      C1=CC1O
      C2=CC2O
C     LENGTH OF COLUMN (M)
      XL=22.4E-3
C     SUPERFICIAL VELOCITY (M/S)
      V=3.799E-3
C     CARBON PARTICLE SIZE (M)
      RO=0.4625E-3
C     COLUMN VOIDAGE
      ETA=0.4655
C     PARTICLE DENSITY (KG/M**3)
      RHO=476.0
C     THE FILM COEFFICIENT (M/S)
      XFILM1=6.00E-5
      XFILM2=3.20E-5
C     DIFFUSION COEFFICIENT AT ZERO CONCENTRATION (M**2/S)
      DS1=2.72E-12
      DS2=1.60E-12
C
C     ***********************************************************
C
C     THE NO. OF RADIAL POINTS INSIDE THE
C     RESIN BEAD IS NX
C
      NX=11
      ALPHA1=-3.0*(1-ETA)*XL*XFILM1/(V*RO)
      ALPHA2=-3.0*(1-ETA)*XL*XFILM2/(V*RO)
      DO 10 I=1,NX
      Y(1,I)=0.0
      Y(2,I)=0.0
      X(I)=SIN(1.57079633*((I-1.0)/(NX-1.0)))*RO
   10 CONTINUE
      X(1)=1.E-13
      TO=0.0
      DO 1 J=1,500
```

```
            CC1(J)=C1
            CC2(J)=C2
    1   CONTINUE
C
C       NBED IS THE NO. OF BEDS THE
C       COLUMN IS SPLIT INTO
C
        NBED=11
C
C       NTIME IS THE NO.
C       OF TIME INTERVALS
C
        NTIME=100
        DO 12 L=1,NBED
        DO 17 I=1,NX
           Y(1,I)=0.0
           Y(2,I)=0.0
   17   CONTINUE
C
C       HPERBOLIC P.D.E. IS PARAMETERISED
C       IN S
C
        S=(FLOAT(L)-1.0)/(FLOAT(NBED)-1.0)
        TO=ETA*S*XL/V
        DO 2 K=1,NTIME
           TEND=(FLOAT(K)-1.0)*100.+ETA*XL*S/V
C
C       TEND IS THE CHARACTERISTIC OF
C       THE PARAMETERISED P.D.E.
C
           C1=CC1(K)
           C2=CC2(K)
           CALL EQN2(TO,TEND,X,Y,CP11,CP12)
           CP1(K)=CP11
           CP2(K)=CP12
           TO=TEND
    2   CONTINUE
C
C       THE SOLUTION OF THE HYPERBOLIC P.D.E. ALONG THE
C       CHARACTERISTIC
C
        DO 8 I=1,NTIME
           CC1(I)=CP1(I)+(CC1(I)-CP1(I))*EXP(ALPHA1*(1./FLOAT(NBED)))
           CC2(I)=CP2(I)+(CC2(I)-CP2(I))*EXP(ALPHA2*(1./FLOAT(NBED)))
    8   CONTINUE
   12   CONTINUE
        DO 13 I=1,NTIME
           WRITE(1,*)(I-1.0)*100.0,CC1(I)/CC10,CC2(I)/CC20
   13   CONTINUE
        STOP
        END
C
C       SUBROUTINE EQN2 SOLVES THE 1 COMPONENT PARABOLIC
C       P.D.E. RATE EXPRESSION
C
        SUBROUTINE EQN2(TO,TEND,X,Y,CP1,CP2)
        IMPLICIT REAL*8 (A-H,O-Z)
        EXTERNAL PDEF,BNDY,MONTR
        REAL*8 TIM(10000),CP(10000),CS(10000)
```

```
      REAL*8 WK(8000),X(50),Y(2,50)
      COMMON DS1,DS2,RO,RHO,XFILM1,XFILM2,CC,C1,C2,NX
      IU=2
      NPDES=2
      RELERR=1.0E-3
      ABSERR=1.0E-4
      INORM=1
      IMON=0
      IBAND=3
      IWK=8000
      IND=0
      M=2
      IFAIL=0
      CALL D03PGE(NPDES,M,PDEF,BNDY,TO,TEND,Y,IU,
     1 NX,X,RELERR,ABSERR,INORM,MONTR,IMON,IBAND,
     2 WK,IWK,IND,IFAIL)
      CALL ISTHRM(Y,CP1,CP2)
      RETURN
      END
      SUBROUTINE PDEF(NPDES,X,T,UX,DUX,F,G,C)
      IMPLICIT REAL*8 (A-H,O-Z)
      REAL*8 UX(2),DUX(2),F(2),G(2,2),C(2)
      COMMON DS1,DS2,RO,RHO,XFILM1,XFILM2,CC,C1,C2,NX
      G(1)=1.0
      F(1)=0.0
      G(1,1)=DS1
      G(1,2)=0.0
      C(2)=1.0
      F(2)=0.0
      G(2,1)=0.0
      G(2,2)=DS2
      RETURN
      END
      SUBROUTINE BNDY(NPDES,T,UX,IBND,P,Q,R)
      IMPLICIT REAL*8 (A-H,O-Z)
      REAL*8 UX(2),P(2),Q(2),R(2)
      COMMON DS1,DS2,RO,RHO,XFILM1,XFILM2,CC,C1,C2,NX
      IF(IBND.EQ.0)THEN
          P(1)=0.
          Q(1)=1.
          R(1)=0.
          P(2)=0.
          Q(2)=1.
          R(2)=0.
      ELSE
          P(1)=0.
          Q(1)=1.
          CALL FCN(UX,AUCPI,ZNCPI)
        P(2)=0.
        Q(2)=1.
        R(2)=XFILM2*(C2-ZNCPI)/(RHO*DS2)
      ENDIF
      RETURN
      END
      SUBROUTINE MONTR(NPDES,X,NPTS,T,TLAST,U,IU,TOUT,DT)
      IMPLICIT REAL*8 (A-H,O-Z)
      REAL*8 X(50),U(2,50)
      COMMON DS1,DS2,RO,RHO,XFILM1,XFILM2,CC,C1,C2,NX
```

```
      RETURN
      END
C
C     SUB. ISTHRM CALCULATES THE LIQID
C     CONC AT THE PARTICLE INTERFACE
C
      SUBROUTINE ISTHRM(CS,CP1,CP2)
      IMPLICIT REAL*8 (A-H,O-Z)
      REAL*8 CS(2,50),XX(2)
      COMMON DS1,DS2,RO,RHO,XFILM1,XFILM2,CC,C1,C2,NX
      XX(1)=CS(1,1)
      XX(2)=CS(2,1)
      CALL FCN(XX,CP1,CP2)
      RETURN
      END
      SUBROUTINE FCN (X,F1,F2)
      IMPLICIT REAL*8 (A-H,O-Z)
      REAL*8   X(2)
      A=501.4935
      B=2.489
      C=33.517
      D=222.7428
      E=0.3922
      F=5.8153
      ALP=0.713
      BET=0.899
      GAM=0.985
      DEL=0.383
      EPS=(C*X(1)/(A-B*X(1)))**1./ALP
      AKA=(E*X(2)/(D-F*X(2)))**1./GAM
      X2=(AKA*EPS**(DEL/GAM))**(1./(1.-BET*DEL/(ALP*GAM)))
      X1=EPS*(X2)**(BET/ALP)
      F1=X1
      F2=X2
      RETURN
      END
```

```
C ***************************************
C                                        *
C * PROGRAM TO SOLVE FOR THE EXTERNAL FILM *
C * AND INTERNAL SURFACE DIFFUSION         *
C * COEFFICIENTS FOR THE SINGLE COMPONENT  *
C * ADSORPTION OFGOLD OR ZINC CYANIDES ONTO *
C * DUOLITE A161                           *
C *                                        *
C ***************************************
C
      IMPLICIT REAL*8 (A-H,O-Z)
      REAL*8 X(50),Y(1,50),CP(50000),CCC(50000)
      COMMON DS,RO,RHO,XFILM,CC,A,GAMMA,NX
C
C     THE REQUIRED DATA IS SPECIFIED HERE
C     ***********************************
C
C     INLET CONCENTRATION (G/M**3)
      CCO=49.7
      CC=CCO
C     LENGTH OF COLUMN (M)
      XL=19.5E-3
C     SUPERFICIAL VELOCITY (M/S)
      V=6.255E-3
C     CARBON PARTICLE SIZE (M)
      RO=0.4625E-3
C     COLUMN VOIDAGE
      ETA=0.4655
C     ISOTHERM PARAMETERS
      A=87.78765
      GAMMA=0.677
C     PARTICLE DENSITY (KG/M**3)
      RHO=476.0
C     THE FILM COEFFICIENT (M/S)
      XFILM=4.63E-5
C     DIFFUSION COEFFICIENT AT ZERO CONCENTRATION (M**2/S)
      DS=2.41E-12
C     ***********************************************************
C
      NX=11
C
C     NX IS THE NO. OF RADIAL POINTS IN THE BEAD
C
      ALPHA=-3.0*(1-ETA)*XL*XFILM/(V*RO)
      DO 10 I=1,NX
      Y(1,I)=0.0
      X(I)=SIN(1.57079633*((I-1.)/(NX-1.)))*RO
   10 CONTINUE
      X(1)=1.E-13
      TO=0.0
      DO 1 J=1,500
         CCC(J)=CC
    1 CONTINUE
C
C     NBED IS THE NO. OF DISCRETISED
C     COLUMN HEIGTHS
C
      NBED=11
```

```
      DO 12 L=1,NBED
      DO 17 I=1,NX
      Y(1,I)=0.0
   17 CONTINUE
      S=(FLOAT(L)-1.0)/(FLOAT(NBED)-1.0)
C
C     S IS THE PARAMETER FOR THE COLUMN EQUATION
C
      TO=ETA*S*XL/V
      DO 2 K=1,100
        TEND=(K*1.0-1.0)*100.+ETA*XL*S/V
C
C     TEND IS THE CHARACTERISTIC FOR THE PARAMETERISED
C     HYPERBOLIC P.D.E.
C
        CC=CCC(K)
        CALL EQN2(TO,TEND,X,Y,CPI)
        CP(K)=CPI
        TO=TEND
    2 CONTINUE
      DO 8 I=1,100
C
C     ANALYTICAL SOLUTION TO THE PARAMETERISED
C     HYPERBOLIC P.D.E. COLUMN EQUATION
C
        CC=CP(I)+(CCC(I)-CP(I))*EXP(ALPHA*(1./FLOAT(NBED)))
        CCC(I)=CC
    8 CONTINUE
   12 CONTINUE
      DO 13 I=1,100
        WRITE(1,*)(I-1.0)*100.0,CCC(I)/CC
   13 CONTINUE
      STOP
      END
C
C     SUBROUTINE EQN2 SOLVES THE PARABOLIC
C     P.D.E. RATE EXPRESSION
C
      SUBROUTINE EQN2(TO,TEND,X,Y,CPI)
      IMPLICIT REAL*8 (A-H,O-Z)
      EXTERNAL PDEF,BNDY,MONTR
      REAL*8 TTM(50000),CP(50000),CS(50000)
      REAL*8 WK(8000),X(50),Y(1,50)
      COMMON DS,RO,RHO,XFILM,CC,A,GAMMA,NX
      IU=1
      NPDES=1
      RELERR=1.0E-3
      ABSERR=1.0E-3
      INORM=1
      IMON=0
      IBAND=1
      LWK=8000
      IND=0
      M=2
      IFAIL=0
      CALL D03PGF(NPDES,M,PDEF,BNDY,TO,TEND,Y,IU,
     1 NX,X,RELERR,ABSERR,INORM,MONTR,IMON,IBAND,
     2 WK,LWK,IND,IFAIL)
      CALL ISTHRM(Y,CPI)
```

```
      RETURN
      END
      SUBROUTINE PDEF(NPDES,X,T,UX,DUX,F,G,C)
      IMPLICIT REAL*8 (A-H,O-Z)
      REAL*8 UX(1),DUX(1),F(1),G(1,1),C(1)
      COMMON DS,RO,RHO,XFILM,CC,A,GAMMA,NX
      C(1)=1.0
      F(1)=0.0
      G(1,1)=DS
      RETURN
      END
      SUBROUTINE BNDY(NPDES,T,UX,IBND,P,Q,R)
      IMPLICIT REAL*8 (A-H,O-Z)
      REAL*8 UX(1),P(1),Q(1),R(1)
      COMMON DS,RO,RHO,XFILM,CC,A,GAMMA,NX
      IF(IBND.EQ.0)THEN
          P(1)=0.
          Q(1)=1.
          R(1)=0.
      ELSE
          P(1)=0.
          Q(1)=1.
          R(1)=CC-(UX(1)/(A-0.1624*UX(1)))**(1./GAM
C         R(1)=CC-(UX(1)/A)**(1./GAMMA)
          R(1)=XFILM*R(1)/(RHO*DS)
      ENDIF
      RETURN
      END
      SUBROUTINE MONTR(NPDES,X,NPTS,T,TLAST,U,IU,TOUT,DT)
      IMPLICIT REAL*8 (A-H,O-Z)
      REAL*8 X(50),U(1,50)
      COMMON DS,RO,RHO,XFILM,CC,A,GAMMA,NX
      RETURN
      END
      SUBROUTINE ISTHRM(CS,CPI)
      IMPLICIT REAL*8 (A-H,O-Z)
      REAL*8 CS(1,50)
      COMMON DS,RO,RHO,XFILM,CC,A,GAMMA,NX
      CPI=CS(1,11)/(A-0.1624*CS(1,11))
C     CPI=CS(1,11)/(A)
      CPI=CPI**(1./GAMMA)
      RETURN
      END
```

APPENDIX 7: EXPERIMENTENAL BREAKTHROUGH DATA AND CONDITIONS

1. GOLD EXPERIMENTS

1.

Gold inlet concentration = 48,9 ppm

Column Length = 20,6 mm

Superficial liquid velocity = 1,44 mm s^{-1}

time [s]	C/C_0
0	0,241
60	0,261
120	0,259
180	0,264
300	0,262
360	0,262
600	0,259
900	0,266
1200	0,263

1500	0,264
1800	0,267
2100	0,266
2400	0,270
3000	0,270
0600	0,271
4200	0,279
4500	0,288
5400	0,285
6000	0,293
6600	0,289
7200	0,295
8100	0,303
9900	0,320

2.

Gold inlet concentration = 45,9 ppm

Column Length = 21,4 mm

Supe ficial liquid velocity = 2,51 mm s-1

time [s]	C/C_0
0	0,358
50	0,360
120	0,361
180	0,362
300	0,361
600	0,365
900	0,365
1200	0,369
1500	0,373
1800	0,376
3000	0,384
3600	0,385
4200	0,391
4800	0,396
5000	0,406
6600	0,414
7200	0,422
8400	0,432
9000	0,433

3.

Gold inlet concentration = 46,4 ppm

Column Length = 22,1 mm

Superficial liquid velocity = 3,80 mm s^{-1}

time [s]	C/C$_o$
0	0,451
60	0,452
120	0,455
180	0,454
300	0,458
600	0,463
900	0,462
1200	0,464
1500	0,466
1800	0,471
2100	0,473
2400	0,475
2700	0,478
3000	0,484
3600	0,488
4200	0,491

4800	0,502
5300	0,523
7200	0,541
8800	0,556

4.

Gold inlet concentration = 52,3 ppm

Column Length = 20[illegible] cm

Superficial liquid velocity = 4,96 cm s

	0,549
300	
420	
600	0,565
900	0,566
	0,570
	0,572
	0,575

2400	0,582
3000	0,590
3600	0,897
4200	0,604
4800	0,614
5700	0,630
6300	0,648
7500	0,665
8400	0,684
9000	0,696
9600	0,707

5.

Gold inlet concentration = 49,7 ppm

Column length = 19,5 mm

Superficial liquid velocity = 6,26 mm s^{-1}

time s	C/C_0
0	0,595
60	0,600
120	0,605
180	0,610

240	0,612
300	0,614
900	0,616
1200	0,618
1500	0,621
2100	0,628
2400	0,632
3000	0,641
3600	0,650
4800	0,669
6000	0,693
6600	0,705
7200	0,717
7800	0,729
9000	0,753
9600	0,764
9900	0,769

2. ZINC EXPERIMENTS

1.

Zinc inlet concentration = 19,7 ppm

Column Length = 43,6 mm

Superficial liquid velocity = 1,44 mm s^{-1}

Time [s]	C/C$_0$
0	0,301
60	0,316
120	0,334
240	0,322
600	0,334
900	0,343
1200	0,348
1500	0,334
1800	0,338
2100	0,338
2700	0,334
3000	0,337
3300	0,335
3600	0,337
3900	0,349
	0,349

4500	0,362
4800	0,365
5100	0,362
5400	0,374
5700	0,378
6000	0,391
6300	0,400
6600	0,400
7200	0,433
7800	0,451
8100	0,456
8400	0,459
8700	0,475
9300	0,501
9600	0,514
9900	0,520

2.

Zinc inlet concentration = 19,1 ppm

Column Length = 19,4 mm

Superficial liquid velocity = 2,51 mm s^{-1}

Time (s)	C/C_0
0	0,421
50	0,441
120	0,437
240	0,423
300	0,439
500	0,441
900	0,441
1200	0,434
1500	0,443
1800	0,440
2100	0,445
2400	0,445
2700	0,448
3000	0,455
3300	0,466
3600	0,474
3900	0,496
4200	0,521
4500	0,522
4800	0,522

5400	0,588
6300	0,625
6600	0,640
6900	0,656
7500	0,688
7800	0,700
8100	0,700
8400	0,712
8700	0,732
9000	0,745
9600	0,770
9900	0,776

3.

Zinc inlet concentration = 19,5 ppm

Column Length = 22,4 mm

Superficial liquid velocity = 3,80 mm s^{-1}

time [s]	C/C_0
0	0,467
30	0,488
60	0,474
120	0,488
180	0,488
240	0,481
300	0,475
360	0,484
420	0,492
600	0,492
720	0,488
900	0,488
1200	0,490
1500	0,478
1800	0,480
2100	0,493
2400	0,506
3000	0,547
3300	0,580
3600	0,600

4800	0,699
5400	0,738
6000	0,767
6600	0,799
7200	0,806
7800	0,811
9000	0,830

4.

Gold inlet concentration = 19,0 ppm

Column Length = 20,3 mm

Superficial liquid velocity = 4,98 mm s^{-1}

time [s]	C/C_0
0	0,531
30	0,566
60	0,568
120	0,569
180	0,572
240	0,561
300	0,561

360	0,569
420	0,577
600	0,570
720	0,570
900	0,568
1200	0,568
1500	0,576
1800	0,599
2400	0,635
3000	0,689
3300	0,706
3600	0,714
4800	0,780
5400	0,822
6000	0,822
6600	0,842
7200	0,838
7800	0,853
9000	0,859
9900	0,877

3. BINARY EXPERIMENTS

1.-

Gold inlet concentration = 44,9 ppm

Zinc inlet concentration = 16,7 ppm

Column height = 22,0 mm

Superficial velocity = 1,44 mm s^{-1}

time [s]	$Au(CN)_2^-$ C / C_0	$Zn(CN)_4^{2-}$ C / C_0
0	0,230	0,269
60	0,238	0,272
120	0,241	0,275
180	0,243	0,278
240	0,241	0,277
300	0,241	0,275
600	0,242	0,273
900	0,247	0,276
1200	0,251	0,276
1500	0,251	0,275
2100	0,270	0,276
2400	0,280	0,277
3000	0,324	0,288
3600	0,324	0,290

4200	0,360	0,295
4700	0,419	0,307
4800	0,425	0,309
5100	0,447	0,315
6000	0,535	0,361
6500	0,611	0,390
8400	0,732	0,452
9000	0,789	0,472
9600	0,842	0,501

2.

Gold inlet concentration = 50,7 ppm

Zinc inlet concentration = 18,4 ppm

Column height = 19,3 mm

Superficial velocity = 2.51 mm s^{-1}

time [s]	$Au(CN)_2^-$ C / C_0	$Zn(CN)_4^{2-}$ C / C_0
0	0,431	0,467
60	0,445	0,470
120	0,450	0,470
180	0,450	0,483
240	0,451	0,477
300	0,451	0,478
600	0,462	0,478
900	0,454	0,476
1200	0,474	0,476
1800	0,511	0,480
2400	0,563	0,487
3000	0,640	0,511
3600	0,716	0,542
4200	0,788	0,580
4800	0,858	0,623
5400	0,931	0,703
6300	0,952	0,749
7500	0,957	0,774
8100	0,960	0,801
9000	0,970	0,827
9900	0,970	0,845

2.

Gold inlet concentration = 45,8 ppm

Zinc inlet concentration = 19,5 ppm

Column height = 22,4 mm

Superficial velocity = 3,80 mm s^{-1}

time [s]	$Au(Cl^-)_2^-$ C / C_0	$Zn(CN)_4^{2-}$ C / C_0
0	0,476	0,511
60	0,478	0,516
120	0,487	0,520
240	0,487	0,525
300	0,491	0,512
600	0,491	0,512
1200	0,522	0,522
1800	0,603	0,538
2400	0,702	0,575
3000	0,789	0,621
3600	0,854	0,672
4800	0,929	0,760
5700	0,939	0,802

	115 V	
6000	0,946	0,816
6600	0,956	0,837
7200	0,959	0,848
9000	0,967	0,891

4.

Gold inlet concentration = 46,2 ppm

Zinc inlet concentration = 20,0 ppm

Column height = 20,0 mm

Superficial velocity = 4,99 mm s^{-1}

Time [s]	$Au(CN)_2^-$ C / C_0	$Zn(CN)_4^{2-}$ C / C_0
0	0,582	0,578
60	0,585	0,588
120	0,592	0,598
240	0,600	0,599
300	0,600	0,600
600	0,600	0,596
900	0,623	0,605
1200	0,652	0,608
2400	0,841	0,720
3600	0,928	0,816
4800	0,943	0,864
6000	0,954	0,884
7200	0,967	0,911
8400	0,975	0,923
9000	0,987	0,938

3.

Gold inlet concentration = 50,3 ppm

Zinc inlet concentration = 20,6 ppm

Column height = 21,5 mm

Superficial velocity = 6,26 mm s^{-1}

Time [s]	$Au(CN)_2^-$ C / C_0	$Zn(CN)_4^{2-}$ C / C_0
600	0,585	0,658
0	0,574	0,651
100	0,580	0,651
200	0,588	0,661
300	0,592	0,662
400	0,592	0,662
500	0,600	0,663
600	0,611	0,664
900	0,641	0,663
1500	0,762	0,684
2100	0,883	0,735
2700	0,922	0,794
3000	0,940	0,819
3600	0,945	0,845
4200	0,959	0,861

5700	0,963	0,908
6000	0,969	0,909
6600	0,979	0,917
7200	0,970	0,927
8400	0,975	0,938
9000	0,972	0,953

APPENDIX 8: PROGRAM TO SOLVE FOR THE BINARY INTRAPARTICLE LOADING PROFILES

```
C
C     ************************************************
C     *                                              *
C     * PROGRAM TO SOLVE FOR THE INTERNAL SURFACE    *
C     * LOADINGS IN AN INFINITE BATH EXPERIMENT      *
C     *                                              *
C     ************************************************
C
      IMPLICIT REAL*8 (A-H,O-Z)
      REAL*8 X(50),Y(2,50)
      COMMON /B1/ DS1,DS2,RO,RHO,XFILM1,XFILM2,CC10,CC20,NX
C
C     THE REQUIRED DATA IS SPECIFIED HERE
C     ***********************************
C
C     INLET CONCENTRATION (G/M**3)
      CC10=100.
      CC20=100.0
C     CARBON PARTIC' : SIZE (M)
      RO=0.4625E-3
C     PARTICLE DENSITY (KG/M**3)
      RHO=476.0
C     THE FILM COEFFICIENT (M/S)
      XFILM1=5.0E-5
      XFILM2=3.5E-6
C     DIFFUSION COEFFICIENT AT ZERO CONCENTRATION (M**2/S)
      DS1=5.0E-12
      DS2=1.5E-12
C
C     ************************************************
C
C     THE NO. OF RADIAL POINTS INSIDE THE
C     RESIN BEAD IS NX
C
      NX=11
      DO 10 I=1,NX
      Y(1,I)=0.0
      Y(2,I)=0.0
      X(I)=SIN(1.57079633*((I-1.)/(NX-1.)))*RO
   10 CONTINUE
      X(1)=1.E-13
      TO=0.0
      TEND=2.0*3600.
      CALL EQN2(TO,TEND,X,Y)
      DO 32 I=1,NX
        WRITE(1,*)X(I)/0.4625E-3,Y(1,I)*0.5,Y(2,I)
   32 CONTINUE
      STOP
      END
      SUBROUTINE EQN2(TO,TEND,X,Y)
      IMPLICIT REAL*8 (A-H,O-Z)
      EXTERNAL PDEF,BNDY,MONTR
      REAL*8 TIM(10000)
      REAL*8 WK(8000),X(50),Y(2,50)
      COMMON /B1/ DS1,DS2,RO,RHO,XFILM1,XFILM2,CC10,CC20,NX
      IU=2
      NPDES=2
      RELERR=1.0E-3
      ABSERR=1.0E-4
```

```
      INORM=1
      IMON=0
      IBAND=3
      IWK=8000
      IND=0
      M=2
      IFAIL=0
      CALL D03PGF(NPDES,M,PDEF,BNDY,TO,TEND,Y,IU,
     1 NX,X,RELERR,ABSERR,INORM,MONTR,IMON,IBAND,
     2 WK,IWK,IND,IFAIL)
      RETURN
      END
      SUBROUTINE PDEF(NPDES,X,T,UX,DUX,F,G,C)
      IMPLICIT REAL*8 (A-H,O-Z)
      REAL*8 UX(2),DUX(2),F(2),G(2,2),C(2)
      COMMON /B1/ DS1,DS2,RO,RHO,XFILM1,XFILM2,CC10,CC20,NX
      C(1)=1.0
      F(1)=0.0
      G(1,1)=DS1
      G(1,2)=0.0
      C(2)=1.0
      F(2)=0.0
      G(2,1)=0.0
      G(2,2)=DS2
      RETURN
      END
      SUBROUTINE BNDY(NPDES,T,UX,IBND,P,Q,R)
      IMPLICIT REAL*8 (A-H,O-Z)
      REAL*8 UX(2),P(2),Q(2),R(2)
      COMMON /B1/ DS1,DS2,RO,RHO,XFILM1,XFILM2,CC10,CC20,NX
      IF(IBND.EQ.0)THEN
          P(1)=0.
          Q(1)=1.
          R(1)=0.
          P(2)=0.
          Q(2)=1.
          R(2)=0.
      ELSE
          P(1)=0.
          Q(1)=1.
          P(2)=0.
          Q(2)=1.
          CALL FCN(UX,AUCPI,ZNCPI)
          R(1)=XFILM1*(CC10-AUCPI)/(RHO*DS1)
          R(2)=XFILM2*(CC20-ZNCPI)/(RHO*DS2)
      ENDIF
      RETURN
      END
C
C     ************************************************************
C
      SUBROUTINE MONTR(NPDES,X,NPTS,T,TLAST,U,IU,TOUT,DT)
      IMPLICIT REAL*8 (A-H,O-Z)
      REAL*8 X(50),U(2,50)
      COMMON /B1/ DS1,DS2,RO,RHO,XFILM1,XFILM2,CC10,CC20,NX
      RETURN
      END

      SUBROUTINE FCN (X,F1,F2)
```

```
      IMPLICIT REAL*8 (A-H,O-Z)
      REAL*8    X(2)
      A=501.4935
      B=2.489
      C=33.517
      D=222.7428
      E=0.3922
      F=3.8153
      ALP=0.718
      BET=0.399
      GAM=0.985
      DEL=0.333
      EPS=(C*X(1)/(A-B*X(1)))**1./ALP
      AKA=(E*X(2)/(D-F*X(2)))**1./GAM
      X2=(AKA*EPS**(DEL/GAM))**(1./(1.-BET*DEL/(ALP*GAM)))
      X1=EPS*(X2)**(BET/ALP)
      F1=X1
      F2=X2
      RETURN
      END
C
```